

Aus dem Fachbereich Medizin
der Johann Wolfgang Goethe-Universität
Frankfurt am Main

betreut am
Zentrum der Molekularen Medizin
Institut für Kardiovaskuläre Pharmakologie
am Max-Planck-Institut für Herz- und Lungenforschung in Bad Nauheim
Direktor: Prof. Dr. Stefan Offermanns

**Deorphanization and in vivo function(s) of the
G-protein-coupled receptor GPR182**

Dissertation
zur Erlangung des Doktorgrades der theoretischen Medizin
des Fachbereichs Medizin
der Johann Wolfgang Goethe-Universität
Frankfurt am Main

vorgelegt von
Alan Le Mercier
M. Sc. Ageing Biology

aus Romilly-sur-Seine, Frankreich

Frankfurt am Main, 2022

Dekan:

Prof. Dr. Stefan Zeuzem

Referent:

Prof. Dr. Stefan Offermanns

Korreferent:

Prof. Dr. Sofia-Iris Bibli

2. Korreferent:

Prof. Dr. Jaya Krishnan

Tag der Mündlichen Prüfung:

7 Juni 2023



SUMMARY

G-protein-coupled receptors (GPCRs) comprise the largest transmembrane receptor family encoded in the human genome. GPCRs mediate the effect of a wide diversity of stimuli including light, odorants, ions, lipids, small peptides, and hormones. GPR182 is a GPCR for which no endogenous ligand has been identified yet. In the absence of an identified ligand, GPR182 remained poorly understood, and its biological functions had remained elusive. The presented work shows that GPR182 is highly and specifically expressed in microvascular endothelial cells. Phylogenetically, GPR182 is closely related to the atypical chemokine receptor 3 (ACKR3). Here, I show that GPR182 binds the chemokines CXCL10, -12 and -13. Similarly to other so-called atypical chemokine receptors, GPR182 is not coupled to G-proteins but is rather constitutively internalized following β -arrestin 2 recruitment. Consistent with potential scavenger functions, we detected increased concentration of the chemokines which bind the receptor in the plasma of Gpr182 deficient mice. Finally, we show that GPR182 plays an essential role in maintaining hematopoietic stem cells within the bone marrow niche. In summary, the data indicate that GPR182 is a novel member of the group of atypical chemokine receptors, which plays an important role in the chemokine/chemokine receptor network.

ZUSAMMENFASSUNG

G-Protein-gekoppelte Rezeptoren stellen die größte Familie von Transmembran-Rezeptoren dar, die im Säuger genom kodiert sind. Sie vermitteln die Effekte einer Vielfalt von Stimuli wie Licht, Geruchsstoffen, Ionen, Lipiden, kleinen Peptiden oder Hormonproteinen. GPR182 ist ein G-Protein-gekoppelter Rezeptor, für den bisher kein endogener Ligand bekannt war. Daher war die biologische Funktion von GPR182 weitgehend unbekannt. Genetisch ist GPR182 am verwandtesten mit dem atypischen Chemokinrezeptor 3 (ACKR3). In der vorliegenden Arbeit konnte erstmals gezeigt werden, dass GPR182 die Chemokine CXCL10, -12 und -13 bindet. Vergleichbar mit anderen sogenannten atypischen Chemokinrezeptoren ist GPR182 nicht an G-Proteine gekoppelt sondern rekrutiert konstitutiv β -Arrestin, was dann zu einer konstitutiven Internalisierung des Rezeptors führt. In Übereinstimmung mit dieser Funktion als sogenannter „Scavenger“ konnte gezeigt werden, dass in Abwesenheit von GPR182 die Plasmakonzentrationen der durch GPR182 gebundenen Chemokine im Plasma signifikant erhöht sind. Schließlich konnten wir zeigen, dass GPR182 zur Aufrechterhaltung der hämatopoetischen Stammzellnische beiträgt und ein Verlust von GPR182 zu einer vermehrten Freisetzung hämatopoetischer Stammzellen führt. Zusammengefasst zeigen diese Daten, dass GPR182 ein neues Mitglied der Gruppe der atypischen Chemokinrezeptoren ist und eine in Teilen noch vollständig zu beschreibende Funktion im komplexen Chemokin/Chemokin-Rezeptor-Netzwerk spielt.

I.	LIST OF ABBREVIATIONS.....	7
II.	LIST OF FIGURES	9
III.	INTRODUCTION.....	11
1)	THE G-PROTEIN COUPLED RECEPTOR FAMILY	11
a)	<i>General Aspects.....</i>	11
b)	<i>GPCR signaling</i>	14
c)	<i>GPR182.....</i>	17
2)	THE CHEMOKINE NETWORK.....	18
a)	<i>Chemokines.....</i>	19
b)	<i>Conventional chemokine receptors.....</i>	21
c)	<i>Atypical chemokine receptors</i>	22
d)	<i>Patho/physiological(s) condition(s) involving the chemokine network.....</i>	24
3)	HEMATOPOIESIS AND THE BONE MARROW NICHE	25
a)	<i>General Aspects.....</i>	25
b)	<i>Hematopoiesis during development</i>	25
c)	<i>Hematopoietic stem cells.....</i>	26
d)	<i>Hierarchy of hematopoietic stem and progenitor cells differentiation</i>	26
e)	<i>Hematopoietic stem cell niche</i>	29
IV.	AIM OF THE STUDY.....	32
V.	MATERIALS	33
VI.	METHODS	42
VII.	RESULTS.....	54
1)	ANALYSIS OF GPR182 EXPRESSION.....	54
a)	<i>Gpr182 mRNA expression.....</i>	54
b)	<i>GPR182 expression.....</i>	55
	57
2)	DEORPHANIZATION OF GPR182	57
a)	<i>GPR182: a chemokine receptor?.....</i>	58
b)	<i>Seeking for a GPR182 endogenous ligand into the blood</i>	59
c)	<i>Seeking for an autocrine/paracrine secretion of GPR182 ligand in the liver</i>	61
d)	<i>Screening a lipid library.....</i>	62
3)	ANALYSIS OF GPR182 KNOCK-OUT FIRST MICE	64
a)	<i>Alteration of blood cells count</i>	64

b)	<i>Hematopoiesis in Gpr182 targeted mice</i>	65
c)	<i>Measurement of plasma cytokine levels highlights CXCL10</i>	66
4)	GPR182: A NOVEL ATYPICAL CHEMOKINE RECEPTOR	67
a)	<i>Specific binding of several recombinant chemokines to GPR182</i>	67
b)	<i>Oppositely to canonical GPCR, GPR182 does not signal through G-protein</i>	70
	72
c)	<i>GPR182 is constitutively highly internalized</i>	73
	74
5)	GPR182: A CHEMOKINE DECOY RECEPTOR DISRUPTING CHEMOKINES´ GRADIENT AND LEUKOCYTES TRAFFICKING.	74
a)	<i>Increased plasma concentration of GPR182´s ligands</i>	74
b)	<i>Decreased leukocytes trafficking into secondary lymphoid organs</i>	75
	76
c)	<i>Increased tumor growth in the lung</i>	77
d)	<i>Increased splenic size is associated with alteration of leukocytes composition</i>	78
6)	GPR182: ROLE IN MAINTENANCE OF QUIESCENT HSC WITHIN THE BONE MARROW NICHE.	80
a)	<i>Blood analysis in KO mice</i>	80
b)	<i>Hematopoiesis</i>	81
	82
c)	<i>Increased extramedullary HSC population</i>	82
d)	<i>Increased HSC population within the circulation</i>	84
7)	MODEL.....	85
a)	<i>Transplantation</i>	87
b)	<i>CXCL12 concentration and localization are not altered in the bone marrow niche</i>	88
VIII.	DISCUSSION	90
IX.	BIBLIOGRAPHY	97
X.	PUBLICATIONS	110
XI.	SCHRIFTLICHE ERKLÄRUNG	113

I. List of abbreviations

ACKR3	Atypical chemokine receptor 3 (formerly CXCR7)
ATP	Adenosine trisphosphate
β -arrst	β -arrestin protein
cAMP	3',5'-cyclic adenosine monophosphate
CAR	CXCL12 abundant reticular cells
CD31	Cluster differentiation 31 (also known as PECAM1)
cDNA	Complementary Deoxyribonucleic acid
CMP	Common myeloid progenitor
COS1	CV-1 in Origin and carrying the SV40 genetic material
CXCL10	C-X-C motif chemokine 10
CXCL12	C-X-C motif chemokine 12
CXCL13	C-X-C motif chemokine 13
CXCR3	C-X-C chemokine receptor type 3
CXCR4	C-X-C chemokine receptor type 4
CXCR5	C-X-C chemokine receptor type 5
CXCR7	C-X-C chemokine receptor type 7 (currently ACKR3)
DAPI	4',6-diamidino-2-phenylindole
DMEM	Dulbecco's modified eagle's medium
DNA	Deoxyribonucleic acid
EC-Gpr182-KO	Tamoxifen inducible endothelial specific knock-out mouse
EDTA	2,2',2'',2'''-(Ethane-1,2-diyldinitrilo)tetraacetic acid
FBS	Fetal bovine serum
GFP	Green fluorescent protein
GPCR	G-protein coupled receptor
HEK293T	Human embryonic kidney cells 293 T
HSC	Hematopoietic stem cell
HSPC	Hematopoietic stem and progenitor cell

IFN γ	Interferon gamma
IP3	Inositol trisphosphate
KDa	Kilo dalton
KO	Knock-out
LDL	Low-density lipoprotein
LMPP	Lymphoid-primed multipotent progenitor
LT-HSC	Long-term HSC
mChe	mCherry protein
MEP	Megakaryocyte and erythroid progenitor
MPP	Multipotent progenitor
oxLDL	Oxidized low-density lipoprotein
PCR	Polymerase chain reaction
PECAM1	Platelet endothelial cell adhesion molecule
PKA	Protein kinase A
PKC	Protein kinase C
PLA	Proximity ligation assay
PLC- β	Phospholipase C isoform β
ROCK	Rho-associated protein kinase
SCF	Stem cell factor
ST-HSC	Short-term HSC
WT	Wild type

II. List of figures

FIGURE 1: PHYLOGENETIC TREE HIGHLIGHTING GPCRS HOMOLOGIES	12
FIGURE 2: MOST COMMON SIGNALING PATHWAY TRIGGERED BY G-PROTEIN ACTIVATION.....	16
FIGURE 3: HIGHLIGHTING GPR182 AND ITS RELATED HOMOLOGUES EXHIBIT THE CHEMOKINE RECEPTOR FAMILY.....	18
FIGURE 4: SCHEMATIC VIEW OF THE STRUCTURE-BASED CLASSIFICATION OF CHEMOKINES	20
FIGURE 5: KNOWN INTERACTIONS BETWEEN CHEMOKINES AND THEIR RECEPTORS.....	22
FIGURE 6: SIMPLIFIED REPRESENTATION OF THE HEMATOPOIETIC DIFFERENTIATION HIERARCHY	28
FIGURE 7: A SCHEMATIC VIEW OF THE HSC NICHE IN THE BONE MARROW	30
FIGURE 8: GPR182 EXPRESSION.....	54
FIGURE 9: GPR182 IS EXPRESSED IN MICROVASCULAR ENDOTHELIAL CELLS.	57
FIGURE 10: SCHEMA REPRESENTING THE TANGO SYSTEM	58
FIGURE 11: GPR182 IS NOT ACTIVATED UPON CHEMOKINES STIMULATION	59
FIGURE 12: GPR182 IS NOT ACTIVATED UPON PLASMA STIMULATION.....	60
FIGURE 13: GPR182 IS NOT ACTIVATED UPON STIMULATION FROM RELEASED HEPATIC FACTORS	62
FIGURE 14: SCREENING AN ENDOGENOUS LIPIDS LIBRARY ON GPR182	63
FIGURE 15 : GPR182 DEFICIENCY LEADS TO LEUKOCYTOSIS	64
FIGURE 16: GPR182 DEFICIENCY RESULTS IN DECREASED BONE MARROW HSC	66
FIGURE 17: GPR182 DEFICIENT MICE DISPLAYED INCREASED CXCL10 PLASMA LEVEL	66
FIGURE 18: GPR182 BINDS THE Fc: CXCL10 FUSION RECOMBINANT PROTEIN	68
FIGURE 19: GPR182 BINDS THE CHEMOKINES CXCL10, CXCL12, AND CXCL13	69
FIGURE 20: GPR182 DOES NOT SIGNAL IN RESPONSE TO LIGAND BINDING	70
FIGURE 21: GPR182 DOES NOT SIGNAL IN RESPONSE TO LIGAND BINDING	71
FIGURE 22: GPR182 DOES NOT SIGNAL IN RESPONSE TO LIGAND BINDING	72
FIGURE 23: GPR182 IS CONSTITUVELY INTERNALIZED	74
FIGURE 24: INCREASED FREE PLASMA CONCENTRATIONS OF CXCL10, CXCL12A, AND CXCL13 IN MICE LACKING GPR182.....	75
FIGURE 25: DECREASED LEUKOCYTES EXTRAVASATION INTO SECONDARY LYMPHOID ORGANS	76
FIGURE 26: INCREASED LUNG METASTASIS FORMATION IN <i>Gpr182-DEFICIENT MICE</i>	77
FIGURE 27: INCREASED SIZE AND ALTERED LEUKOCYTES COMPOSITION OF THE SPLEEN OF MICE LACKING THE RECEPTOR.	79
FIGURE 28: GPR182 DEFICIENCY LEADS MAINLY TO AN INCREASED MCV/MCH, WHILE ERYTHROCYTES AND RETICULOCYTES COUNTS ARE SLIGHTLY RISEN.	80
FIGURE 29: <i>Gpr182-DEFICIENCY</i> RESULTS IN DECREASED BONE MARROW HSC	82
FIGURE 30: INCREASED HSC POPULATION WITHIN THE SPLEEN OF KO MICE.....	83
FIGURE 31: INCREASED HSC NUMBER WITHIN THE BLOODSTREAM.....	84
FIGURE 32: MODEL OF GPR182 BEHAVING AS A CHEMOKINE DECOY RECEPTOR	85
FIGURE 33: THE ENGRAFTMENT AND THE PERSISTENCE OF <i>Gpr182-KO</i> DONOR- HSCS APPEARS NORMAL	88

FIGURE 34: THE LOCALIZATION AND QUANTIFICATION OF CXCL12 WITHIN THE BONE MARROW NICHE IS NOT ALTERED BY THE LACK OF GPR182 88

III. Introduction

1) The G-protein coupled receptor family

a) General Aspects

More than 3% of the genes of the human genome encode over 800 so-called G-protein-coupled receptors, characterized by 7-transmembrane spanning domains [9]. In response to their specific stimulus, these receptors recruit and signal through heterotrimeric G-protein [10]. Thereby, these receptors have been renamed: G-protein coupled receptors (GPCR). Outstandingly, scientists working on GPCR were rewarded by the Nobel Prize at several times through history (Nobel Prize in Physiology or Medicine in 1971 and 1994; the Nobel Prize in Chemistry in 2012); highlighting the tremendous role of GPCRs in patho/-physiological processes and their therapeutic targeting potential.

These 800 GPCRs are dichotomized into two subfamilies; the first half is involved in sensing various odorants, bitter and sweet taste molecules, while the second subfamily represents the non-olfactory GPCRs [11]. Noticeably, most of our knowledge is related to non-olfactory GPCR, while the olfactory receptors remain largely evasive.

A different classification of the GPCR family is available in the literature. This sequence-similarity-based analysis allows classifying GPCR into five classes:

Rhodopsin (Class A), Secretin (Class B), Metabotropic Glutamate (Class C), Frizzled and Adhesion GPCR [12] (Figure 1):

- Class A represents the largest subclass and contains nearly all olfactory GPCRs as well as receptors for light, peptides, lipids, and neurotransmitters [13].
- Class B is the narrower subfamily, represented by ~25 GPCRs that mainly signal through G_s protein. These GPCRs bind hormones such as glucagon, secretin, vasoactive intestinal peptide, the growth-hormone-releasing-factor, and calcitonin [14].

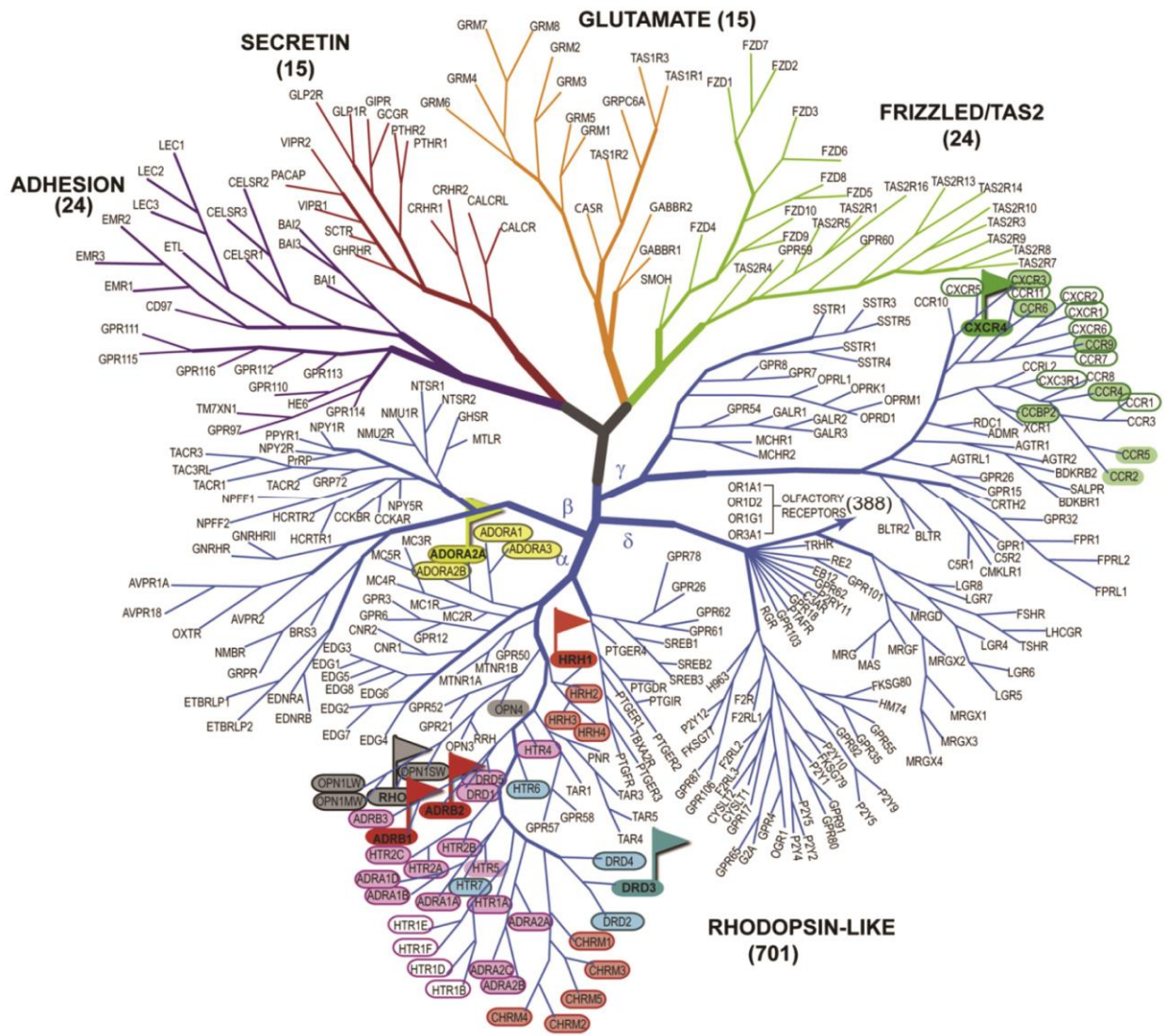


Figure 1: Phylogenetic tree highlighting GPCRs homologies

The phylogenetic analysis performed on the GPCR Family exhibits 5 distinct branches. Homologies within the TM domain are circled when superior at 35% whereas high homology within the binding pocket, superior at 50%, are displayed using similar color regrouping the GPCRs. [2]

- Class C is a small subfamily, characterized by a lengthy extracellular agonist binding region. Most class C receptors respond to neurotransmitters such as GABA or glutamate. However, some olfactory GPCR also belongs to this subfamily [15].
- The Frizzled GPCRs represent the most conserved GPCRs since metazoan evolution which, could be linked to their critical role during embryo development, cell polarization, and proliferation [16, 17].
- Finally, the human proteome codes for 33 adhesion GPCRs. Indeed, the extracellular region of these GPCRs consists of multiple protein/protein interaction domains suggesting that these GPCRs interacts with the extracellular matrix rather than responding to soluble ligands [18]. Furthermore, adhesion GPCRs are discernible because of their excessively long extracellular region [19, 20]. For instance, GPR98 has an extracellular domain that contains almost 6000 amino acids [21], while most GPCRs only display a ~100 amino acids N-terminal extremity.

As depicted above, GPCRs are receptors for a wide range of stimuli covering odorants molecules, hormones, neurotransmitters, chemokines, ions, and even photons of light [22]. Consequently, GPCRs are involved in most key physiological processes and, subtle dysregulation of GPCR signalling is found in many pathologies such as, non-exhaustively, hypertension [23], diabetes [24], cancer [25], Parkinson disease [26], mental disorders [27, 28]. As a result, ~35% of commonly used medicines in clinic target GPCR [29]. However, up to ~150 non-olfactory GPCR, considered orphan receptors, have not yet been paired to their endogenous ligand [30]. In consequence, the absence of endogenous ligands ultimately complicates their study and biological function(s) understanding.

Because orphan GPCR represent high potential drug-target, deorphanizing and getting a better understanding of those orphans GPCR remains a very active area of research.

b) GPCR signaling

Upon ligand binding, GPCRs undergo conformational changes resulting in the recruitment/ activation of guanine nucleotide-binding protein (G-proteins) [10]. G-protein consists of proteic complexes made up of three different subunits namely: α -subunit, β -subunit and a γ -subunit [10]. Upon receptor activation, a soluble GTP exchanges a phosphate with the inactive GDP- $G\alpha$ subunit resulting in the active form: GTP- $G\alpha$ subunit. Simultaneously, the active $G\alpha$ subunit dissociates from the $G\beta$ - γ dimer.

Both $G\alpha$ and $G\beta$ - γ dimer can trigger distinct effector [31, 32]. Additionally, each of these subunits is acknowledged as a gene family comprising 16 $G\alpha$, 5 $G\beta$ and 12 $G\gamma$ genes resulting in great combinatorial complexity and an immense range of possibilities of fine signaling [33]. Among all these signaling feasibilities, we retain the five most-characterized and understood downstream signaling: $G_{\alpha s}$, $G_{\alpha i/o}$, $G_{\alpha q/11}$, $G_{\alpha 12/13}$, and $G\beta$ - γ dimer signaling (Figure 2).

- $G_{\alpha s}$ activates the adenylyl cyclase which, catalyzes the conversion of adenosine triphosphate (ATP) into 3',5'-cyclic adenosine monophosphate (cAMP). Hereafter, cAMP behaves as an allosteric positive regulator of an essential secondary effector: the cAMP-dependent protein kinase (PKA). Finally, PKA activation results in the regulation of numerous proteins' activities through a specific phosphorylation of their serine-threonine amino acids [34, 35].
- Oppositely, $G_{\alpha i/o}$ protein inhibits the adenylyl cyclase activity, resulting in a decreased intracellular cAMP level [36].
- GPCRs coupled to $G_{\alpha q/11}$ activate phospholipase C- β (PLC- β) which, is known to hydrolyze the plasma membrane component, phospholipid, into diacylglycerol

and inositol 1,4,5-triphosphate (IP3). Then, IP3 promotes an intracellular calcium transient allowing the activation of another major secondary effector named calcium-dependent protein kinase (PKC). Finally, PKC governs numerous proteins activity by modifying their phosphorylation status [37, 38].

- $G\alpha_{12/13}$ controls the activity of a small monomeric G-protein family: the RhoA family. The understanding of RhoA functions requires further study; however, the Rho-associated protein kinases (ROCK) family appear to be a major downstream effector of the RhoA protein [37, 39, 40].
- Historically, $G\beta\text{-}\gamma$ dimers have been discovered to control K^+ and Ca^{2+} channels [41, 42]. However, $G\beta\text{-}\gamma$ dimers have more recently been described for regulating the adenylyl cyclase and phospholipase C- β/ϵ activity [43-45].

Besides these well-understood signaling pathways, several other effectors have been uncovered such as cadherins, A-kinase anchoring proteins (AKAP), non-receptor tyrosine kinases and protein phosphatases [46].

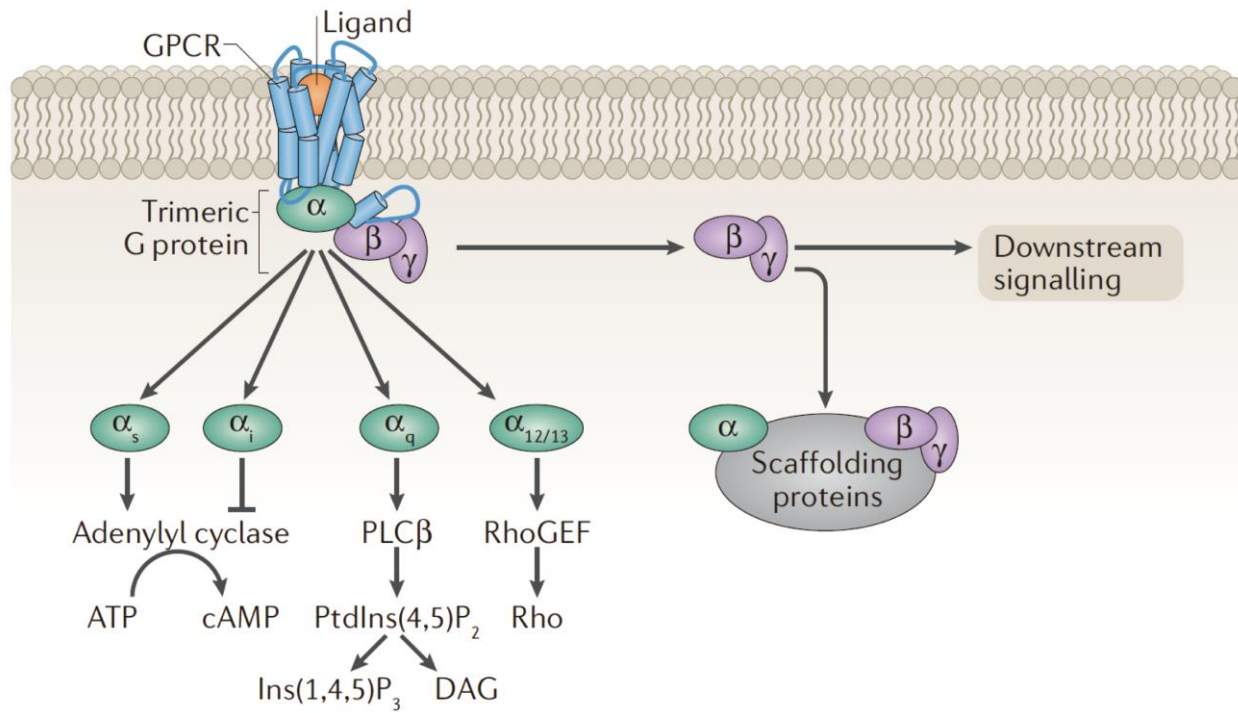


Figure 2: Most common signaling pathway triggered by G-protein activation

Upon GPCR activation by their ligands, inactive G protein heterotrimers dissociate into active G α and G $\beta\gamma$ subunits. These subunits differentially control downstream signal transduction [1].

c) GPR182

GPCRs represent the most successful drug target because they are the upstream specific trigger of most key biological functions and because they are pharmacologically manipulable. Thus, deorphanizing and gaining a better understanding of poorly studied GPCR embody a high potential for future therapeutic drugs. Regarding this context, we decided to study one of these orphan receptors: G-protein-coupled receptor 182 (GPR182).

Historically proposed to respond to adrenomedullin, a vasodilator hormone [47], further analysis could not confirm this observation [48]. Expression analysis performed on whole tissue described that GPR182 is widely expressed in various organs [4]. Further analyses in developing zebrafish and adult mice revealed that *Gpr182* is preferentially expressed in the vascular endothelium [49, 50]. Widespread expression in endothelial cells of mice was shown by using a mouse line expressing β -galactosidase under the control of the *Gpr182-promoter* [51]. Additionally, expression of the receptor was reported in human sinusoidal endothelial cells [52]. Whereas the role of GPR182 in endothelial cells is unknown, GPR182 expression in intestinal stem cells seems to negatively regulate proliferation during regeneration and adenoma formation [51].

Interestingly, the closest paralogue of GPR182 is a chemokine receptor: the atypical chemokine receptor 3 (ACKR3, previously described as CXCR7) (Figure 3) [2].

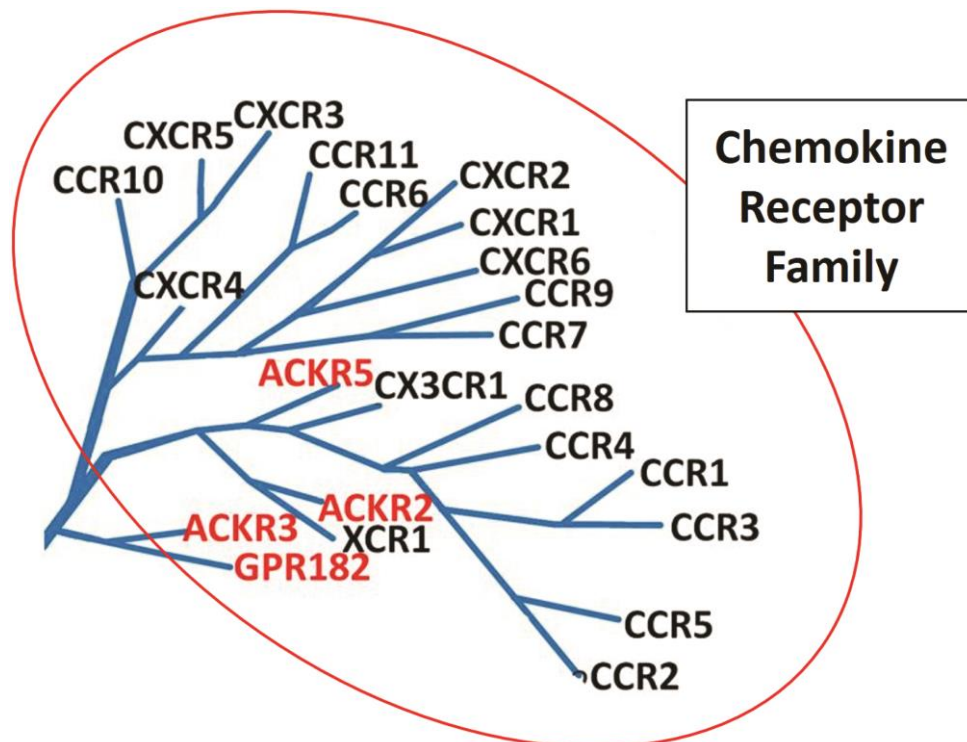


Figure 3: Highlighting GPR182 and its related homologues exhibit the chemokine receptor family.

Conventional chemokine receptors are represented in black while decoy receptors are depicted in red. To note, ACKR1 and ACKR4 are not represented because of their weak homology to this receptor family. Adapted from [2]

2) The chemokine network

Chemokines are small chemotactic cytokines (8-10 kDa) that mainly control migrations and positioning of immune cells, likewise any other cells expressing chemokine receptors [53]. Even though the first chemokines was discovered 40 years ago, chemokines remain of particular interest because of their substantial contribution to patho-/physiological processes. Indeed, chemokine receptors have since been largely and efficiently targeted in clinic. Nevertheless, understanding the chemokine network is extremely complex due to a large number of ligands, receptors and regulatory factors.

a) Chemokines

Chemokine constitutes the largest family of cytokines with ~50 chemokines in both humans and mice. A nomenclature based on the precise configuration of the two cysteines close to the N-terminal extremity allows classifying chemokines into four subfamilies: CC, CXC, CX3C, and XC chemokines (Figure 4A-D) [53]. In CC chemokines, the two first N-terminal cysteines involved in disulfide bond with further cysteine are adjacent to each other (Figure 4A). In CXC chemokines, these two cysteines are spaced by one amino acid, and the only CX3C chemokine has three amino acids in between these two cysteines (Figure 4B-C). Finally, the XC chemokines subfamily represented by two chemokines in human and one murine orthologue lack one of the two N-terminal cysteines (Figure 4D). Unconventionally, a second classification based on chemokines' function split chemokines into two subfamilies: inflammatory chemokines (CCL chemokines) and homeostatic chemokines (CXCL, CX3CL, and XCL chemokines).

Alongside these 50 chemokines, a multitude of mechanisms evolved to regulate chemokines' activities.

Mainly, post-translational modifications such as nitration, citrullination, or cleavage by matrix metalloproteinase have been shown to substantially tune chemokines activities. CCL2 nitration on its tyrosine residues has been shown to greatly reduce CCR2-expressing monocyte migration [54]. Additionally, the conversion of arginine residues into citrulline by an endogenously expressed peptidylarginine deiminase strongly reduces CXCL8, -10, and -11 chemotactic activities [55, 56]. Occasionally, chemokines such as CXCL16 and CX3CL1 are anchored to the plasma membrane and can be proteolytically cleaved, thereby releasing in the extracellular matrix an active chemokine fragment [57-61]. Furthermore, some secreted chemokines such as CCL6, -9, or -23 showed a strengthened activity after cleavage of their N-terminal appendix [62]. Uncommonly, post-transcriptional modifications have been shown to regulate chemokine activity. Indeed, *cxc12* is known to have six different spliced isoforms, each linked to distinct biological functions [63, 64].

Another significant way to regulate chemokine activity is to control chemokine availability after secretion. While some chemokines such as CCL19 and CXCL12 are soluble and freely diffusing within the extracellular matrix [65, 66], most chemokines are immobilized due to interaction with the extracellular matrix, especially glycosaminoglycans [67, 68]. By capturing monomeric chemokines, glycosaminoglycans have been shown to influence the formation of homodimers, heterodimers, or more elaborated chemokines complexes ending up with modified chemokine activity [69-72].

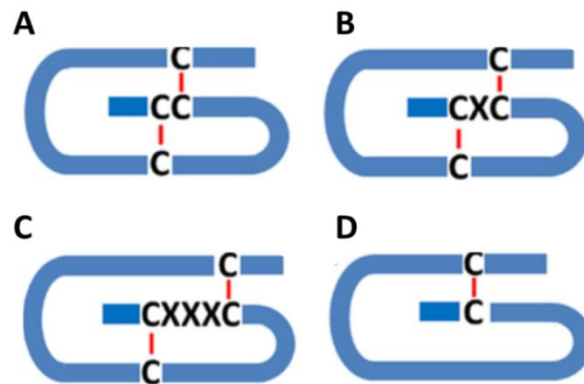


Figure 4: Schematic view of the structure-based classification of chemokines

Simplified view depicting the structurally-based difference between the four subtypes of chemokines. In Figure 4A, CCL-chemokines display two adjacent cysteines involved in disulfide bond while, the Figure 4B shows that disulfide bonds in CXCL-chemokines are spaced by a single aminoacid. Finally, Figure 4C and 4D, exhibit the small CX3CL- and XCL-chemokines subfamilies, in which disulfide bond are respectively spaced by three aminoacid or display one disulfide bond less. Adapted from [7]

b) Conventional chemokine receptors

The chemokine family contains ~19 receptors named according to the classification of chemokine they bind: CCR, CXCR, CX3CR or XCR receptors.

Interestingly, receptor specificity among the chemokine family is complex since chemokines bind several receptors and reciprocally [6]. That is mainly true for inflammatory chemokines that bind several receptors, while homeostatic chemokines bind only one or two receptors (Figure 5) [73]. Additionally, chemokines' affinity to receptors varies whether the receptor is monomeric, homodimerized, heterodimerized with another chemokine receptor or with a non-chemokinic receptor [74-80].

When a chemokine binds to a receptor, it induces a conformational change which is followed by intracellular signal triggering [81, 82]. Although most chemokine receptors have been shown to signal through Gai/o protein, other signaling pathways such as β -arrestin and JAK-STAT pathways have been identified [83, 84]. The most studied chemokine function is leukocytes' migration. Indeed, leukocytes require effective migration out of the bone marrow, likewise into, within and out of other organs to achieve precise localized and directed immune surveillance [73]. Besides leukocytes migration through gradients, chemokines have also been identified in maintaining chemokine-responsive cells within specialized environments such as hematopoietic stem cells (HSC) within the bone marrow niche [85]. Finally, it is well accepted that chemokines are also engaged in a wide range of cellular processes covering cell adhesion, survival, proliferation, differentiation, cytokine production and respiratory burst [86-100].

Chemokine ligand (alternative name)	Chemokine receptor														
	Conventional											Atypical			
	CCR1	CCR2	CCR3	CCR4	CCR5	CCR6	CCR7	CCR8	CCR9	CCR10	CCR11	CCR12	ACKR1	ACKR2	ACKR4
CC-chemokines															
CCL1 (I-309)															
CCL2 (MCP1)															
CCL3 (MIP1 α)															
CCL3L1 (LD78)															
CCL4 (MIP1 β)															
CCL5 (RANTES)															
Mouse CCL6 (C10)															
CCL7 (MCP3)															
CCL8 (MCP2)															
CCL9 (MIP1 γ)															
CCL11 (Eotaxin)															
CCL12 (MCP5)															
CCL13 (MCP4)															
CCL14 (HCC1)															
CCL15 (HCC2)															
CCL16 (HCC4)															
CCL17 (TARC)															
CCL18 (PARC)															
CCL19 (MIP3 β)															
CCL20 (MIP3 α)															
CCL21 (SLC)															
CCL22 (MDC)															
CCL23 (MPIF1)															
CCL24 (Eotaxin 2)															
CCL25 (TECK)															
CCL26 (Eotaxin 3)															
CCL27 (CTACK)															
CCL28 (MEC)															

Chemokine ligand (alternative name)	Chemokine receptor										
	Conventional										Atypical
	CXCR1	CXCR2	CXCR3	CXCR4	CXCR5	CXCR6	CXCR8	XCR1	CX ₃ CR1	ACKR1	ACKR3
CXC-chemokines											
CXCL1 (GRO α)											
CXCL2 (GRO β)											
CXCL3 (GRO γ)											
CXCL4 (PF4)											
CXCL5 (ENA78)											
CXCL6 (GCP2)											
CXCL7 (NAP2)											
CXCL8 (IL-8)											
CXCL9 (MIG)											
CXCL10 (IP10)											
CXCL11 (I-TAC)											
CXCL12 (SDF1)											
CXCL13 (BCA1)											
CXCL14 (BRAK)											
Mouse CXCL15 (Lungkine)											
CXCL16 (SR-PSOX)											
CXCL17 (DMC)											
C-chemokines											
XCL1 (Lymphotactin)											
XCL2 (SCM1 α)											
CX₃C-chemokine											
CX ₃ CL1 (Fractalkine)											

Figure 5: Known interactions between chemokines and their receptors

Table summarizing the known interaction between chemokines and their receptors and shedding light on the complex network of such interactions[6]

c) Atypical chemokine receptors

Recently, four atypical receptors were unable to initiate classical downstream signaling despite binding chemokines with high affinity [83]. Indeed, all these atypical receptors lack within their structure the canonical motif *DRYLAIV*, required for G-protein interaction [101]. Therefore, none of atypical chemokine receptor (ACKR) mediates the G-protein-signaling-dependent cell migration; instead, they internalize chemokines thereby,

regulating the extracellular chemokines' localization and abundance, implying that ACKRs shape chemokines' gradient [101].

ACKR1, previously described as Duffy and DARC, binds up to 20 different CCL and CXCL chemokines [102, 103]. ACKR1 is expressed in venular endothelial cells, erythrocytes and neurons. In endothelial cells, ACKR1 performs chemokines transcytosis; meaning, that it transports chemokine across the cell [104, 105]. In erythrocytes, ACKR1 behaves either as a chemokine reservoir or a sink [106-108]. As a result of the incredibly high number of erythrocytes, ACKR1 may buffer plasma's chemokine levels. Besides, ACKR1 is also the binding entry site in red blood cells for the pathogens causing malaria [109, 110]. Interestingly, an evolutive adaptation leading to ACKR1 lack of expression in human erythrocytes has been shown to protect Africans' subpopulation from developing malaria [111, 112].

Human ACKR2, also known as D6, binds at least 12 CCL chemokines [113, 114]. Briefly, ACKR2 is constitutively trafficking between the plasma membrane and lysosomes via endosomes [113, 115-117]. Such constitutive trafficking allows to quickly internalizing chemokines. Following internalization, the low pH in endosomes disrupts the covalent bonding between the receptor and its ligand. Then, the chemokine is degraded within lysosomes while the receptor is either degraded or recycled back to the plasma membrane for further scavenging. Through repeated cycles, ACKR2 may progressively deplete the extracellular matrix of chemokines; resulting in shaping the chemokine gradient.

ACKR3, exhaustively described as CXCR7, only binds CXCL11, and -12 [118, 119]. However, ACKR3 has recently been described to scavenge other families of proteins such as opioid peptides [120] and a vasodilator peptide: adrenomedullin [121, 122]. Mechanistically, ACKR3 is also a scavenger receptor that constitutively traffics between plasma membrane and lysosome.

Similarly to ACKR3, hACKR4 also binds, internalizes and degrades few chemokines; CCL19, -21, -25 [123, 124].

Finally, it is still controversial whether CCRL2 should be considered as an atypical chemokine receptor. Initially discovered as an atypical receptor for chemerin, a chemoattractant protein, it has additionally been shown to bind and internalize CCL5, -19 chemokines [125-127].

d) Patho/physiological(s) condition(s) involving the chemokine network

The chemokine network is involved in the regulation of a myriad of physiological processes. These physiological processes can be divided into two branches:

- The inflammatory reaction mediated by inflammatory chemokine:

Inflammatory chemokines are only produced under pathological conditions and contribute to inflammatory response [128, 129]. Notably, inflammatory responses are triggered following pathogens infections, and pathogen-free conditions: sterile inflammation (non-exhaustively: fatty liver disease, chronic kidney disease, auto-immune diseases, atherosclerosis, post-myocardial infarction, and most cancers) [6, 130-132].

Inflammatory responses are characterized by initial tissue damage. Subsequently, tissue-resident macrophages release a cytokine cocktail which “freely” diffuses within the tissue and generates a chemokine gradient. This cytokine gradient ultimately reaches the bloodstream where the circulating leukocytes sense it and migrate upward it until accessing the inflammation site [133]. Under “physiological” condition the inflammation is resolved, whereas abnormally sustained inflammation leads to the establishment of the pathologies previously mentioned [134].

- The homeostatic chemokines network:

Homeostatic chemokines are constitutively produced and contribute to the basal circulation of inactive leukocytes between the different lymphoid organs. Besides, homeostatic chemokines contribute to the maintenance of migrating cells within a

specific environment.

For instance, thymus-originating T cells entering the spleen are trapped within the splenic T cell follicle. However, these T cells do not remain immobile; they rather migrate through a circular gradient of homeostatic chemokines which indefinitely maintain T cells within the T follicle.

Another interesting example of homeostatic chemokine implication is the maintenance of the hematopoietic stem cells (HSC) within the HSC niche in bone marrow [85].

3) Hematopoiesis and the bone marrow niche

a) General Aspects

Hematopoiesis is a complex and still poorly understood biological process consisting in blood components production. All highly and differentially specialized blood cell lineages arise from a unique cell type: hematopoietic stem cell (HSC). Through successive rounds of differentiation and proliferation, the hematopoietic stem and progenitor cells (HSPC) spawn all mature blood cells: erythrocytes, leukocytes, and thrombocytes.

Erythrocytes, providing oxygen supply and CO₂ expelling, represent the most abundant cell type in human (~84% of eukaryotic cells!) [135]. Following a ~120 days' life span, removal of senescent erythrocytes' from the circulations is mainly assured by splenic macrophages [136-138]. Consequently, hematopoiesis compensates with millions of newly formed erythrocytes every second of life [5]. Leukocytes gather differently specialized cell types contributing all together in innate and adaptive immunity. Thrombocytes are remnants fragment originating from megakaryocytes that are mainly involved in hemostasis and wound healing.

b) Hematopoiesis during development

In utero, hematopoiesis appears around the fourth weeks of development. Before this stage, the embryo is small enough to receive the required amount of oxygen and nutrients from the placenta. Thus, hematopoiesis begins slightly before heart and

vasculature development and is undertaken by a primitive HSC population localized in the embryonic yolk sac [139]. Later on, the definitive HSC population emerges de novo from extra/ and intraembryonic tissue [140-142] and migrates to the fetal liver [143, 144]. Around the third month of development, hepatic hematopoiesis declines because of the HSC migration and colonization in the spleen. Finally, HSCs migrate shortly before birth into their final environment: the bone marrow niche [144]. However, under certain pathological conditions, extra-medullary hematopoiesis may principally occur in the liver, spleen and occasionally in lymph nodes [145-147].

c) Hematopoietic stem cells

HSC is a cell type characterized by two main features:

- First, HSCs are undifferentiated and multipotent cells; meaning, they can differentiate into several specialized cell lineages. As mentioned above, they form all the different blood cell types.

- Secondly, HSC division is asymmetric; conversely to somatic cells mitosis' that engenders two identical daughter cells, HSC division gives two functionally different cells. One daughter cell, named long-term HSC (LT-HSC), remains quiescent, undifferentiated, and self-renewing: allowing a perpetual pool of stem cells (Figure 6). The second daughter cell, referred to as short-term HSC (ST-HSC), highly proliferates and differentiates into the diversified blood progenitors (Figure 6).

d) Hierarchy of hematopoietic stem and progenitor cells differentiation

Hematopoiesis analysis is best realized by flow cytometry because it allows discriminating a horde of scarce cell types simultaneously. Indeed, HSC represents only 0,002% of all bone marrow cells [5].

First, isolating HSPC population requires ignoring the abundant mature blood cells (or lineage positive population). Additionally, all HSPC highly express Sca1 and the tyrosine

kinase receptor, c-Kit. Together, these three markers allow characterizing the Lin-/Sca1+/ c-Kit+ (LSK) population (0,06% of bone marrow cells). Additional markers identified HSC as the CD48-/CD34low/CD150+ LSK subpopulation [148]. The highest multipotent progenitor (MPP) differentiates into three distinct progenitors: megakaryocyte–erythroid progenitor (MEP), the common myeloid progenitor (CMP) and the lymphoid-primed MPP (LMPP) [5]. While progressing through this cascade of differentiation, these three progenitors lose some of their precursor multi-lineages potential. The MEP progenitor generates platelets and erythrocytes while the CMP progenitor produces most of the leukocytes cell types: Granulocytes (eosinophils, basophils and neutrophils), monocytes and dendritic cells. Finally, the LMPP progenitor engenders the remaining leukocytes that evolutionary appeared with the adaptive immune response, lymphocytes' cell types: B cells, T cells, natural killer cells (NK cells) (Figure 6).

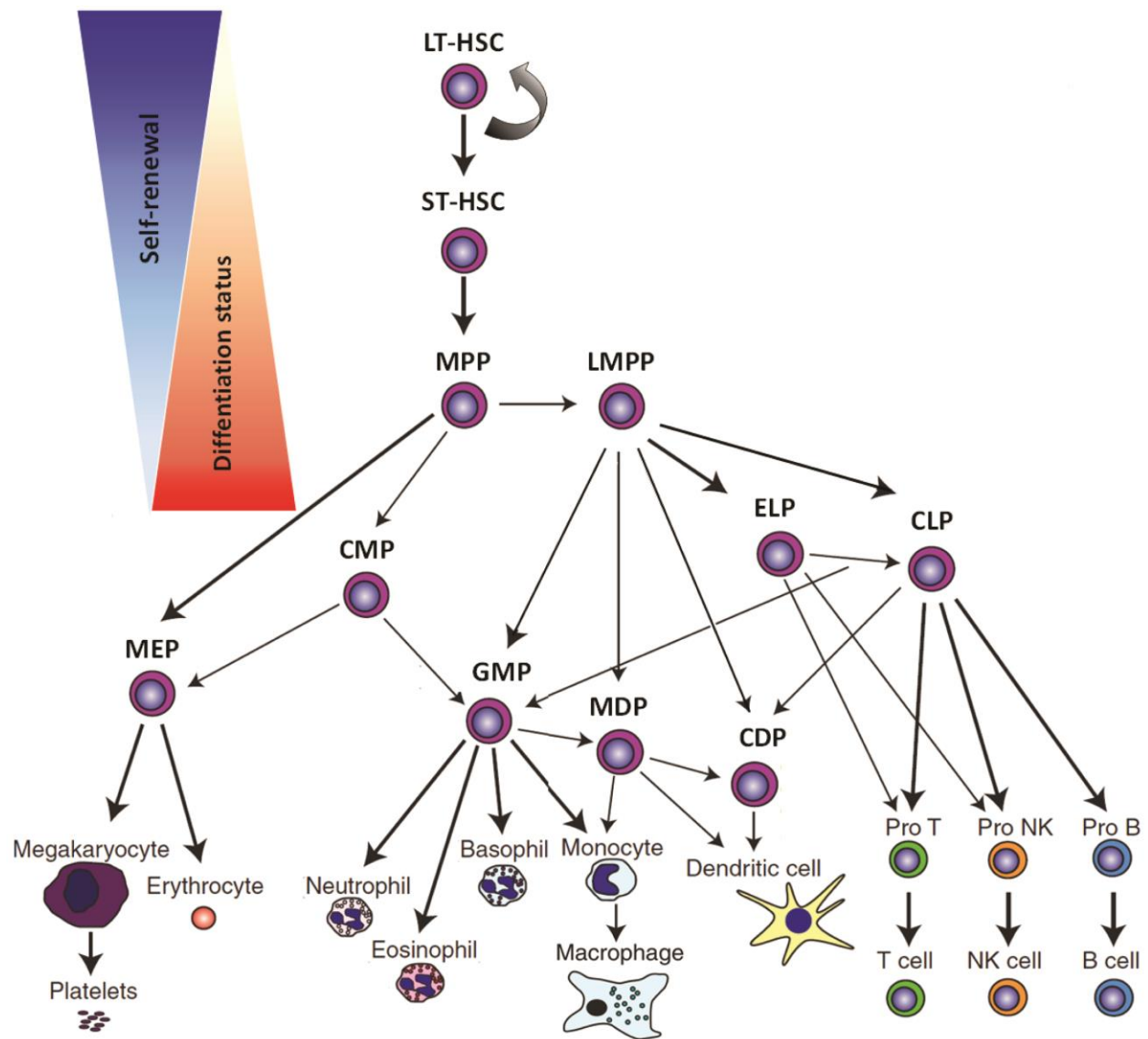


Figure 6: Simplified representation of the Hematopoietic differentiation hierarchy

Long-term self-renewing HSCs differentiate into all blood cell lineages through distinct hematopoietic stem and progenitors cell stages. Adapted from [5]

e) Hematopoietic stem cell niche

By definition, the hematopoietic stem cell niche is a highly specialized microenvironment that allows HSCs maintenance and functions [8]. Such environment implies the support of several cell types, locally released factors, and long-ranged factors. Markedly, since a niche is a highly specialized interface of a cellular function with its environment, it is now well-established that each HSPC has its own niche within the bone marrow [149].

Historically, several studies pointed out the role of osteoblasts in regulating HSC functions [150, 151]. However, an extensive work performed hereafter excluded any direct role of osteoblast and progenitors in regulating HSC [148, 152-154]. Accordingly, our comprehension of the HSC niche is sparse and ongoing.

As mentioned above, HSCs are best characterized by flow cytometry, using various markers. Therefore, identifying with confidence which cells neighbours HSC within the niche remained a real challenge. However, few elegant, yet debated immunohistochemical studies identified HSCs as a CD150⁺/CD48⁻/CD41⁻ population adjacent to sinusoidal blood vessels (Figure 7) [148, 153, 155]. More precisely, HSCs were mainly found in bone diaphysis' vasculature, almost excluding HSCs from bone metaphysis (extremity of the bone where osteoblasts are found) [8, 156].

As previously described, HSC specifically expresses a tyrosine kinase receptor: c-Kit. The c-Kit/SCF (**S**tem **C**ell **F**actor) interaction represents the most decisive axis for the HSC retention within the bone marrow niche. Interestingly, SCF is expressed both as a membrane-bound protein and a soluble released factor. Whereas no data specifically uncover the role in the bone marrow of the soluble form, mice lacking the membrane-bound SCF exhibited an impaired HSC retention [157-159]. Such observation highlights the importance of a direct interaction between c-Kit⁺ HSCs and the CAR cells expressing the membrane-bound SCF.

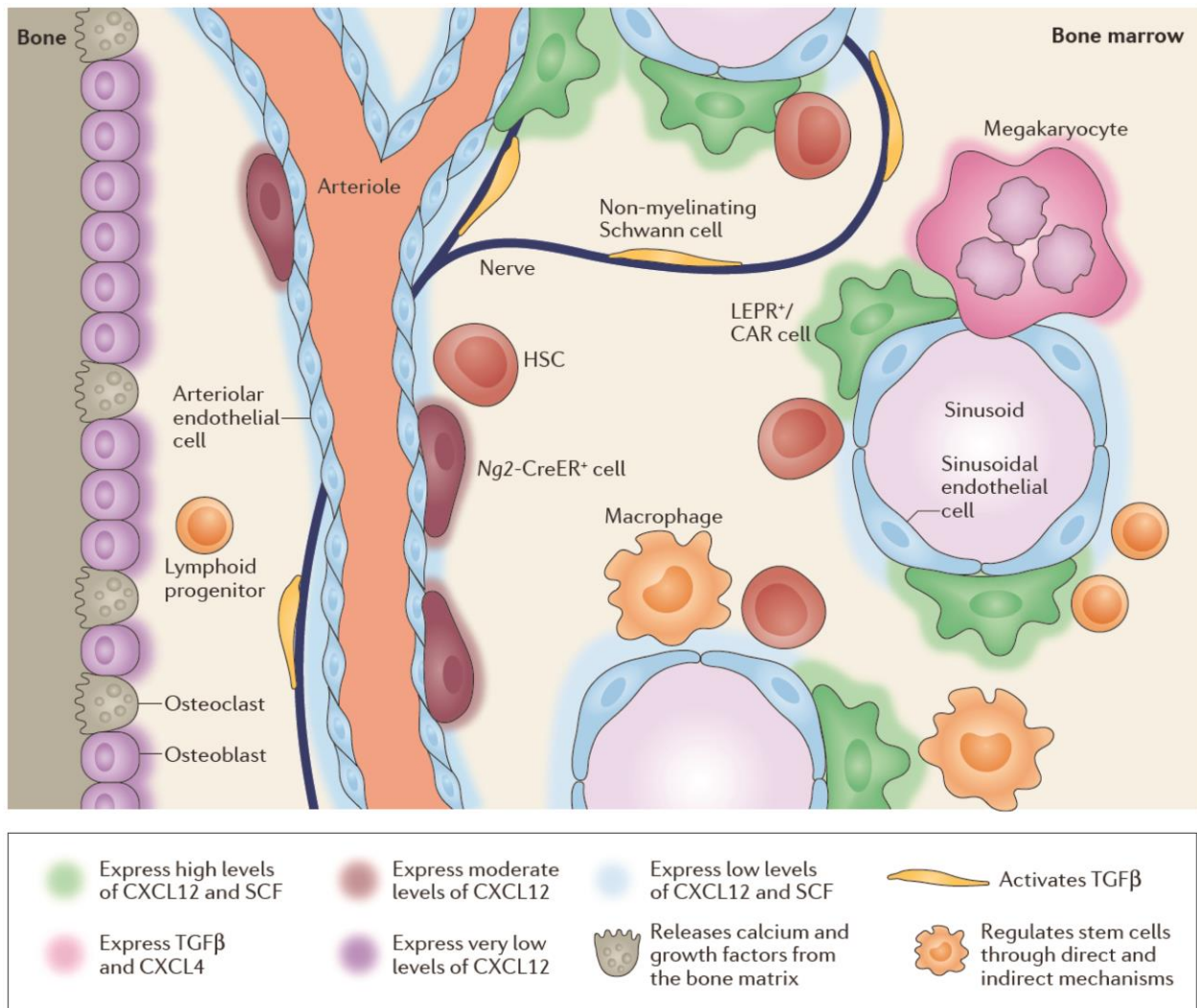


Figure 7: A schematic view of the HSC niche in the bone marrow

Most haematopoietic stem cells (HSCs) localize adjacent to sinusoids where they are in close contact with endothelial and CXCL12-abundant reticular (CAR) cells. Only 10% of HSCs localize near to small-diameter arterioles. Schwann cells associated with nerve fibers also regulate HSC maintenance through daily oscillation of CXCL12. Osteoblasts do not directly regulate HSC maintenance through any known mechanism, but they probably indirectly regulate HSC maintenance through crosstalk with other cell. Adapted from [8]

CAR cells are mesenchymal stromal cells directly surrounding endothelial cells. Apart from their SCF expression, CAR cells were found to highly express CXCL12 (CAR cells stands for **C**XCL12 **A**bundant **R**eticular cell). Soon after, the substantial contribution of the CXCL12/CXCR4 axis in HSC mobilization was discovered [160, 161]. Surprisingly, CXCL12 release by CAR cells is controlled by the sympathetic nervous system, which confers circadian oscillation of CXCL12 level throughout the day [162]. Coherently, physiological HSC mobilization from the bone marrow to blood circulation follows the CXCL12 oscillations [162].

Thrombopoietin is a hormone highly produced by liver sinusoidal endothelial cells, to a lesser extent in the kidney and physiologically not expressed within the bone marrow. Thrombopoietin is principally known for activating megakaryocytes and boosting their production of thrombocytes. Nevertheless, both thrombopoietin and its tyrosine kinase receptor were shown to play a role in HSC retention within the bone marrow [163, 164].

These few axes do not permit a tolerable comprehension of the HSC niche complexity. Therefore, outstanding questions remained to be sought. For instance, the HSC niche might be dynamic and involves additional factors during regeneration following severe haemorrhage, or irradiation. Besides, other factors than receptors/ligands interactions may be relevant for an appropriate niche. To date, it is acknowledged that HSCs are localized within a hypoxic environment [165, 166], although it is not clear whether hypoxia is required for HSC, or the result of high oxygen consumption by surrounding cells engaged in hematopoietic proliferation and differentiation. Finally, preliminary observations raised the concern of a metabolic aspect of the HSC niche while unearthing the HSC sensitivity to valine depletion in the environment [167, 168].

IV. Aim of the study

G-protein coupled receptors (GPCRs) are commonly used as drug targets. However, more than one hundred of the non-olfactory GPCRs remain poorly understood, because their endogenous ligand is unknown, which makes these receptors so-called “orphan receptors”. The field of GPCRs therefore remains an active area of research intending to discover novel drug targets. The aim of this project was to gain insight into the function of the orphan receptor GPR182, because of its interestingly high and specific expression in microvascular endothelial cells. To do so, I planned to identify what could be the endogenous ligand and the signaling of the receptor. A parallel goal was to generate a genetic expression reporter for GPR182 as well as a constitutive and conditional knock-out to uncover the physiological and pathophysiological functions of GPR182.

V. Materials

Antibody

Supplier

7-AAD - Dil. 1/10	BD Biosciences Horizon
A488 Donkey anti -rat - Dil. 1/500	Life Technologies
A488 Donkey anti-rabbit - Dil. 1/500	Life Technologies
A594 Donkey anti-rabbit - Dil. 1/500	Life Technologies
A647 Donkey anti-rabbit - Dil. 1/500	Life Technologies
A488 Donkey anti-rat - Dil. 1/500	Life Technologies
A594 Donkey anti-rat - Dil. 1/500	Life Technologies
A647 Goat anti-rat - Dil. 1/500	Life Technologies
α -SM actin eFluor660 - Ms - Clone 1A4 - Dil. 1/200	eBioscience™ Antibodies
B220 biotin - Rat - Clone RA3-6B2	eBioscience™ Antibodies
CD3 ϵ biotin – Hamster - Clone 145-2C11	eBioscience™ Antibodies
CD3 ϵ PE – Hamster - Clone 145-2C11	eBioscience™ Antibodies
CD4 APC – Rat – Clone RM4-5	eBioscience™ Antibodies
CD8 PECy7 – Rat – Clone 53-6.7	eBioscience™ Antibodies
CD11b /Mac1biotin - Rat - Clone M1/70	eBioscience™ Antibodies
CD19 biotin – Rat - Clone eBio1D3 (1D3)	eBioscience™ Antibodies
CD19 BV510 – Rat - Clone eBio1D3 (1D3)	eBioscience™ Antibodies
CD31 AF647 - Rat - Clone MEC13.3 - Dil. 1/100	Biologend
CD31 \emptyset - Rat - Clone MEC13.3 - Dil. 1/100	BD Biosciences Horizon
CD34 eF660 - Rat - Clone RAM34	eBioscience™ Antibodies
CD45 eF450 – Rat – Clone 30-F11	eBioscience™ Antibodies
CD48 APC-Cy7 - Hamster - Clone HM48-1	Biologend
CD150 PE-Cy7 - Rat - Clone TC15-12F12.2	Biologend
c-Kit BV421- Rat - Clone 2B8	Biologend
CXCL12 \emptyset - Rabbit - Polyclonal (PLA assay)	Abcam
DAPI - Dil. 1/1000	Life Technologies
Endomucin \emptyset - Rat - Clone V.7C7 - Dil.1/100	Santa Cruz Biotechnology
ERG \emptyset - Rabbit - Clone EPR3864 - Dil.1/100	Abcam
Fixable viability dye eF506	eBioscience™ Antibodies

Antibody	Supplier
FLAG® M2 - Ms - Clone M2 - Dil. 1/1000 IF	Sigma-Aldrich
FLAG® M2 - Ms - Clone M2 - Dil. 1/500 Flow cyt.	Sigma-Aldrich
Gr1 biotin - Rat - clone RB6-8C5	eBioscience™ Antibodies
HEV AF488 - Rat - Clone MECA-79 - Dil.1/100	eBioscience™ Antibodies
Lyve-1 Ø - Rabbit - Poly clonal - Dil. 5 µg/mL	ReliaTech
Prox-1 Ø - Goat - Poly clonal - Dil. 1/100	R&D System
Sca-1 PerCp-Cy5.5 - Rat - Clone D7	eBioscience™ Antibodies
Streptavidin BV711	BD Biosciences Horizon
Ter119 biotin - Rat - Clone TER-119	eBioscience™ Antibodies
Ter119 FITC - Rat - Clone TER-119	eBioscience™ Antibodies

Cell line	Supplier
B16F10	ATCC
B16F10 GFP-Luc	homemade
HTLA	gift from Dr. Gilad Barnea
HEK 293T cells	ATCC

Chemicals & Reagents	Supplier
Ammonium Chloride Solution (NH ₄ Cl)	StemCell Technologies
Blasticidin	Thermo Fischer Scientific
BrightGlo Reagent TM	PROMEGA
Bovin Serum Albumin (BSA)	SERVA Electrophoresis
Calcium chloride dihydrtate (CaCl ₂ - 2 H ₂ O)	ROTH
Coelenterazine H	Thermo Fischer Scientific
Collagenase II	Worthington
Dimethyl sulfoxide DMSO	SERVA Electrophoresis
Dithiotreithol (DTT)	New England Biolabs
DNase I	New England Biolabs
dNTPs	New England Biolabs

Chemicals & Reagents	Supplier
Dulbecco's Modified Eagle Medium (DMEM)	Thermo Fischer Scientific
Dulbecco's Phosphate Buffer saline (PBS)	Thermo Fischer Scientific
Ethanol	ROTH
Etylenediaminetetraacetic acid (EDTA)	ROTH
Fetal bovine serum	Gibco
Fetal bovine serum	StemCell Technologies
Fluoromount W	SERVA Electrophoresis
Glucose	ROTH
Glycerol	ROTH
Heparin	Merck Millipore
HEPES free acid	Sigma-Aldrich
Horse Serum New Zealand origin	Gibco
Iscove's modified Dulbecco's medium (IMDM)	StemCell Technologies
Iscoves MDM + 2% FBS	StemCell Technologies
Iscoves MDM with 25 mM Hepes	StemCell Technologies
L-Glutamine	Gibco
Lipofectamine 2000	Thermo Fischer Scientific
Lipofectamine RNAiMAX	Invitrogen
Magnesium chloride hexahydrate (MgCl ₂ ·6 H ₂ O)	ROTH
Methylcellulose-based medium MethoCult M3434	StemCell Technologies
Human CXCL10-AF647	Almac
Human CXCL12-AF647	Almac
Hygromycin B	Gibco
Methylcellulose-Based Media	StemCell Technologies
Miglyol 812	Local Pharmacy
Opti-MEM	Thermo Fischer Scientific
Paraformaldehyde (PFA)	ROTH
Penicilin/Streptomycin	Gibco
Pertex mounting medium	VWR
Phenol Red solution	Sigma-Aldrich
Photocript II Reverse Transcriptase	New England Biolabs
Proteinase K	ROTH
Potassium chloride (KCL)	ROTH
Recombinant human/murine Chemokines	PeproTech
Red Blood cell lysis buffer	Thermo Fischer Scientific
OCT cryo-tissue embedding compound	Sakura FineTechnical
Sucrose	Sigma-Aldrich
Sodium chloride (NaCl)	Roth
Sodium Pyruvate	Gibco

Chemicals & Reagents**Supplier**

T4 DNA ligase	New England Biolabs
Triton X-100	Merck Millipore
Trypsin-EDTA	Gibco
XenoLight Luciferin K ⁺ Salt Bioluminescent Substrate	PerkinElmer

Consumables**Supplier**

BD Pharm lyse™ buffer	BD Biosciences Horizon
Cell Strainer 40 µm	Corning
Cell Strainer 70 µm	Corning
Cell Strainer 100 µm	Corning
EDTA-coated microtubes	Thermo Fischer Scientific
Fixation/Permeabilization concentrate	BD Biosciences Horizon
Histopaque	Sigma-Aldrich
SmartDish 6-well plates	StemCell Technologies
SuperFrostUltra slides	Thermo Fischer Scientific
Syringe	B. Braun

Drugs**Supplier**

Cayman Bioactive Lipid I Screening Library	Cayman
Ketamine	Sigma-Aldrich
Tamoxifen	Sigma-Aldrich
Xylazine	Bayer

Instruments & Equipment**Supplier**

Thermo cycler	Analytik Jena
NanoDrop ND1000 Spectrophotometer	Thermo Fischer Scientific
Lightcycler 480 qPCR cycler	Roche
Cryotome	Leica
Microtome	Leica
Epifluorescence Zeiss Axio Observer microscope	Carl Zeiss
Inverted confocal microscope SP8	Leica
IVIS Lumina S5 Imaging System	PerkinElmer
VacuFuge Plus Vacuum Concentrator	Eppendorf
Peristaltic pump	Eckert & Ziegler
Magpix System	Merck Millipore
Flexstation 3 Plate reader	Molecular Devices
FACS Canto II Flow cytometer	BD Biosciences
FACS Forterssa Flow cytometer	BD Biosciences

Kit**Supplier**

Bright-Glo™ Luciferase Assay System	PROMEGA
Customed human Luminex® Performance Assay	R&D System
DNase-Free DNase Set	Qiagen
LightCycler 480 Probe Master	Roche
Mouse Cytokine/Chemokine Magnetic Bead Panel	Merck Millipore
Nano-Glo® Live Cell Assay System	PROMEGA
Photocript II cDNA synthesis Kit	New England Biolabs
Qiagen Plasmid Maxi Kit	Qiagen
Red/ET kit	Gene Bridges
RNA Microprep Kit	Zymo Research
RNeasy micro kit	Qiagen

Mouse Line	Supplier
ACTB-Flpe - Tg(ACTFLPe)9205Dym	The Jackson Laboratory
BAC Gpr182-mCherry	homemade
Cdh5CreERT2 - Tg(Cdh5-cre/ERT2)1Rha	Gift from Pr. Dr. R. Adams
EIIA-Cre - Tg(EIIa-cre)C5379Lmgd	The Jackson Laboratory
Gpr182floxed	homemade
Gpr182 KO-Lacz - Gpr182tm2b(KOMP)Wtsi	Bred in house
<i>Gpr182 Targeted - Gpr182tm2a(KOMP)Wtsi</i>	EUCOMM

Plasmids & Vectors	Supplier
Aequorin-GFP (pG5A)	10.1073/pnas.97.13.7260
BAC mouse RP23-119B1 containing Gpr182 locus	bacpacresources.org
BAC Gpr182-mCherry	homemade
Empty-Tango	homemade
FLP 705 plasmid to remove FRT-AMP-FRT cassette	Gene Bridges
Galphai-LgBit	DOI:10.1016/j.cell.2019.04.044
Gβ, GySmbit	DOI: 10.1016/j.cell.2019.04.044
Human CXCR3 (pcDNA3.1+)	cDNA Resource Center
Human CXCR4 (pcDNA3.1+)	cDNA Resource Center
Human CXCR5 (pcDNA3.1+)	cDNA Resource Center
Human ACKR3 (pcDNA3.1+)	cDNA Resource Center
HumanGPR182-FLAG (pcDNA3.1)	Homemade
HumanGPR182 (pcDNA3.1)	Homemade
MouseGPR182-FLAG (pcDNA3.1)	Homemade
MouseGPR182 (pcDNA3.1)	Homemade
PRESTO-TANGO GPCR Kit	doi: 10.1038/nsmb.3014

Medium	Composition	Recipe
DMEM Culture medium:	DMEM	450 mL
	FBS	50 mL
	Penicillin/Streptomycin	5 mL
	L-Glutamine	5 mL
	Sodium Pyruvate	5 mL

Buffers	Composition	Recipe
Phosphate-Buffered Saline:	KCl	2,7 mM
	Na ₂ HPO ₄	10 mM
	KH ₂ PO ₄	2 mM

Blocking Buffer:	PBS	47,5 mL
	Horse Serum	2,5 mL
	Triton X-100	100 µL

Ligand binding buffer:	H ₂ O mq	1 L
	NaCl	125 mM
	KCl	5,9 mM
	MgCl ₂ . 6H ₂ O	1 mM
	HEPES free acid	25 mM
	CaCl ₂ . 2H ₂ O	2,56 mM
	Bovine Serum Albumin	0,1 %
	Adjust to pH 7,4	

Buffers	Composition	Recipe
Calcium assay buffer:	HBSS ^{-/-}	50 mL
	D-Glucose	90 mg
	CaCl ₂ 1M	90 µL
	Add 10 µL Coelenterazine H for 5,5 mL of Buffer	
TANGO buffer:	HBSS ^{-/-}	50 mL
	HEPES	20 mM
	CaCl ₂ 1M	90 µL
	Adjust pH to 7,4	
Add 1 mL Bright Glo reagent for 9 mL Tango buffer		
FACS Buffer:	PBS CaCl ₂ free/MgCl ₂ free	1 L
	Bovine Serum Albumine	0,1 %
	EDTA	2 mM
Buffer A:	PBS	
	HEPES	1M
	KCl	5 %
	Adjust to pH 7,4	
Liver perfusion medium I:	PBS	500 mL
	Buffer A	5 mL
	D-Glucose 1M	2,5 mL
	EDTA 200 mM	0,5 mL
	Phenol red solution	1 mL
	Adjust to pH 7,4	

Buffers	Composition	Recipe
Liver perfusion medium II:	PBS	500 mL
	Buffer A	5 mL
	HEPES 1M	10 mL
	D-Glucose 1M	2,5 mL
	CaCl ₂ 500 mM	1 mL
	Phenol red solution	1 mL
	Adjust to pH 7,4	
Collagenase solution:	Liver perfusion medium II	25 mL
	Collagenase II	2 mg/mL

VI. Methods

RNA Extraction and Real-Time Polymerase Chain Reaction

We performed RNA isolation and reverse transcription according to the manufacturer's instructions. Transcript levels of genes were analyzed by real-time polymerase chain reaction using the LightCycler 480 Probe Master System (Roche). Gene expression was normalized to water and calculated using the $\Delta\Delta C_t$ method. The following primers used for this analysis were designed with the online tool provided by Roche:

Probe #45

F: AAGTTGGCCCTCATGTCAGT

R: ATTGTCCGGTTCCAAGGTG

Histology and microscopy

For the expression analysis of mCherry reporter mice, animals were sacrificed by CO₂ and perfused with 20 ml PBS through the left ventricle, followed by 4% paraformaldehyde in PBS (PFA).

Following the perfusion, tissues were fixed in PFA 4% at 4°C for one hour (lymph nodes, Peyer's Patches, aorta) or overnight. After fixation, organs were washed three times with PBS and transferred to sucrose 30% (w/v) at 4°C for 24 h. Tissues were then embedded in OCT and stored at -80°C until further processing. OCT blocks were sectioned using a cryostat, and 12 μ m sections were dried on SuperFrost PLUS microscope slides.

For immunofluorescence staining, cryosections were thawed at room temperature for 30 min, washed three times with PBS and blocked/permeabilized with antibody diluent (PBS containing 5% horse serum and 0.1% Triton X-100) for one hour at room temperature. Then cryosections were incubated with primary antibodies overnight at 4°C. After three washes with PBS, sections were incubated for one hour at room temperature with AlexaFluor-488, -594 or -647 conjugated secondary antibodies in antibody diluent containing DAPI. After three washes with PBS, sections were mounted in Fluoromount and analyzed by confocal microscopy using Leica TCS SP8 confocal microscope.

Cell lines

HEK293T cells were obtained from ATCC (American Type Culture Collection). HTLA cell line (a HEK293 cell line stably expressing a tTA-dependent luciferase reporter and a β -arrestin2-TEV fusion gene) was a gift from Dr. Gilad Barnea (Brown University, Providence, USA). The two cell lines were maintained in Dulbecco's modified Eagle's medium (DMEM) supplemented with 10% FBS, 2 mM L-glutamine, 5 units/ml penicillin/streptomycin.

Beta-arrestin assay

The TANGO assay was specifically designed to monitor ligand-induced interaction between GPCRs and β -arrestin. The Tango plasmid library, a gift from Bryan Roth, was obtained from Addgene Kit #1000000068. HTLA cells were transfected with TANGO-receptors in 96-well plates. Afterwards, cells were incubated for 4 hours in a serum-free medium and stimulated overnight with the mentioned ligands. The following day, the supernatant was replaced by 100 μ L assay buffer containing 10% Bright-Glo reagent (Promega). After an incubation of 20 min at room temperature, luminescence was assessed in a plate reader (Flexstation-3, Molecular Devices) and expressed as fold change compared to non-stimulated transfected cells.

To compare the basal activity of TANGO-CXCR3, -4, -5, TANGO-ACKR3, and TANGO-GPR182; transfected cells (in quadruplicates) were fixed with 4% PFA for 10 min at room temperature. Then, cells were washed three times with PBS, blocked and permeabilized with PBS containing 5% horse serum and 0.1% Triton X100 for 5 min at room temperature. To detect total receptor expression, the cells were then incubated with a mouse anti-FLAG M2 antibody for one hour at room temperature. After three washes with PBS, the cells were incubated with Alexa488 coupled anti-mouse secondary antibodies and DAPI for 30 min at room temperature. Afterwards, imaging was performed using an epifluorescence microscope Zeiss Axio Observer and the Axio Vision software. The mean fluorescence intensity of the FLAG staining was quantified using ImageJ and corrected by subtracting the background fluorescence from untransfected cells.

Plasma preparation and fractioning

Blood sampling was performed on animals sacrificed in a CO₂ chamber, and blood was collected intracardiacally. A heparin-coated syringe and an Eppendorf tube were used for the preparation of plasma, while a regular syringe and tube were used for serum preparation. The blood was then; either immediately processed at low temperature (4°C) to prepare plasma or kept 2 hours at room temperature for serum preparation. Following a centrifugation step at 1.500 g for 10 min, the upper phase containing either plasma or serum was transferred to an Amicon® Ultra-15 size-exclusion column (Merck Millipore) and centrifuged at 4.500 g for 10 min. Successive centrifugation using distinct size-exclusion featured columns were performed until obtaining the desired elution. Finally, the elution was collected and aliquoted in several Eppendorf tubes and placed in a rotating evaporator for 30 min (CONC/VACUF, Eppendorf). Finally, the various aliquoted concentrated plasma/serum were pooled together and stored at -20°C until their use to stimulate cells-expressing receptor.

Isolation and culture of isolated hepatic cells

The isolation and culture method used was similar to previously established methods [Ref, Ref]. Shortly, animals were anesthetized with a mixture of ketamine and xylazine. Once fully anesthetized, animals limbs were taped to the heating pad, the fur was sprayed with ethanol and the abdominal cavity was opened. Subsequently, a catheter linked to a peristaltic pump was placed within the hepatic portal vein. Once the disposal settled, we sectioned the inferior vena cava and started perfusing the liver with 15 mL of Perfusion medium I. Following, we perfused the liver with 10mL of a collagenase solution. Then, the liver was resected and placed in a petri dish filled with perfusion medium II. The gallbladder was removed, and shaking the liver using two forceps allowed the isolation of liver cells. Liver cells were further isolated through successively tinnier tea-strained filter. Liver cells were centrifugated at 50 g for two minutes. The pellet containing living hepatocytes was washed three times with DMEM medium, counted and seeded on 12-well plate. The supernatant containing non-parenchymal cells (NPC) was further centrifugated at 300 g for 15 minutes. The pellet containing

NPCs was gently disposed on top of a 50%/25% Percoll gradient and centrifuged at 900 g for 25 minutes without brake. NPCs were pipetted out of the 50%-25% gradient interface and washed three times with PBS. Finally, NPCs were resuspended in DMEM medium, counted and seeded in 12-well plates. After optimization, seeding conditions were performed on 12-well plate coated with Collagen I and with a cellular density of 300.000 hepatocytes and 1 million NPCs. After one day in culture, the culture medium was replaced with 500µL of fresh medium for half a day. Finally, the medium culture was collected and processed as described in the plasma fractioning preparation.

Stably TANGO-GPR182 expressing cell line establishment

A vial of HTLA cells frozen at a low passage was thawed and placed in culture for two regular passages. When reaching a confluence of 85%, HTLA cells were transiently transfected with the TANGO-GPR182 vectors using Lipofectamine 2000 transfection reagent according to the manufacturer's instructions. Receptor-expressing cells were maintained in DMEM and selected with 15 µg/ml blasticidin, 100 µg/ml hygromycin B, and 100 IU Penicillin and 100 µg/ml Streptomycin for two weeks. Cells resisting to the blasticidine were presumed to stably express TANGO-GPR182 Confirmation of receptor expression was performed in different clones through immune blot using an anti-FLAG antibody.

Blood analysis

Blood was collected similarly than previously described, although we used EDTA-coated tubes. Blood samples and blood smear were sent to the IDEXX Laboratories for a standard and complete analysis of blood parameters.

In House flow cytometry analysis of hematopoietic stem cells

Both femurs were collected from each mouse for single mouse analysis. Bones were cleaned from all remaining muscular and tendinous tissue before flushing out of the bones with a syringe and cold PBS the medullary bone marrow cells.

Bone marrow cells were first stained with biotinylated antibodies against mature blood cells (CD3, CD11b, CD19, CD41, B220, Gr-1 and Ter119) for 15 min. After three wash with PBS, cells were stained for one hour on ice and protected from light with the following stem cell markers (Streptavidin-PE-Cy7; Sca1-APC-Cy7; cKit-PE; CD48-Pacific Blue; CD150-PerCP-Cy5.5; CD34-FITC; Propidium iodide). After washing them three times with PBS to remove unbound antibodies, cells were resuspended in FACS buffer and analyzed on a FACS Fortessa (Becton Dickinson) with FACS Diva 7 software (Becton Dickinson).

Lineage-negative cells were gated out from the viable mononuclear cells. From those cells, the Sca1, c-Kit double-positive hematopoietic stem progenitor cells (LSK; lineage-, Sca1+, c-Kit+) were distinguished and exhibited long-term repopulating hematopoietic stem cells (LT-HSCs as; LSK, CD150+, CD48-, CD34^{low}) and the multipotent progenitors (MPPs as; LSK, CD150-, CD48+). The gating strategy is illustrated in Figure 16A.

Determination of chemokine levels

Blood sampling was performed from the facial vein bleeding. The blood was collected into EDTA coated tubes and immediately placed on ice. Plasma was then prepared as previously described and frozen at -80°C until analysis. Plasma cytokines and chemokines levels were determined by Milliplex map magnetic bead-based multi-analytes panel mouse Cytokine/Chemokine 25 Plex or a custom-made designed Mouse Magnetic Luminex Assay plex panel for CXCL10, CXCL12 α and CXCL13. Samples were analyzed using the MAGPIX system and the Milliplex Analyst 5.1 software (Merck Millipore).

Ligand binding assay

HEK293T cells were plated in 6-well plates with a density of 500.000 cells per well. Those cells were immediately transfected with eukaryotic expression plasmids carrying the GPR182 and GFP cDNA. Two days post-transfection, a single cell suspension was prepared using a brief trypsin/EDTA treatment. The single cell suspension was washed once with medium to remove the trypsin. Soon after, cells were incubated for one hour at room temperature allowing the receptor to be re-exposed to the plasma membrane. Cells were rinsed with binding buffer (HBSS pH 7.4) and dispensed in a V-bottom 96-well plate. Cells were resuspended and incubated in 90 μ L of binding buffer at room temperature for one hour with variable concentration of fluorescently labelled chemokine. Afterwards, cells were washed thrice with binding buffer, fixed for 10 minutes with PFA 1% and washed thrice with PBS. Later, cells were resuspended into 100 μ l PBS and transferred to a 96-well plate with black-wall and transparent glass bottom. Cells were then allowed to settle down for one hour and were analyzed with an epifluorescence Zeiss Axio Observer microscope using the AxioVision software. Pictures were analyzed with Fiji software, and CXCL10-AF647 or CXCL12-AF647 fluorescent signal was quantified in GFP positive cells. Competition binding assay was performed by incubating increasing concentration of non-labelled chemokine shortly before adding the fluorescently labelled chemokine at the indicated concentration. The screening of the chemokine family was performed with 40nM of fluorescently labeled CXCL10 and 120 nM of non-labelled chemokines. For quantification of binding affinity, curve fitting and K_d were determined using one site-specific binding equation in GraphPad Prism 6.07 after subtracting the total binding fluorescence value by the non-specific fluorescence binding in cells transfected with the control vector. In competitive experiments, curve fitting and K_i was determined using one site fit K_i equation in GraphPad Prism 6.07 by providing the concentration (40 nM) and K_d values of fluorescently labelled Alexa647 chemokine ("hot" ligand).

Calcium mobilization assay

HEK293 T cells were seeded in 96-well plates with white walls and transparent bottom with a density of 20.000 cells per well. These cells were transfected using Lipofectamine 2000 with the corresponding receptor plasmids as well as a cDNA coding for GFP (basically a transfection control), a promiscuous G-protein α -subunit and aequorin: a calcium-sensitive bioluminescent fusion protein. Two days post-transfection, cells were loaded with HBSS containing 5 μ M Coelenterazine H for 2 hours at 37°C. Measurements were performed using a luminometric plate reader (Flexstation 3, Molecular Devices). The area under each calcium transient was determined using the SoftMaxPro software and expressed as area under the curve (AUC).

G α i activation assay

To determine the ligand-induced G α i signaling, we used the recently developed NanoBiT assay. HEK293 cells were seeded onto a 96-well plate and transfected with Galphai-LgBit, Gbeta, GgammaSmbit and the receptor using Lipofectamine 2000. After 24 hours, the supernatant was replaced by 50 μ l of Coelenterazine H (10 μ M) and then incubated at 37°C for one hour. Then, the plate was placed in a plate reader (Flexstation 3), and the luciferase activity was monitored in real-time before and after stimulation with the indicated chemokine for 5 min. Data were expressed relative to baseline (before chemokine stimulation). Lastly, data were processed in GraphPad Prism 6.07 and expressed as area under the curve.

GPR182 and CXCL10 internalization study

Adherent HEK293T cells were transfected using Lipofectamine 2000 either with the N-terminally FLAG-tagged hGPR182 or with the control pcDNA3 vector. The next day, trypsin/EDTA treatment allowed single cell suspensions and cells were incubated for one hour at room temperature in complete culture medium. After three washes with ice cold binding medium (containing serum-free DMEM, 0.5% BSA, 10 mM HEPES), cells were incubated with 100 nM of fluorescently labelled chemokine CXCL10-AF647 for one

hour at 4°C with gentle rocking allowing chemokines' binding to the cell surface. After three washes with ice cold binding medium, cells were resuspended and incubated at 4°C or 37 °C for 30 min with gentle rocking. After three additional washes with ice cold binding medium, cells were fixed in 1% PFA for 10 min at room temperature, washed and stained with Hoechst for 15 min. Then, cells were settled down in Ibidi 8-well chamber slides and analyzed using an inverted Leica SP8 confocal microscope.

For analyzing GPR182 internalization, cells were seeded and transfected as previously described. Then, cells were incubated with anti-FLAG-M2 antibody in binding medium for one hour at 4°C with gentle rocking. After three washes, cells were incubated with or without 100 nM of recombinant hCXCL10 as indicated and placed at 37 °C for 15, 30 or 60 min with gentle rocking, or maintained at 4°C to determine the basal surface expression. After three washes, cells were incubated with AlexaFluor 488-conjugated donkey anti-mouse IgG in ice cold binding buffer containing the cell viability dye 7AAD for 30 min at 4°C with gentle rocking. Finally, cells were washed three times with ice cold PBS before analysis by flow cytometry using a FacsCanto (BD Biosciences). The total amount of cell surface receptor was set by median fluorescence intensity and expressed as a percent of GPR182 basal cell-surface expression from cells maintained at 4°C without chemokine treatment.

Flow cytometry analysis for lymphoid organs analysis

Immediately after CO₂-induced sacrifice, spleens were collected into FACS buffer (PBS + 0.1% BSA + 2 mM EDTA). Spleens were minced with surgical scissors and smashed onto a 40 µm tea-strainer. Single-cell suspension was washed twice with FACS buffer and resuspended to 100 million cells per mL. Twenty million cells were blocked with CD16/CD32 antibody for 10 minutes at room temperature. Then, cells were washed thrice and incubated for 30 minutes at 4°C with a mix of antibodies (7-AAD, Ter119-FITC, CD45-Efluor450, CD3-PE, CD4-APC, CD8-PECy7, CD19-BV510). Finally, cells were washed thrice with FACS buffer and analyzed with a CANTO II flow cytometer (Becton Dickinson). Lastly, data were analyzed with the FlowJo software and plotted with GraphPad prism.

Adoptive transfer of CFSE-stained leukocytes

Splenocytes were collected from the spleen of wild-type mice. Following a mincing and smashing procedure of the spleen similar to previously described, the single-cell suspension was washed twice with FACS buffer and resuspended to 100 million cells per mL. Then, cells were stained with CarboxyFluorescein Succinimidyl Ester (CFSE) for 8 min at 37°C in a shaking water bath. Following three additional washes with PBS, recipient mice were injected intravenously in the tail vein with 20 million CFSE positive cells. After 90 min, mice were sacrificed in a CO₂ chamber. Spleen, lymph node and Payer's patches were collected in FACS buffer. Organs were processed for flow cytometry analysis as mentioned above.

Lung tumor growth

B16F10 Luc cells were thawed and maintained in a 100mm culture dish for two passages. When arriving at 85% confluence, cells are briefly treated with trypsin/EDTA to prepare a single cell suspension. Then, cells are counted and resuspended in 3 million cells per mL. Soon after, mice are anesthetized with isoflurane and injected in the tail vein with 300.000 cells. After several days, anesthetized mice were injected subcutaneously with the XeloLight Luciferin reagent according to the manufacturer recommendations. During a ten minutes incubation period allowing the diffusion of the Lucifer reagent into tumor cells and its catalyze into a bioluminescent signal, mice were gently placed and tapped onto the IVIS heating/Isoflurane pad. Following the incubation, the bioluminescent signal was recorded using the IVIS Lumina S5 Imaging System (PerkinElmer) and the signal intensity was analyzed using the Living Image software.

Lineage and Progenitor staining of BM cells

Bone marrow cells were isolated as mentioned above. The bone marrow cells were gently placed on top of Histopaque® and centrifugated on Ficoll gradient at room temperature without brake, 400 g for 30 min. The interphase, enriched in bone marrow mononuclear cells (BMMNC) was collected and washed twice with PBS. For stem and

progenitor analyses, the BMMNCs were stained against mature blood cells with biotinylated antibodies (CD3, CD11b, CD19, CD41, B220, Gr-1 and Ter119) for 15 min before staining progenitors for 30 min (Sca1-PerCPCy5.5 CD48-APCCy7, Streptavidin-BV711, cKit-BV421, CD150-PECy7, CD34-eF660, Fixable Viability Dye eF506). After a PBS wash to remove unbound antibodies, the cells were resuspended in FACS buffer and analyzed on a FACS Fortessa (Becton Dickinson) with the FACS Diva 7 software. Lineage-negative cells were gated out from the viable mononuclear cells. Among the Sca1, c-Kit double positive population (LSK; lineage-, Sca1+, c-Kit+) we sub-gated the long-term quiescent hematopoietic stem cells (LT-HSCs; LSK/CD150+/CD48/CD34^{low}), multipotent progenitors (MPPs; LSK/CD150-/CD34+). The Lin-/Sca1-/c-Kit+ myeloid committed progenitors (LK) were further subgated on megakaryocyte-erythroid-progenitors (MEP; LK/CD150+) and pre-granulocyte-macrophage-progenitors (pre-GMP; LK/CD150-/CD34+).

c-kit staining of spleen cells

As previously described, spleens from each mouse were separately collected, minced and meshed through a 40 µm cell filter. Ten million splenocytes were stained with cKit-BV421 and Fixable Viability Dye eF506 for 30 min. Then, we washed cells once with PBS to remove excessive antibodies and cells were resuspended in FACS buffer for the quantification on a FACS Fortessa (Becton Dickinson) with the FACS Diva 7 software.

Colony-forming unit assay

Mouse blood was collected using a heparin-coated syringe and was placed in an Eppendorf containing heparin. Subsequently, spleens were collected and placed in IMDM medium supplemented with 2% FBS. Spleens were minced and smashed on a 40 µm cell strainer. Splenocytes were washed twice with IMDM medium containing 2% FBS, resuspended in IMDM medium and counted using a Neubauer hemocytometer. Whole blood was treated with nine volumes of ammonium chloride solution. Afterwards, blood cells were washed twice with IMDM medium and counted again. Splenocytes and erythrocyte-depleted blood cells were resuspended into Methocult medium and plated in

Smart 6-well plates. Finally, the quantification of formed colonies was assessed after 12 days of incubation at 37 °C, 5% CO₂ and \geq 95% humidity.

Animal models

All mice were backcrossed onto a *C57BL/6J* background at least 8 to 10 times, and experiments were performed with littermates as controls. Male and female animals (8-12 weeks old) were used unless stated otherwise. Mice were housed under a 12-hour light-dark cycle, pathogen-free conditions and without any restriction to food nor water. Transgenic mice expressing mCherry under the control of the *Gpr182* promoter (*Gpr182-mCherry*) were generated using the bacterial artificial chromosome (BAC) clone RP23-119B1 from mouse chromosome 10. The coding sequence of *Gpr182* on the BAC was replaced by a cassette carrying the mCherry cDNA, a polyadenylation signal and an FRT-flanked ampicillin-resistant gene using the Red/ET recombination kit. Correct insertion of the cassette was verified by restriction digestion and DNA sequencing. Following Flp-mediated excision of the ampicillin-resistant gene and linearization, the recombined BAC was injected into the pronuclei of FVB/N oocytes. The transgenic offspring was genotyped for BAC insertion by PCR. In total, four independent BAC transgenic lines engendered showed a similar mCherry expression pattern. Mice lacking GPR182 were obtained from the Knockout Mouse Project Repository (knock-out first allele *Gpr182tm2a(KOMP)Wtsi*). To generate a conditional allele of *Gpr182*, a cassette flanked by FRT-sites was removed by crossing mice with the Flp-deleter mouse line. After Flp-mediated recombination, mice were crossed with *Cdh5-CreERT2* mice to obtain animals with inducible endothelium-specific deficiency. Maintenance of the animals was in agreement with German animal welfare legislation.

Statistics

Statistical analysis was performed using the GraphPad Prism software v.6.07 from GraphPad Software Inc. (La Jolla, CA, USA). Values are presented as mean \pm SEM; n represents the number of independent experiments or animals. Statistical analysis between two groups was performed with an unpaired two-tailed Student's t-test, or

nonparametric Mann-Whitney U test when appropriate while multiple group comparisons were analyzed with one-way ANOVA followed by Tukey's post-hoc test unless stated otherwise, and comparisons between multiple groups at different time points were performed using two-way ANOVA followed by Bonferroni's post-hoc test. A p-value lower than 0.05 was considered to be statistically significant.

VII. Results

1) Analysis of *Gpr182* expression

a) *Gpr182* mRNA expression

Aiming at studying *Gpr182* expression, we first attempted to reproduce results from a large-scale GPCR expression or transcriptomic analysis [4]. Regard et al. described a very high expression of the receptor in the atrial heart, the lung, the vena cava and the liver (Figure 8A). Using qPCR on cDNAs from C57BL/6J mice organs, we confirmed the highest expression of *Gpr182* in the liver, the heart atrium and the lung. To a lower extent, we observed an expression in kidneys, lymph nodes and brown adipose tissue. However, the vena cava expression was much weaker than published result (Figure 8B).

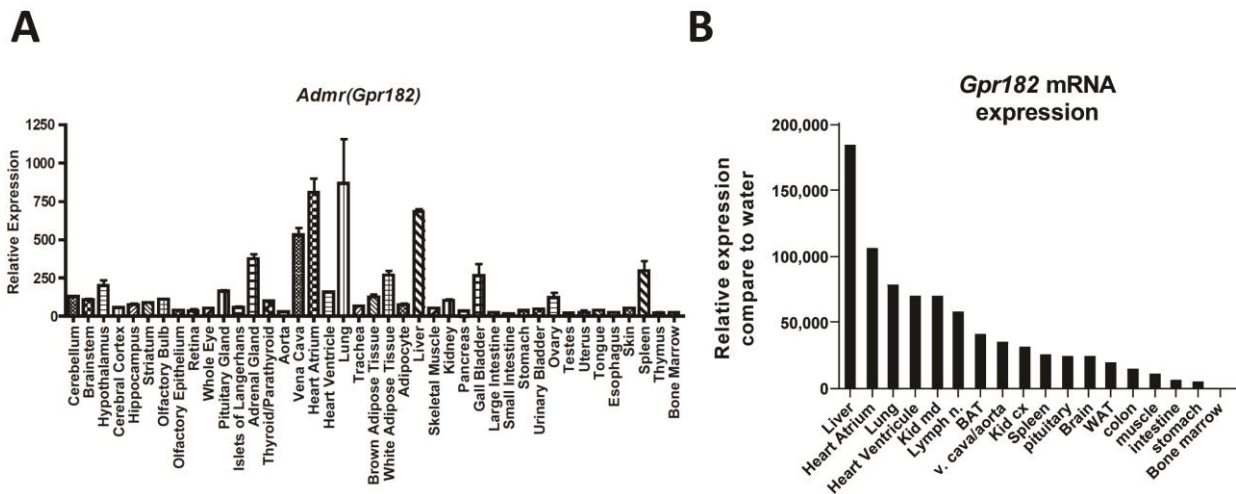


Figure 8: *Gpr182* expression

A large-scale GPCR expression from a transcriptomic analysis published by Regard et al. [4] displays *Gpr182* expression in different tissues (A). Homemade analysis of *Gpr182* mRNA levels using real-time polymerase chain reaction (B).

b) GPR182 expression

RT-PCR on whole organ sample does not allow distinguishing the specific cell type expressing a given transcript. To study the cell-specific expression of *Gpr182*, we generated a bacterial artificial chromosome (BAC)-based transgenic mouse line expressing the monomeric red fluorescent protein mCherry under the control of *Gpr182* promoter (Figure 9A). The injection of the modified BAC into a mouse zygote gave birth to 24 pups. Among them, four animals were mCherry positive and maintained a germline transmission. A preliminary analysis of the four different founders did not reveal any significant differences in the mCherry profile; therefore, we further studied two randomly selected mice lines. Similar to published expression data and our qPCR expression analysis, the *Gpr182*-mCherry signal was observed in most organs such as the liver, lungs, spleen, lymph nodes, Peyer's patches, adrenal gland, bone marrow, kidney, intestine and aorta (Figure 9B-K). Co-staining with different markers confirmed that GPR182 expression was localized in vascular endothelial cells. For instance, using the nuclear endothelial marker, ERG, and the plasma membrane endothelial cell marker, CD31 on lung sections, unveiled a superposition with the mCherry signal (Figure 9C). Besides, the mCherry signal was observed in splenic and hepatic sinusoidal endothelial cells, and to a lower extent, in hepatic arteries and central veins (Figure 9B). In lymph nodes, mCherry signal was detected in sinusoidal endothelial cells and high endothelial venules (Figure 9E). Additionally, GPR182 was found in endomucine-positive cells in the bone marrow, which is a specific marker of sinusoidal endothelial cells in bone marrow (Figure 9H) [156]. Interestingly, bone marrow arteries identified as α SMA+/endomucine-structure were not expressing mCherry (Figure 9H). Briefly, mCherry was also found in endothelial cells of several others tissues such the as heart, Peyer's patches, adrenal gland, renal vasa recta endothelial cells, and even slighter in renal glomerular endothelial cells and lamina propria endothelium of the small intestine (Figure 9). Conversely, to the published literature [51], our mCherry founders did not reveal any expression in intestine epithelial cells (Figure 9J). While Regard et al. reported a strong expression of *Gpr182* in conductive arteries and venous vessels [4], the analysis of our mCherry reporter mice did not show any fluorescent signal in the aorta and inferior vena cava (Figure 9K).

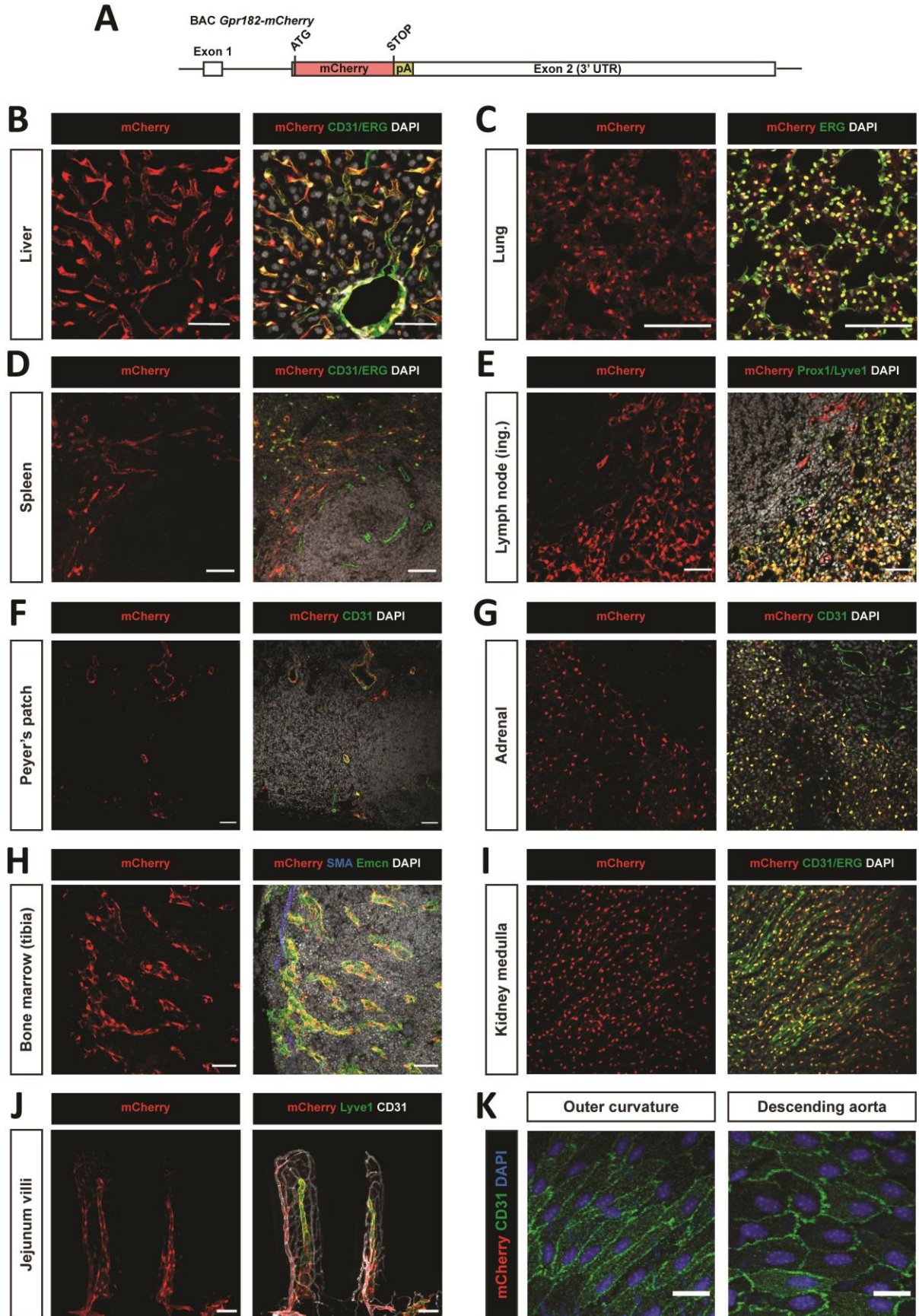


Figure 9: GPR182 is expressed in microvascular endothelial cells.

Schematic view of the BAC-based mouse Gpr182-mCherry reporter transgene which had a total length of 234 kb. UTR: untranslated region (A). Representative immunofluorescence confocal images of cryosections of the indicated organs from Gpr182-mCherry transgenic mice. The mCherry signal corresponds to endogenous mCherry fluorescence. Cryosections were stained with antibodies against vascular or lymphatic endothelial markers (CD31, ERG, Prox1, Endomucin, α -SMA and Lyve1 respectively) (B–K). Shown are results of representative experiments of at least three independently performed experiments (Scale bars, 50 μ m).

2) Deorphanization of GPR182

Another important aspect of studying an orphan GPCR such as GPR182 is deorphanization. Deorphanization consists of identifying endogenous ligand, which physiologically activates the receptor.

For this purpose, we decided to use a recently described system, specifically designed for GPCR deorphanization [3]. This system is based on the fact that β -arrestin protein is involved in GPCR internalization: a key feature of GPCR desensitization (Figure 10).

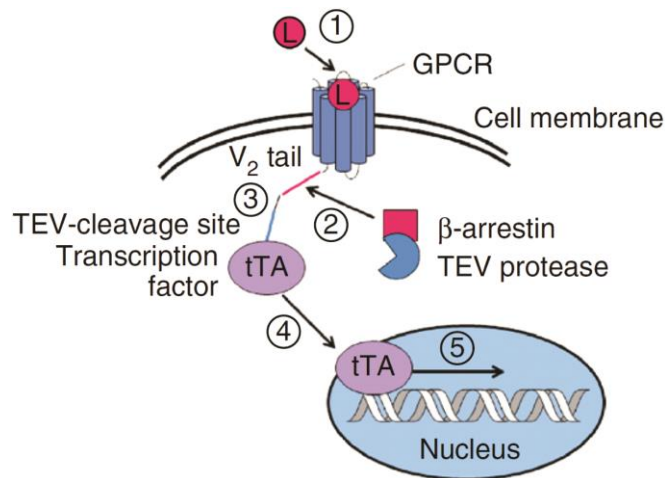


Figure 10: Schema representing the TANGO system

This artificial system involves a cell line stably expressing a fusion protein: β -arrestin/protease. In addition, this system requires the transfection of a GPCR of interest fused to a transcriptional factor (tTA). Upon receptor activation, it naturally results in the recruitment of the fusion β -arrestin/protease, which ultimately induces the cleavage of the link between GPCR/tTA. Following such cleavage, the released tTA transcriptional factor is translocated into the nucleus and induces the luciferase reporter gene expression. Thus, activation of the receptor can be easily monitored by measuring luciferase activity [3]

a) GPR182: a chemokine receptor?

Phylogenetically, the closest paralogue of GPR182 is the atypical chemokine receptor 3 (ACKR3), a chemokine receptor for CXCL11 and CXCL12. Regarding that, chemokines bind several chemokine receptors and reciprocally, we tested whether CXCL11, -12 and few other related chemokines could activate GPR182. As a control, CXCL1 and -10 did not activate ACKR3 (Figure 11A). However, upon CXCL11 and -12 stimulations, we could respectively detect a 10- and 15-fold increase of luciferase bioluminescence (Figure 11A). Unfortunately, GPR182 stimulation with these chemokines did not lead to receptor activation (Figure 11B).

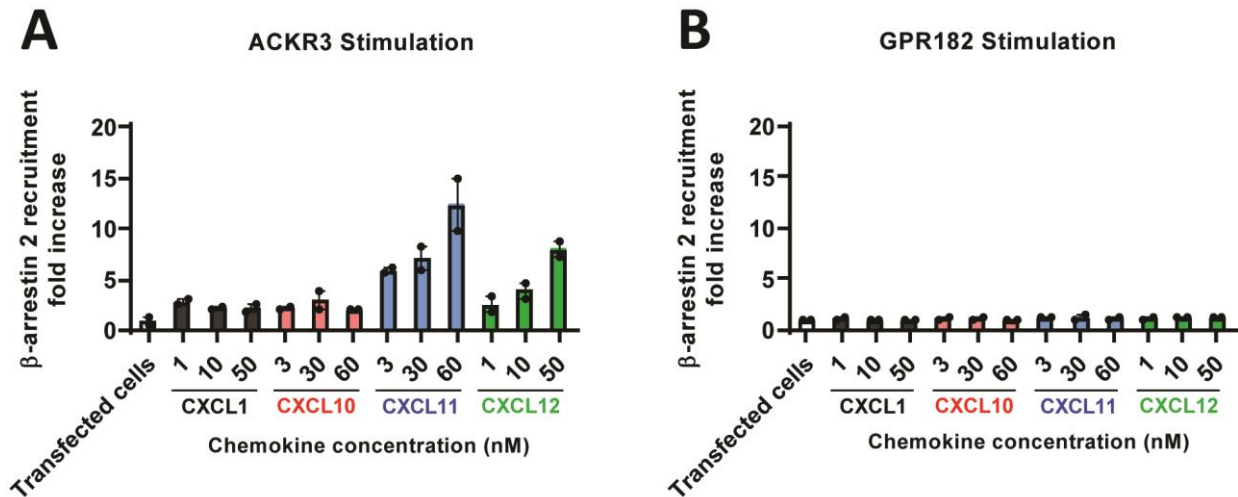


Figure 11: GPR182 is not activated upon chemokines stimulation

Effect of the indicated chemokines on β -arrestin recruitment to ACKR3 (A) and GPR182 (B). Data are means \pm SEM.

b) Seeking for a GPR182 endogenous ligand into the blood

Considering that GPR182 is an endothelial cell receptor, we tested whether GPR182’s ligand is present in the blood. To answer that question, we adapted the ultra-filtration method established by Benedikter *et al.* [169]. Briefly, the principle is based on separating the different blood components according to their molecular weight using successive size-exclusion chromatography columns.

First, we depleted human plasma of its low and high molecular weight constituents, retaining only plasma components sized between 3-50 kDa. Then, we concentrated this 3-50 kDa plasma phase twenty times. As shown in Figure 12A, stimulation of the TANGO-GPR182 receptor with this preparation induced a 3-fold increase in luciferase activity. To determine more precisely GPR182’s potential ligands, plasma samples were processed to generate 3-10 kDa, 10-30 kDa, and 30-50 kDa eluates. While most of these different plasma elutions did not affect GPR182 activation, the 3-10 kDa phase showed a slight increase (Figure 12B). However, the 3-fold increase observed in GPR182 positive cells was extremely weak compared to the 100-fold increase observed in the positive control receptor (Figure 12C). Moreover, a similarly prepared serum could

not reproduce GPR182 activation (Figure 12D). Altogether, these experiments did not allow identifying an endogenous ligand within the blood.

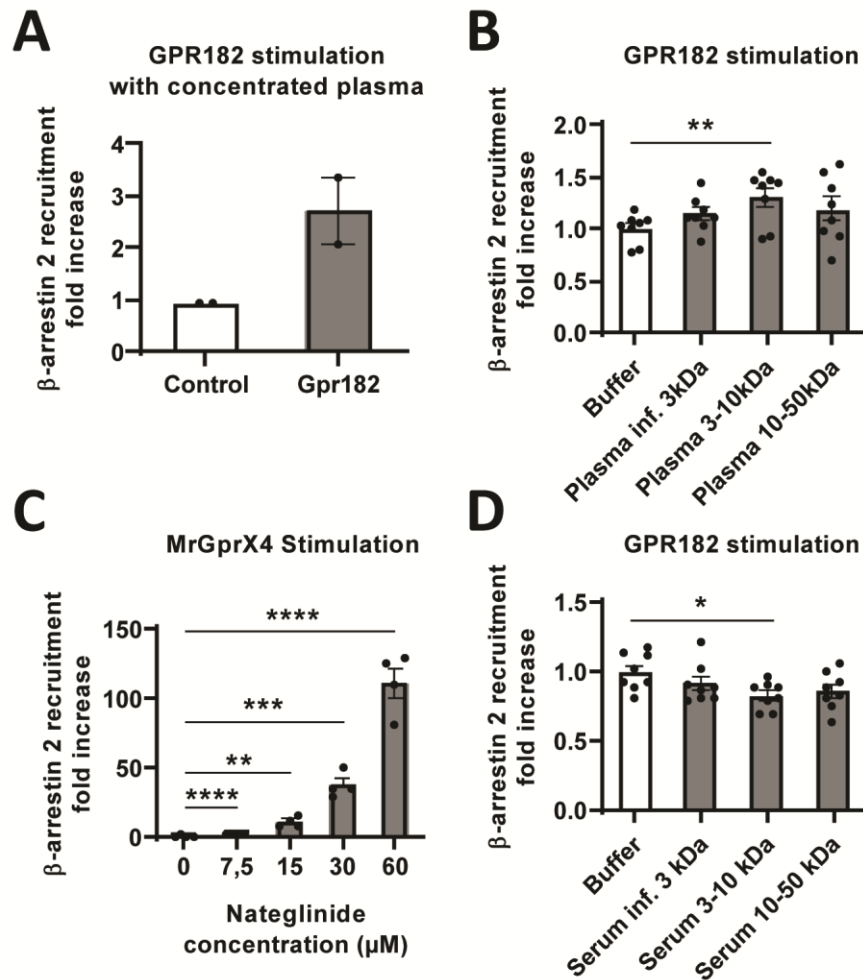


Figure 12: GPR182 is not activated upon plasma stimulation

Analysis of β -arrestin recruitment to GPR182 in response to plasma stimulation (A-B). Comparison with the β -arrestin recruitment to a MrGprX4 and its known ligand Nateglinide (C). Effect of GPR182 stimulation with serum on the recruitment of β -arrestin to the receptor (D). Data are means \pm SEM; differences between groups were analyzed using paired Student's t-test. * P < 0.05; ** P < 0.01; *** P < 0.001; **** P < 0.0001

c) Seeking for an autocrine/paracrine secretion of GPR182 ligand in the liver

Since liver sinusoidal endothelial cells are highly expressing GPR182, we asked whether hepatic cells are locally producing and secreting GPR182 ligand. To verify this hypothesis, we first established a primary cell culture of hepatic cells by adapting the protocol published by Li *et al.* [170]. After isolation, we seeded single cells in different culture conditions (figure 13A-C). While isolated hepatocytes were successfully attaching and proliferating (Figure 13A), the attached non-parenchymal cells, mainly composed of liver endothelial cells, were not proliferating (data not shown). Since primary cell culture of endothelial cells remains challenging [171], we adapted the co-culture of endothelial cells with hepatocytes (Figure 13B). In co-culture, endothelial cells shape and proliferation rate appeared enhanced. The medium of these different culture conditions was collected, filtered, and used to stimulate *Gpr182* positive cells. Unfortunately, none of these preparations led to GPR182 activation (Figure 13D).

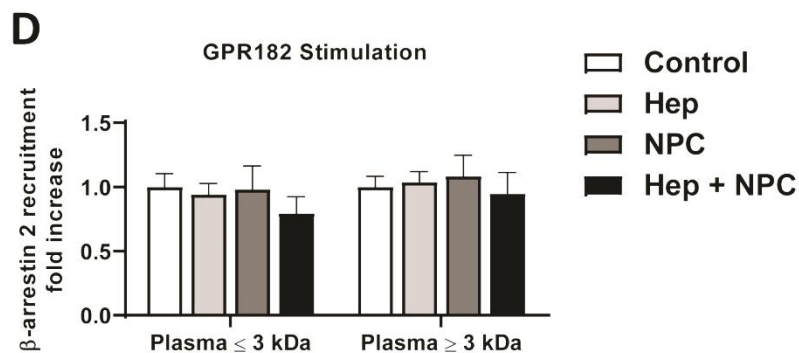
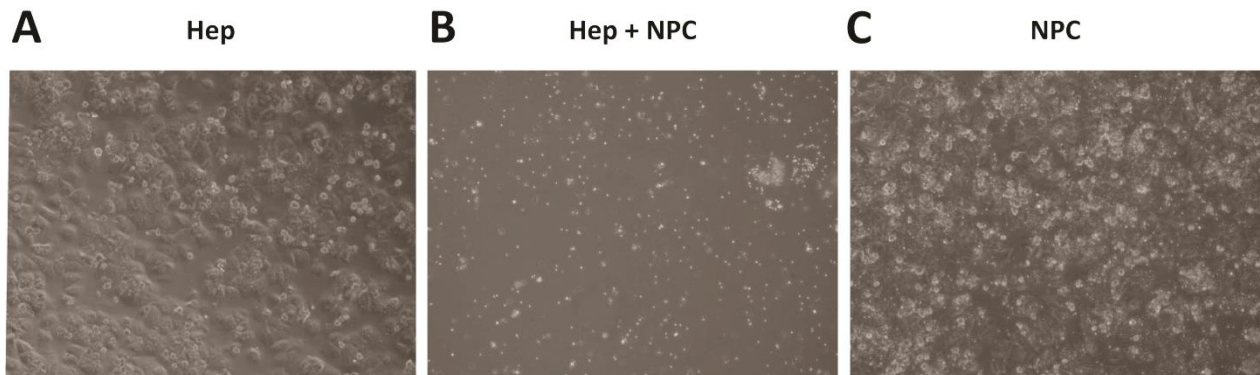


Figure 13: GPR182 is not activated upon stimulation from released hepatic factors

Establishment of hepatic primary cell culture of hepatocytes (Hep), Non-parenchymal cell (NPC) and Hep+NPC (A-C). The effect of GPR182 stimulation with the factors released by the hepatic cell cultures is monitored by the β -arrestin recruitment to the receptor and expressed as a relative increase compared to the stimulation of mock transfected cells medium (D)

d) Screening a lipid library

We ordered a ~900 compounds library designed especially for GPCR deorphanization. This library contained various endogenous lipids such as prostaglandins, thromboxanes, cannabinoids, inositol-phosphates, phosphatidylinositol-phosphates, sphingolipids, inhibitors, receptor agonists and antagonists, ceramide derivatives, and several other complex polyunsaturated fatty acids.

Having the intention to screening more than 800 compounds, we decided to optimize the TANGO system by generating a cell line stably expressing the TANGO-GPR182 receptor. Then, we screened the Cayman library in two different clones stably expressing the receptor (Figure 14A).

Screening results from the two clones highlighted significant differences. Indeed, in the top 20 hits, only three compounds were shared by the two clones (Figure 14B). We randomly decided to analyze further in transiently transfected cells the potentials agonists/antagonists observed with clone 6. When comparing the effect of the top four agonists and top three antagonists to five unrelated GPCR, we observed that these compounds had a similar effect on all tested receptors (Figure 14C). Therefore, we concluded that the initial observation was not specific to GPR182, rather drugs that directly disturb the TANGO-system.

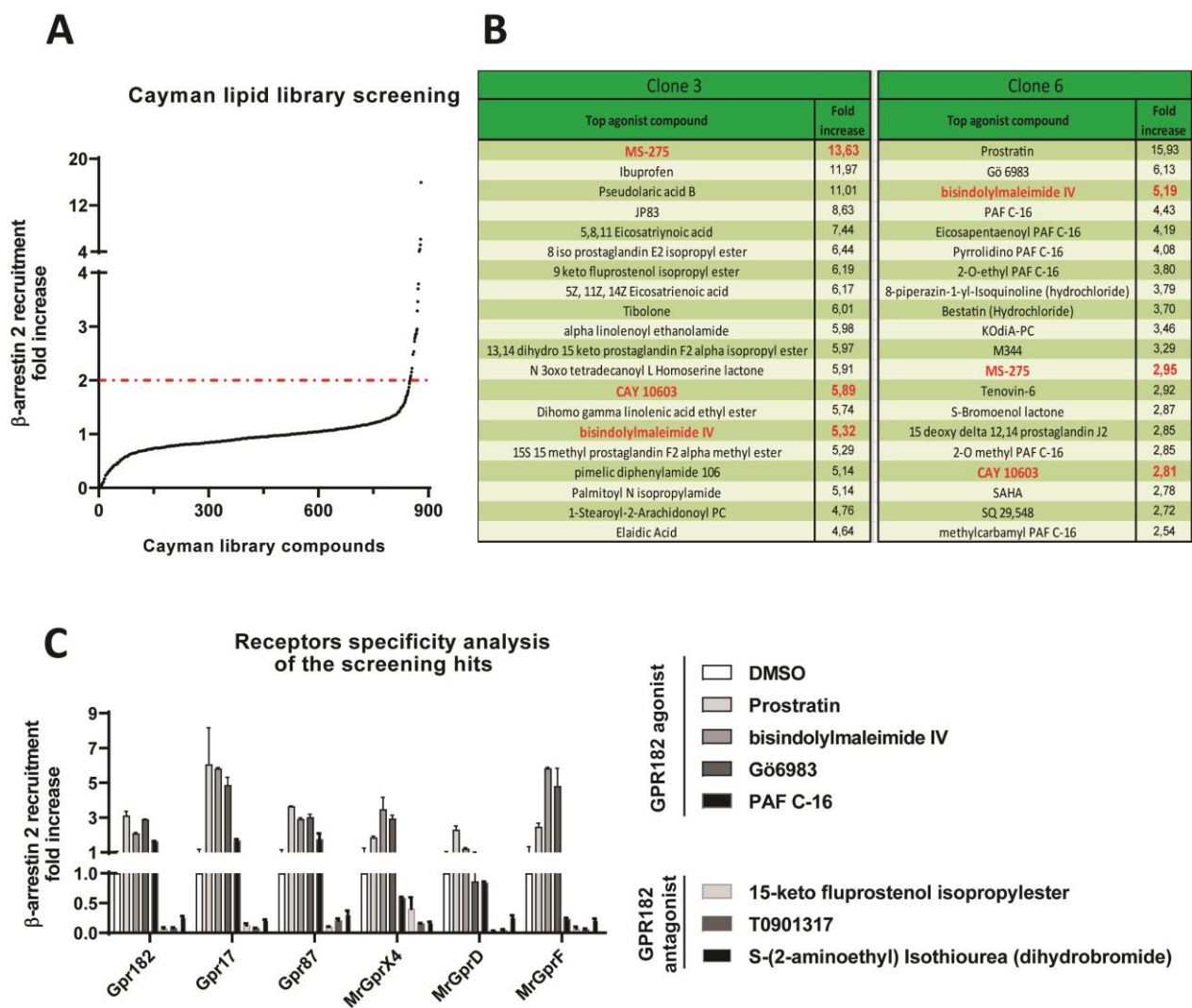


Figure 14: Screening an endogenous lipids library on GPR182

Analysis of β -arrestin recruitment to GPR182 in response to each of the ~900 lipids from the CAYMAN library (A). Table showing the top 20 compounds inducing the highest recruitment of β -arrestin in clone stably expressing TANGO-GPR182. Experiment performed independently in two different clones stably expressing the receptor. In red are highlighted compounds found in both clones (B). Analysis of the relative recruitment of β -arrestin to GPR182 compared to several non-related GPCRs in response to some agonists and antagonists (C). Data are means \pm SEM.

3) Analysis of *Gpr182* Knock-out first mice

a) Alteration of blood cells count

The International Mouse Phenotyping Consortium previously described that *Gpr182* targeted mice exhibit an increased mean corpuscular volume (MCV). Consequently, we performed blood sampling using the same "first KO" mice. While the erythrocyte and reticulocyte number was unchanged, we confirmed the significant MCV increase in *Gpr182* deficient mice (Figure 15C). Interestingly, the mean corpuscular Chemoglobin (MCH) (Figure 15D) and the mean corpuscular hemoglobin concentration (MCHC) were unaltered (data not shown), nor hematocrit, hemoglobin and thrombocytes (Figure 15 E-G). Strikingly, the leukocyte population was enlarged in *deficient* mice (Figure 15H). Indeed, that rise affected several leukocyte subpopulations: eosinophils, neutrophils, monocytes, and lymphocytes (Figure 15 I-L).

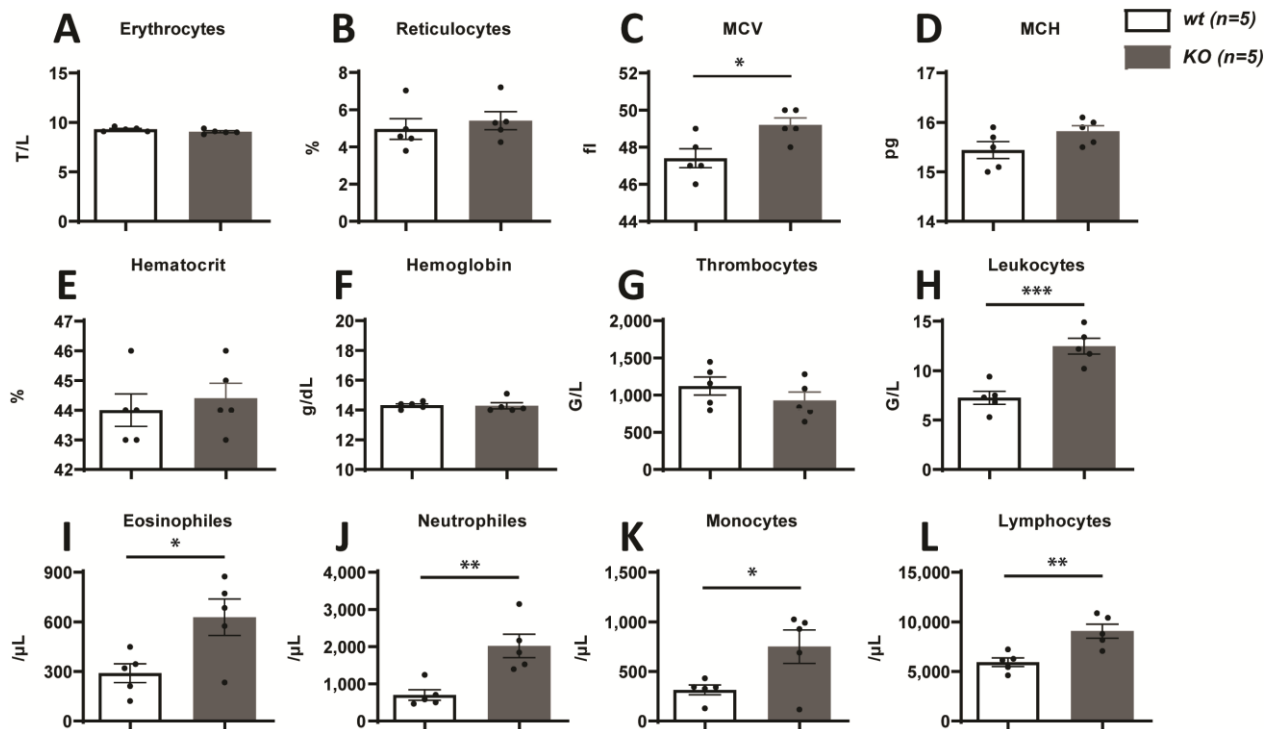


Figure 15 : GPR182 deficiency leads to leukocytosis

Blood cell count and parameters of circulating cells in 10-weeks-old KO first male and their control littermates (A-L). Data are means \pm SEM; differences between genotypes were analyzed using paired Student's t-test. * $P < 0.05$; ** $P < 0.01$; *** $P < 0.001$

Possible explanations for swelling leukocyte population could either be; an increased leukocyte production during hematopoiesis or an increased leukocyte mobilization into the bloodstream due to systemic inflammation.

b) Hematopoiesis in *Gpr182* targeted mice

Because most of leukocyte subpopulations were increased (Figure 15H-L), we favoured the hypothesis that a major dysfunction occurred during haematopoiesis of mice lacking *GPR182*. To test this hypothesis, we aimed analysing the hematopoietic stem and progenitors cells subpopulations according to a method published by Duchene *et al.* [172]. The gating strategy used for this purpose is shown in Figure 16A. Our preliminary result exhibited a significant reduction of HSC number whereas multipotent progenitors remained unchanged (Figure 16B-E).

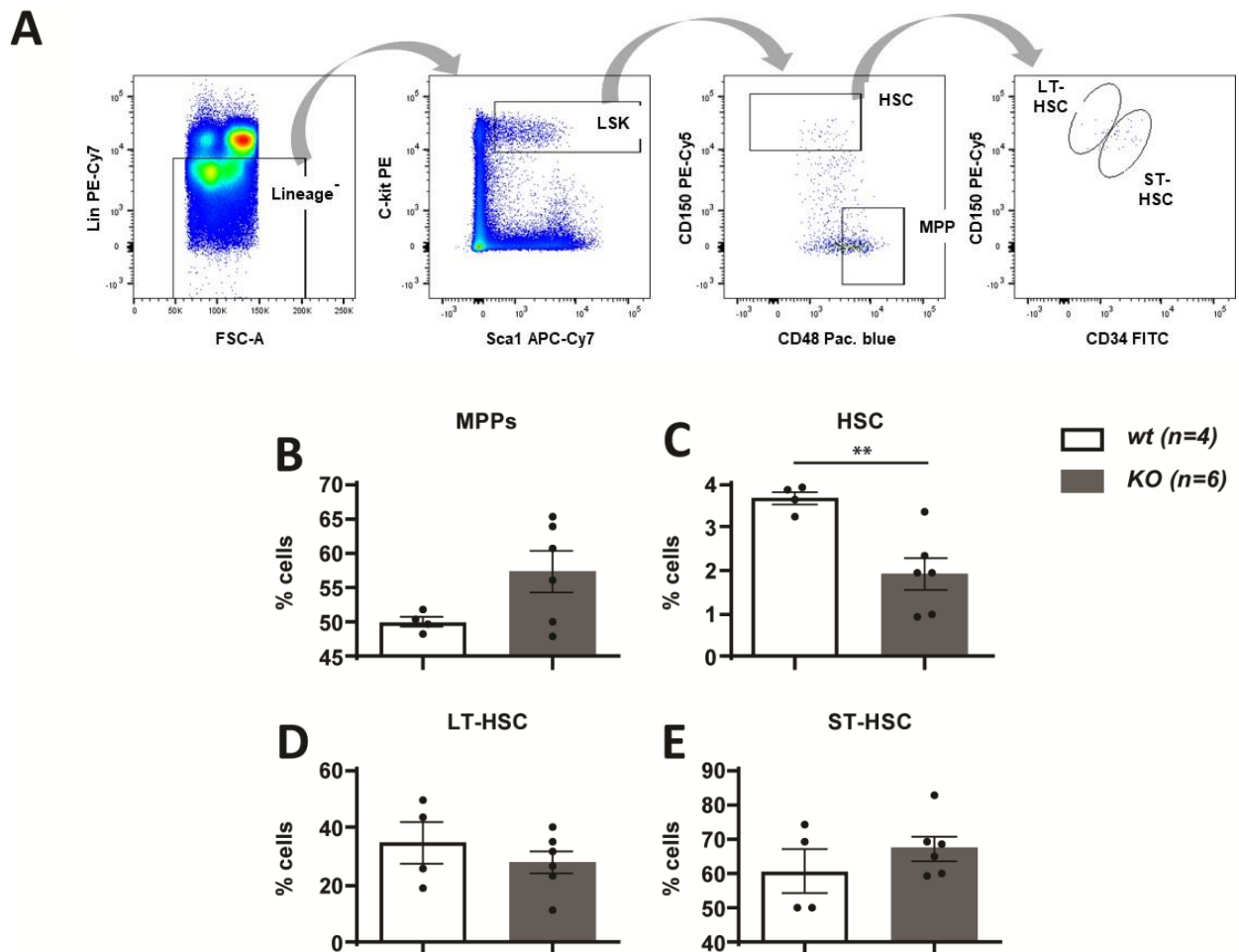


Figure 16: GPR182 deficiency results in decreased bone marrow HSC

Gating strategy used to distinguish the different populations (A). Hematopoietic stem cells (HSC) and multipotent progenitors (MPP) were quantified (B-C). A deeper analysis of the HSC subpopulations into the long-term repopulating HSC (LT-HSC) and the short-term differentiating HSC (ST-HSC) was assessed (D-E). Data are means \pm SEM; differences between genotypes were analyzed using paired Student's t-test. ** P < 0.01

c) Measurement of plasma cytokine levels highlights CXCL10

Simultaneously, we tested whether a general mobilization of leukocytes occurred in the bloodstream of *Gpr182* targeted mice. We performed a Magpix milliplex[®] analysis on plasma samples from the same cohort of mice that exhibited enlarged leukocyte's subpopulations. The plasma level of most inflammatory cytokines was unchanged; however, we noticed an intriguing two-fold increase of CXCL10 in the plasma of mice bearing the targeted allele (Figure 17A).

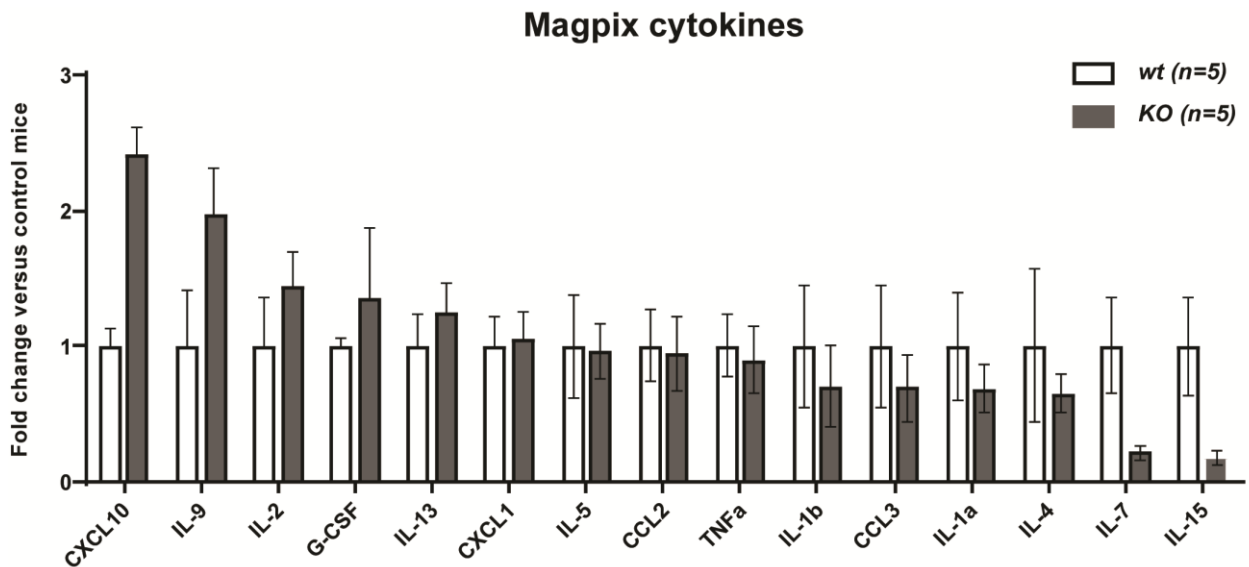


Figure 17: GPR182 deficient mice displayed increased CXCL10 plasma level

Assesment of plasma concentrations of the indicated cytokines in GPR182 deficient mice and their control littermates. Shown are mean values \pm S.E.M.

4) GPR182: a novel atypical chemokine receptor

a) Specific binding of several recombinant chemokines to GPR182

As previously mentioned, GPR182 is related to a chemokine decoy receptor. Consequently, we wondered whether the rise of CXCL10 plasma concentration in deficient mice, indeed, reflected a lack of CXCL10 scavenging. Using the TANGO system, we examined whether CXCL10 stimulation promoted β -arrestin recruitment to the receptor (Figure 11B). However, international consensus decided to rename atypical chemokine receptors this way, principally because of their atypical signaling.

Therefore, to exclude definitely whether chemokines are endogenous ligands for GPR182, we decided to assess CXCL10 binding to GPR182. We generated a construct coding for a Fc-CXCL10 fusion protein and its mock control: Fc (Figure 18A). Following transfection, the medium of culture, enriched in fusion proteins was collected and incubated with GPR182+ cells. As a control, the mock protein did not bind to HEK cells nor *Gpr182*+ cells (Figure 18B). However, the Fc-CXCL10 fusion protein specifically bound to GPR182 (Figure 18C).

However, this experiment does not indicate whether the CXCL10 concentration used was physiologically relevant. To determine CXCL10 affinity to GPR182, we switched to a commercially available chemokine: fluorescently labelled CXCL10 (hCXCL10-AF647). The binding analysis of hCXCL10-AF647 to hGPR182 positive cells revealed an affinity for the human receptor with a K_d around ~ 19 nM (Figure 19A) likewise the murine receptor with a slightly lower affinity: 35 nM (Figure 19B). Then, we sought whether non-labelled CXCL10 could displace CXCL10-AF647 binding to the receptor. Indeed, we observed that increasing concentration of non-labelled CXCL10 nicely displaced CXCL10-AF647 binding to GPR182 with a K_i of 10 nM (Figure 19C). Accordingly, we systematically studied the ability of 42 different chemokines to displace CXCL10-AF647 binding. While most of the tested chemokines did not alter CXCL10-AF647 binding to the receptor, the three chemokines CXCL13, -10, and -12 showed the most substantial binding competition (Figure 19D). Finally, we validated the best candidates in

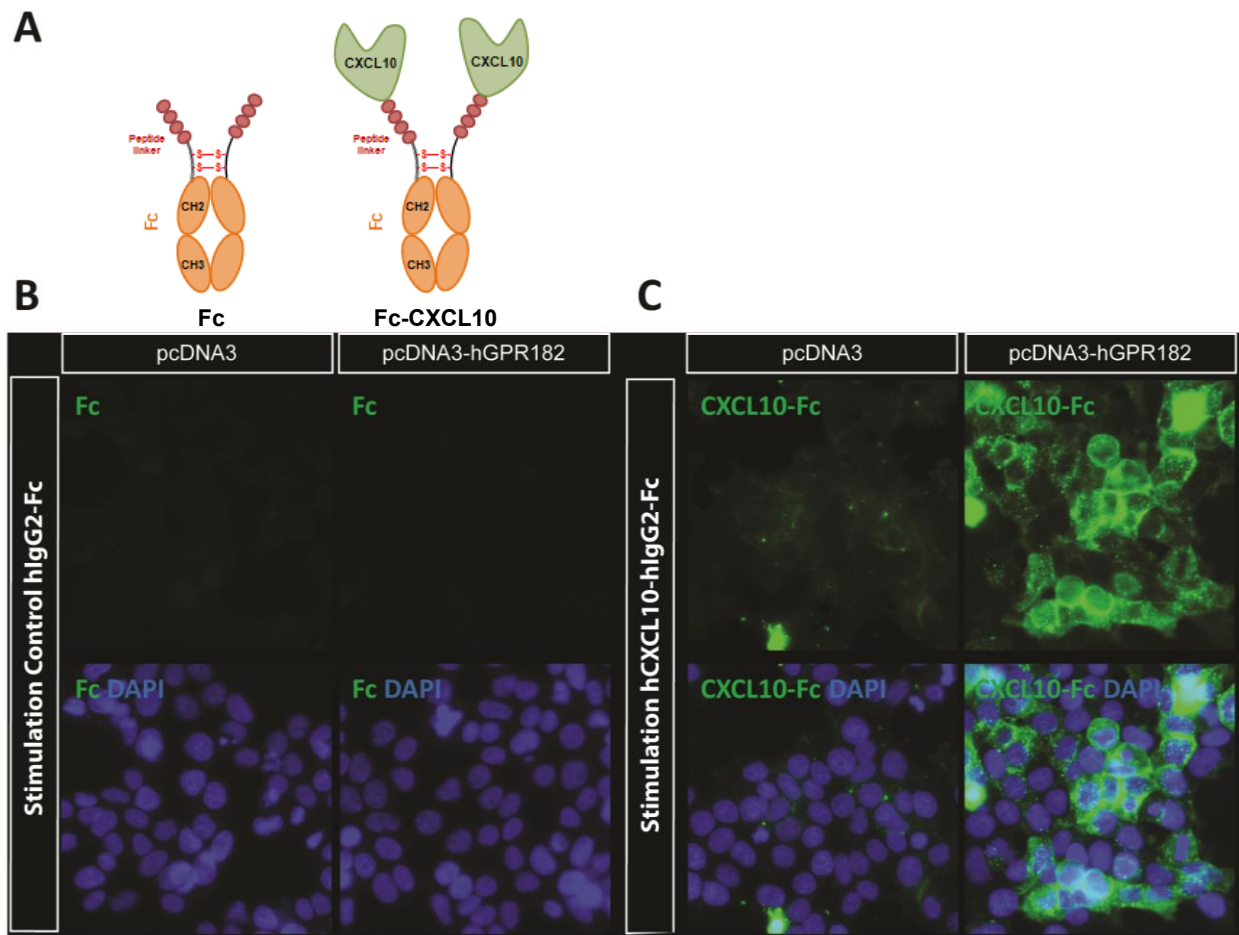


Figure 18: GPR182 binds the Fc: CXCL10 fusion recombinant protein

Schematic view of the engineered Fc-CXCL10 recombinant protein and its mock control (A). Representative immunofluorescence images of HEK293 cells overexpressing GPR182 after incubation with the mock protein (B) or the Fc: CXCL10 fusion protein (C).

competition-binding studies until K_i values ceased to be physiologically relevant. We observed the highest binding affinity for CXCL13 and CXCL10, with K_i values of 9 and 10 nM, respectively (Figure 19E). To a lower extent, both isoforms of CXCL12, α , and β showed a binding affinity to GPR182 with K_i values of 31 and 19 nM, respectively (Figure 19E). Finally, CCL19 had a much lower binding affinity (K_i : 260 nM), and CCL16 competition was too weak to be analyzed (Figure 19E). Convincingly, similar results with the murine receptors/chemokine strengthened this finding (Figure 19F).

b) Oppositely to canonical GPCR, GPR182 does not signal through G-protein

Then, we wondered how GPR182 signals in response to its ligands.

First, we followed an established method based on monitoring GPCRs activation by measuring the intracellular calcium transient induced by a promiscuous G-protein activation[173]. As a positive control, CXCR3, -4 and -5 expressing cells induced Ca²⁺ mobilization in response to their respective ligands: CXCL10, -12 and -13. Conversely, GPR182 positive cells exposure to each of the four chemokines did not result in Ca²⁺ transient (Figure 20). Similarly to GPR182, ACKR3 stimulation with CXCL12 did not lead to G-protein activation (Figure 20B-C). Recently, a study reported the interaction of GPR182 with receptor activity-modifying proteins (RAMPs) [174]. Therefore, we tested whether co-expression of GPR182 with RAMP-1, -2 or -3 mediated chemokine-induced G-protein signaling. However, none of each RAMPs promoted GPR182 downstream signaling (Figure 20).

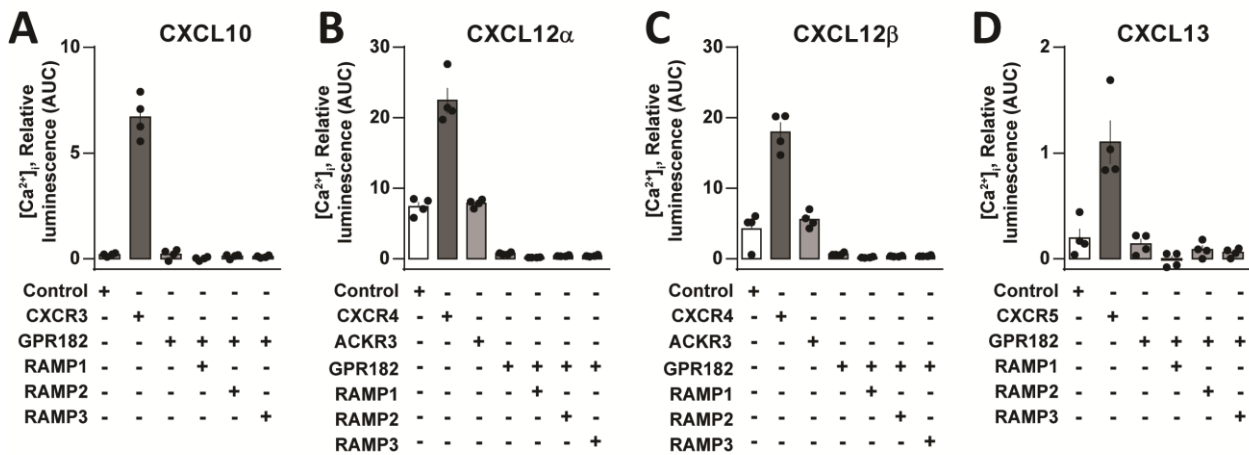


Figure 20: GPR182 does not signal in response to ligand binding

Assessment of intracellular calcium transient in HEK293 cells expressing the indicated receptors together with Ca²⁺-sensitive bioluminescent fusion protein in response to CXCL10 (A), CXCL12a (B), CXCL12b (C) and CXCL13 (D). Shown are mean values \pm SEM.

Secondly, the use of the NanoBiT-Gprotein dissociation assay established by Inoue *et al.* [175] reproduced very similar results (Figure 21).

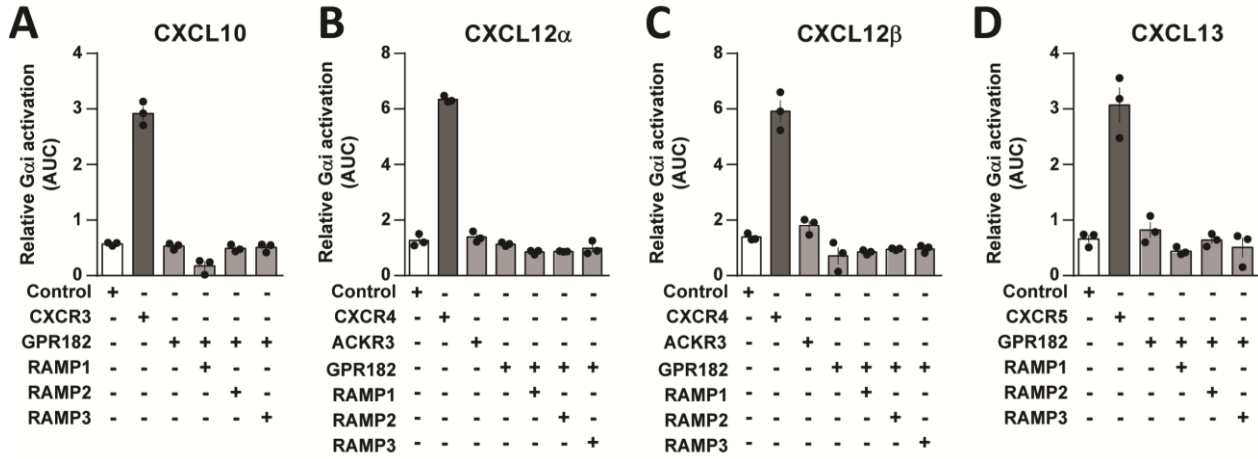


Figure 21: GPR182 does not signal in response to ligand binding

Assessment of intracellular cAMP formation upon stimulation with CXCL10 (A), CXCL12a (B), CXCL12b (C) and CXCL13 (D). Shown are mean values \pm SEM.

Lastly, we used the PRESTO-Tango system [3] to study the potential effects of chemokines on GPR182-dependent β -arrestin-recruitment. All four chemokines increased β -arrestin recruitment through their conventional receptors, CXCR3, CXCR4, and CXCR5, whereas they had hardly any effect on β -arrestin recruitment to GPR182 (Figure 22). However, as previously shown in figure 11A, CXCL12 strongly induced β -arrestin recruitment to its atypical receptor ACKR3 (figure 22B-C). Interestingly, compared to other chemokine receptors, GPR182 showed substantial recruitment of β -arrestin in the absence of any ligand, indicating high constitutive activity (Figure 22E). Regarding the physiological role of β -arrestin, such basal activity suggests a constitutively high internalization of the receptor.

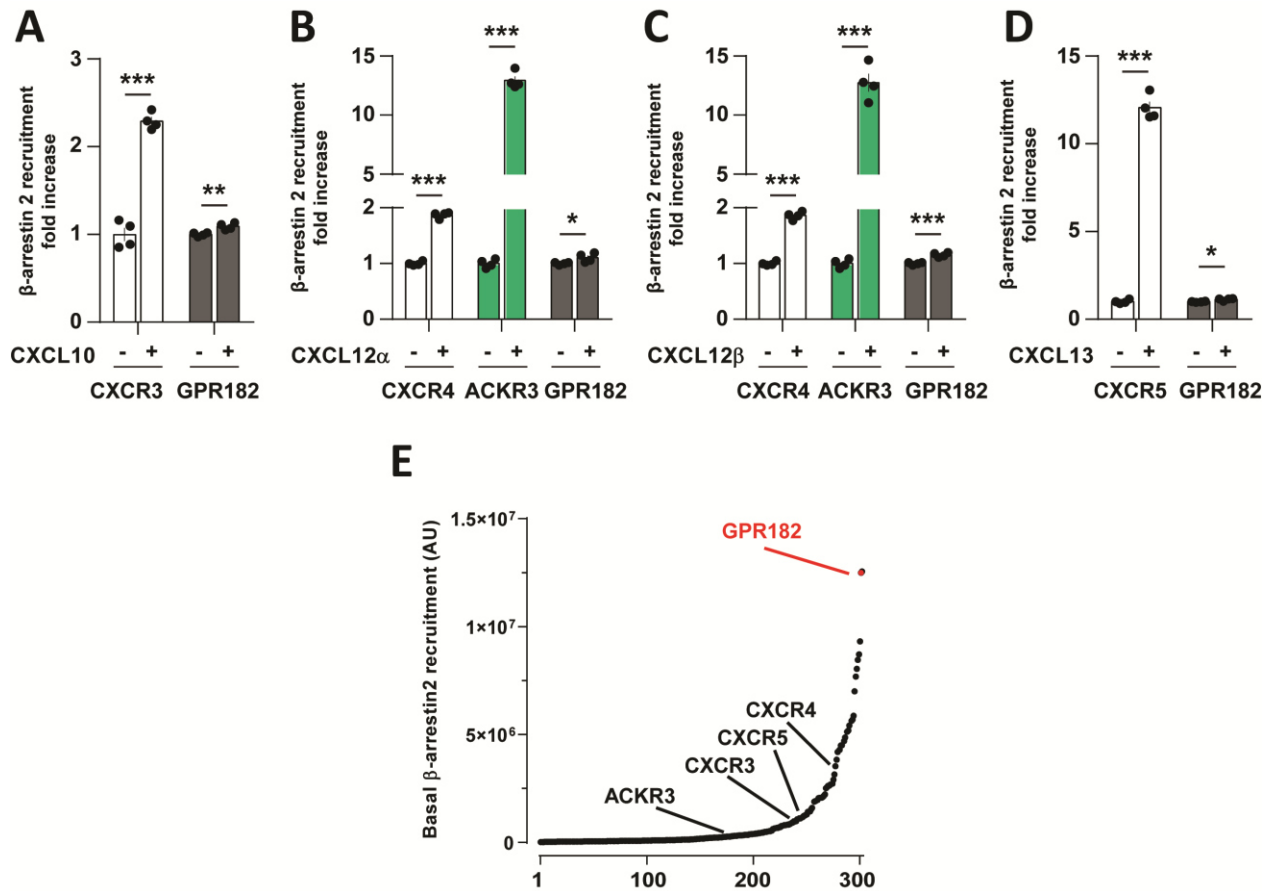


Figure 22: GPR182 does not signal in response to ligand binding

Measurement of β -arrestin recruitment to GPR182 in response to CXCL10 (A), CXCL12a (B), CXCL12b (C) and CXCL13 (D). Basal activity of β -arrestin recruitment to the 300 TANGO-GPCRs (E). Shown are mean values \pm SEM. * $P < 0.05$; *** $P < 0.001$

c) GPR182 is constitutively highly internalized

To demonstrate whether GPR182 is constitutively internalized we expressed an N-terminal Flagged-GPR182 fusion protein in HEK cells. We noticed that staining the extracellular Flag-tag during cold exposure exhibit a membrane localization of the receptor; however, GPR182 is quickly internalized when cells are incubated back to 37°C (Figure 23A). Furthermore, the internalization of GPR182 was unchanged when incubated with CXCL10 (Figure 23B). Finally, we observed that β -arrestin 1/2 knockdown substantially inhibited the internalization of GPR182 (Figure 23C). Altogether, these *in vitro* data indicate that GPR182 is an atypical chemokine receptor for CXCL-10, -12, and -13, which binds and internalizes chemokines, rather than inducing conventional downstream signaling in response to ligand binding.

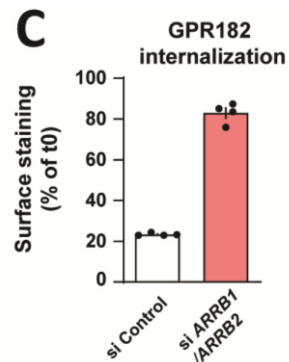
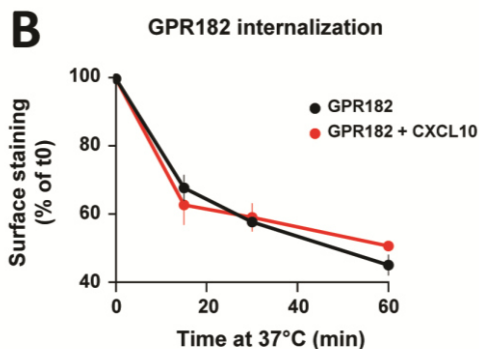
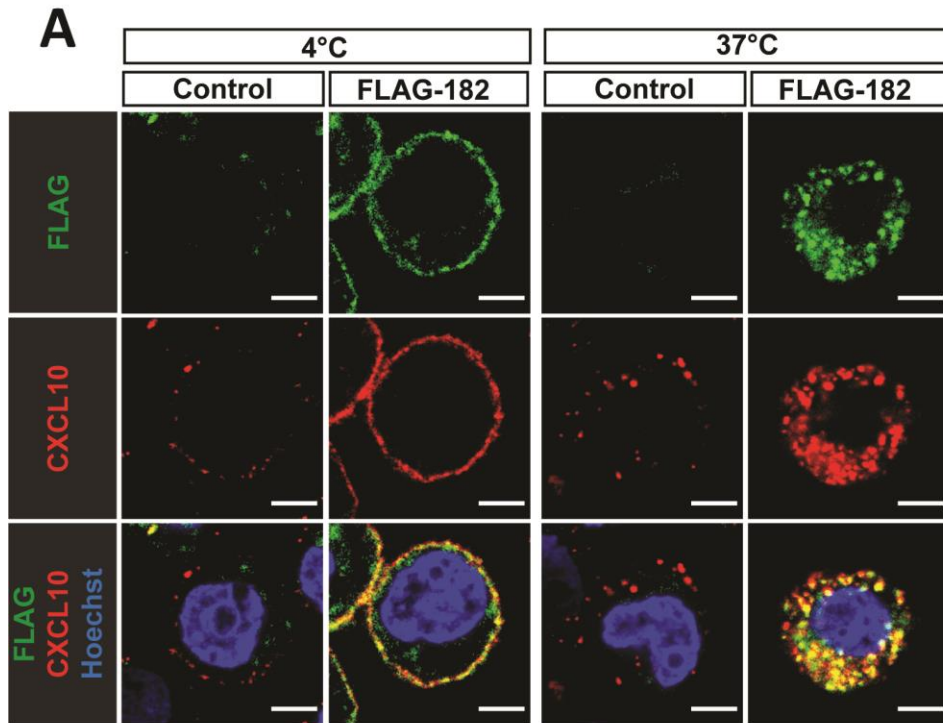


Figure 23: GPR182 is constitutively internalized

Representative immunofluorescence confocal images of Single-cell suspension of HEK293T cells expressing FLAG-GPR182 or the control vector. The cellular localization of the receptor and CXCL10-AF647 is shown at 4°C and following 30 minutes incubation at 37°C (A). The location of FLAG-GPR182 was measured by flow cytometry in the presence or absence of hCXCL10 (100 nM) (n =3 replicates) (B). Internalization of FLAG-GPR182 was assessed after knock-down of β -arrestin-1 and β -arrestin-2 (si ARRB1/ARRB2) (C). Shown are mean values \pm SEM of one experiment; unpaired two-tailed Student's t test

5) GPR182: a chemokine decoy receptor disrupting chemokines' gradient and leukocytes trafficking.

a) Increased plasma concentration of GPR182's ligands

Since *Gpr182* is specifically expressed in endothelial cells, we tested whether the loss of GPR182 affected plasma chemokine levels. Plasma concentrations of each three chemokines were significantly increased in GPR182-deficient mice. While CXCL10 and CXCL12 levels were two- to threefold increased, CXCL13 levels were increased more than tenfold (Figure 24A-C). To validate these findings and test whether the acute loss of endothelial GPR182 would result in elevated plasma levels of chemokines, we generated inducible endothelium-specific GPR182-deficient mice (*Cdh5-CreERT2; Gpr182^{flox/flox}* (EC-Gpr182-KO)). The induction of EC-Gpr182-KO mice resulted in a rapid increase in the plasma concentration of CXCL10, CXCL12, and CXCL13 (Figure 24D-F). Similarly to the constitutive GPR182-deficient mice, the increase in CXCL13 levels was more pronounced than increases in CXCL10 and CXCL12 plasma levels. Indeed, CXCL13 plasma levels continued to rise after induction of endothelial GPR182, while the increases of CXCL10 and CXCL12 plasma levels appeared to remain stable over 20 days (Figure 24D-F).

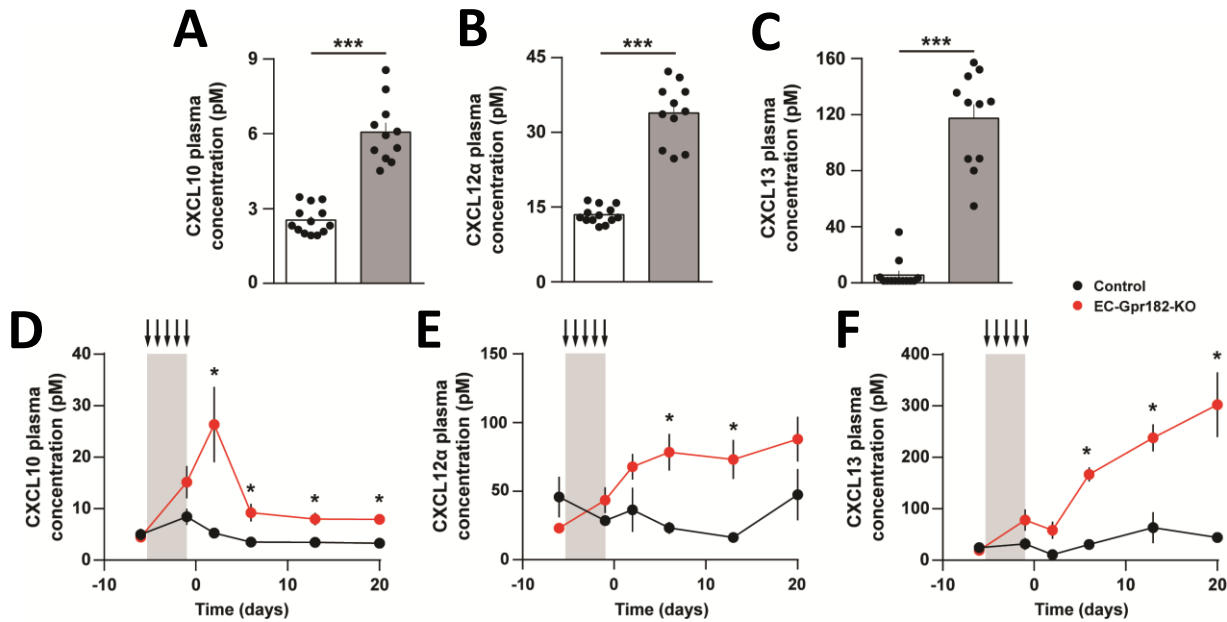


Figure 24: Increased free plasma concentrations of CXCL10, CXCL12 α , and CXCL13 in mice lacking GPR182.

Plasma concentrations of the indicated chemokines in GPR182-deficient mice (grey; n = 13) and their littermate control (white; n = 11) (A-C). Plasma concentrations of the indicated chemokines 1 day before as well as 1, 3, 7, 14, and 21 day after tamoxifen treatment for five consecutive days (arrows) in control mice and in EC-Gpr182-KO animals (n = 4 to 7 mice per genotype) (D - F). Shown are mean values \pm SEM. * P < 0.05; *** P < 0.001. Statistical analysis using an unpaired two-tailed Student's t test (A-C) or multiple t-test with Sidak correction (D-F)

b) Decreased leukocytes trafficking into secondary lymphoid organs

To test whether leukocytes' trafficking into lymphoid organs is disturbed in *Gpr182* deficient mice, we performed an adoptive transfer experiment. Briefly, we monitored by flow cytometry the trafficking behavior of CFSE-labelled leukocytes within lymphoid organs of receiver mice (Figure 25A). We observed a decreased extravasation of CFSE positive leukocytes of 20% and 30% respectively, in the mesenteric lymph node and the spleen of KO mice (Figure 25B). Additionally, we noticed an overall

reduction in splenic extravasation affecting all B/T cells and myeloid cells (Figure 25C). Interestingly, we observed declined extravasation of myeloid and T cells within the mesenteric lymph node while the B cell population was not affected (Figure 25D).

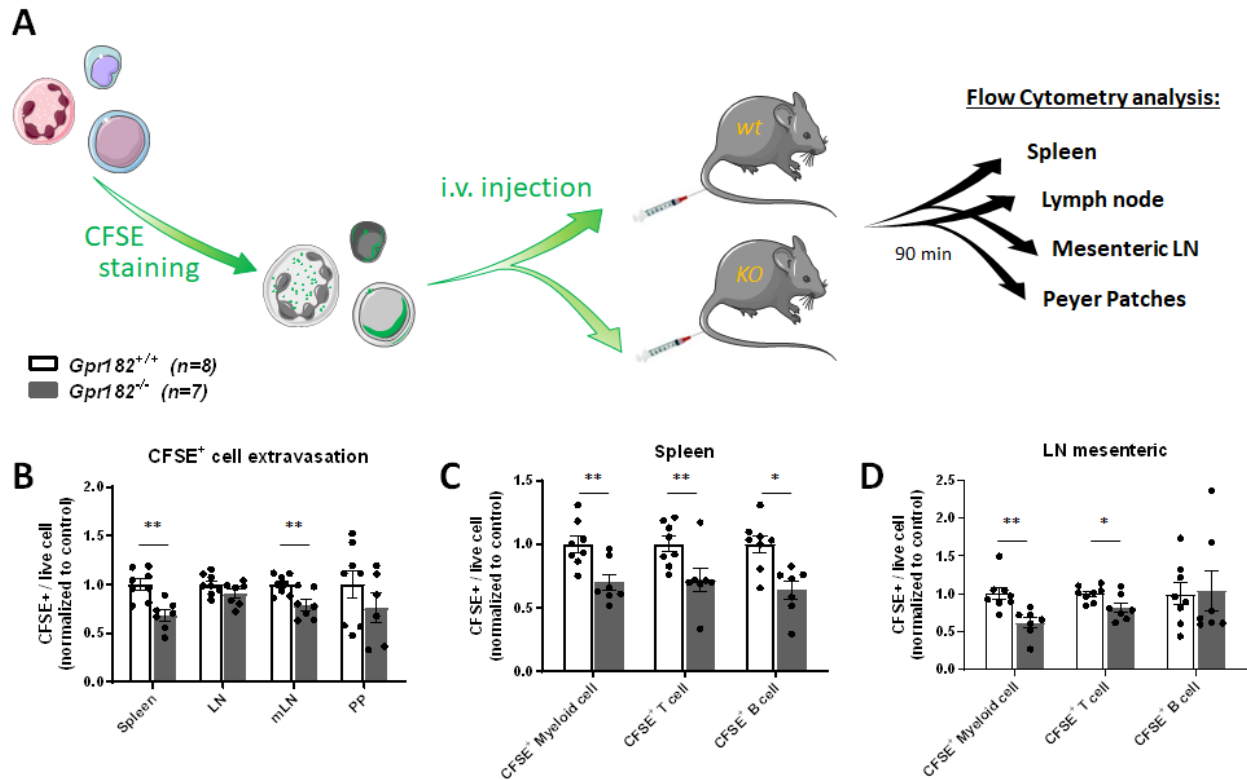


Figure 25: Decreased leukocytes extravasation into secondary lymphoid organs

Schematic view of the adoptive transfer experiment protocol (A). Leukocytes were isolated from the spleen of C57BL/6J mice and stained with CarboxyFluorescein Succinimidyl Ester (CFSE) before to be reinjected into the tail vein of GPR182-deficient mice and their control littermates. The number of CFSE positive leukocytes detected in the spleen, peripheral lymph node (LN), mesenteric lymph node (mLN) and Peyer's Patches (PP) were assessed by flow cytometry 90 minutes after the CFSE-stained cells infusion (B). A more detailed analysis of the CFSE-labeled leukocytes subpopulation trafficking into the spleen and mesenteric lymph node is shown (C-D). Shown are mean values \pm SEM. * $P < 0.05$; ** $P < 0.01$. Statistical analysis using an unpaired two-tailed Student's t test.

c) Increased tumor growth in the lung

Since *Gpr182* deficiency is associated with reduced leukocytes trafficking *in vivo*, we aimed to decipher whether we would observe such impairments in pathological conditions. Given the substantial role supported by leukocytes in tumor immunity through leukocytes recruitment within the tumors, we studied the tumor growth of B16F10 firefly-luciferase positive tumor cells in the lung of *Gpr182* KO mice and its littermate control. The bioluminescence levels measured during the first week were similar in both groups whereas we observed a significant bioluminescent increase 12 days after the tumor cells injections in *Gpr182* KO mice (Figure 26A).

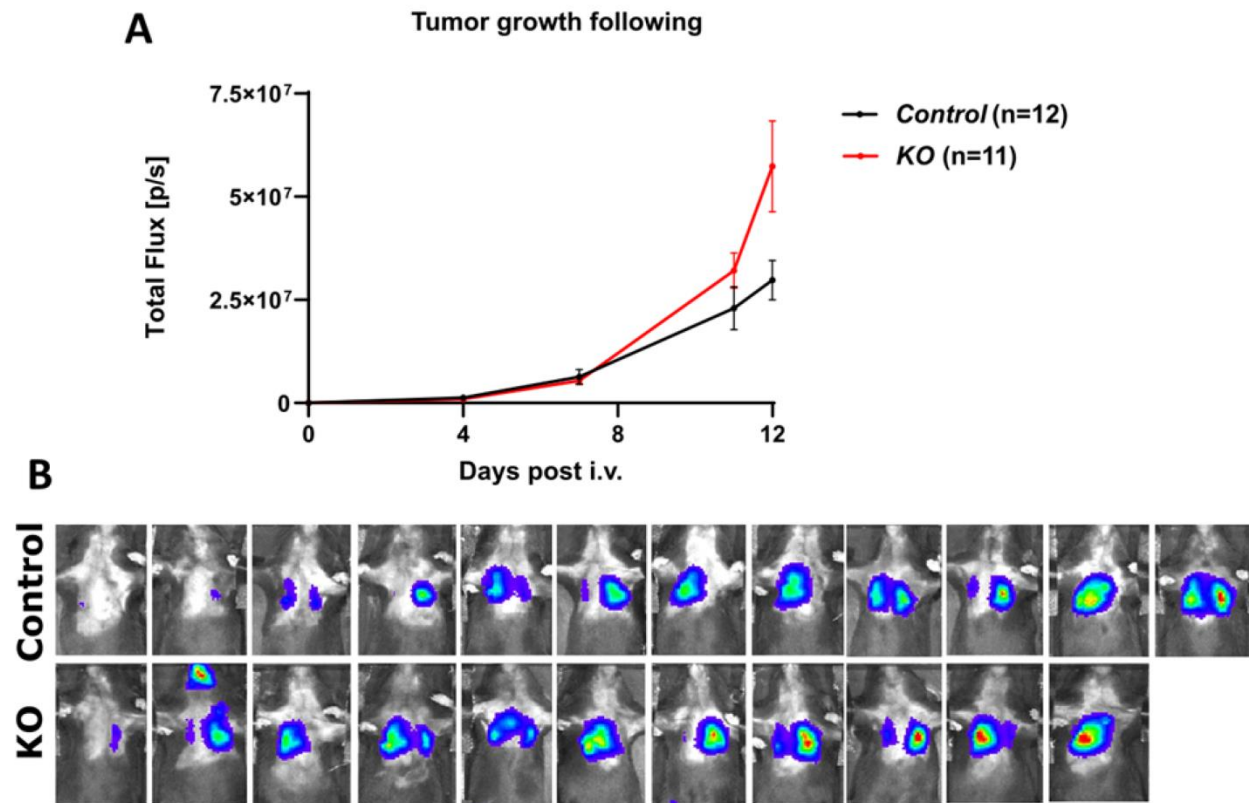


Figure 26: Increased lung metastasis formation in *Gpr182*-deficient mice.

Follow-up of *Gpr182*-deficient mice and their control littermates at 7, 11 and 12 days after the i.v. injection of B16F10Luc cells using the IVIS System (A). Images of each mouse showing the lung tumors taken with the IVIS system of day day12 (B).

d) Increased splenic size is associated with alteration of leukocytes composition

We observed that spleens were significantly enlarged in GPR182 deficient mice (Figure 27A-B). Additionally, further analysis revealed a decline of the lymphocytes T population counterbalanced by a rise of the myeloid population (Figure 27C). In the meanwhile, the study of GPR182 acute loss of function provided striking observations. The net increase of the myeloid population observed three days after tamoxifen injection came back to normal over time (Figure 27C). Conversely, the acute loss of GPR182 did not immediately affect the T cell population but prolonged time (Figure 27E). Lastly, we did not discern significant alterations within the B cells of global KO mice. However, we measured a rapid drop of B cells after tamoxifen injection while the B cell population appeared normal after a prolonged period (Figure 72D). To conclude, we identified that leukocytes' homeostasis is disrupted after the loss of GPR182. Nevertheless, it is unclear whether these modifications reflect an altered leukocyte homing and retention within the spleen or reflected a potential inflammation status in the spleen.

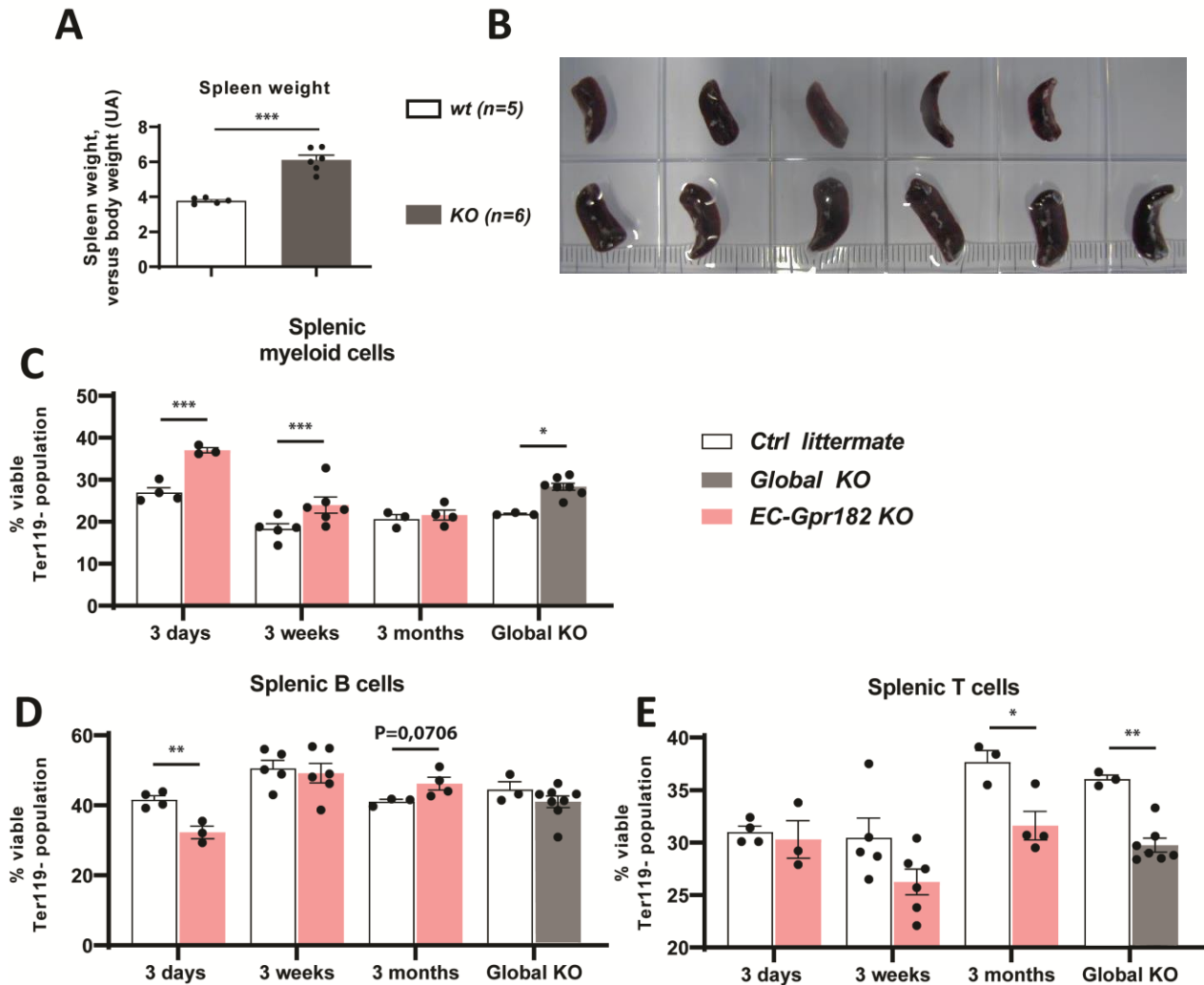


Figure 27: Increased size and altered leukocytes composition of the spleen of mice lacking the receptor.

Splenic weight of Gpr182-deficient mice and their control littermates expressed as Arbitrary Unit (U.A.) (A). Representative pictures showing the size of the spleen in KO mice and their control (B). A more detailed analysis was performed to quantify the splenic subpopulation of myeloid cells, B cells and T cells in EC-Gpr182-KO animals 3 days, 3 weeks and 3 months after tamoxifen injections (C-E). Similarly, the analysis was performed in 10 weeks-old Gpr182 global KO mice. Shown are mean values \pm SEM. * $P < 0.05$; ** $P < 0.01$; *** $P < 0.001$. Statistical analysis using an unpaired two-tailed Student's t test.

6) GPR182: role in maintenance of quiescent HSC within the bone marrow niche.

a) Blood analysis in KO mice

To validate the blood analysis performed in the KO first mouse line, we performed blood sampling in the EC-GPR182 mouse line. While we could confirm the increase in MCV and MCH, we observed some differences within the other blood parameters (Figure 28). For instance, we noticed a slight, yet significant rise in erythrocytes and reticulocytes number (Figure 28A-B). Additionally, we observed an increased monocytes number while the other leukocytes subpopulations were unchanged (Figure 28I-L).

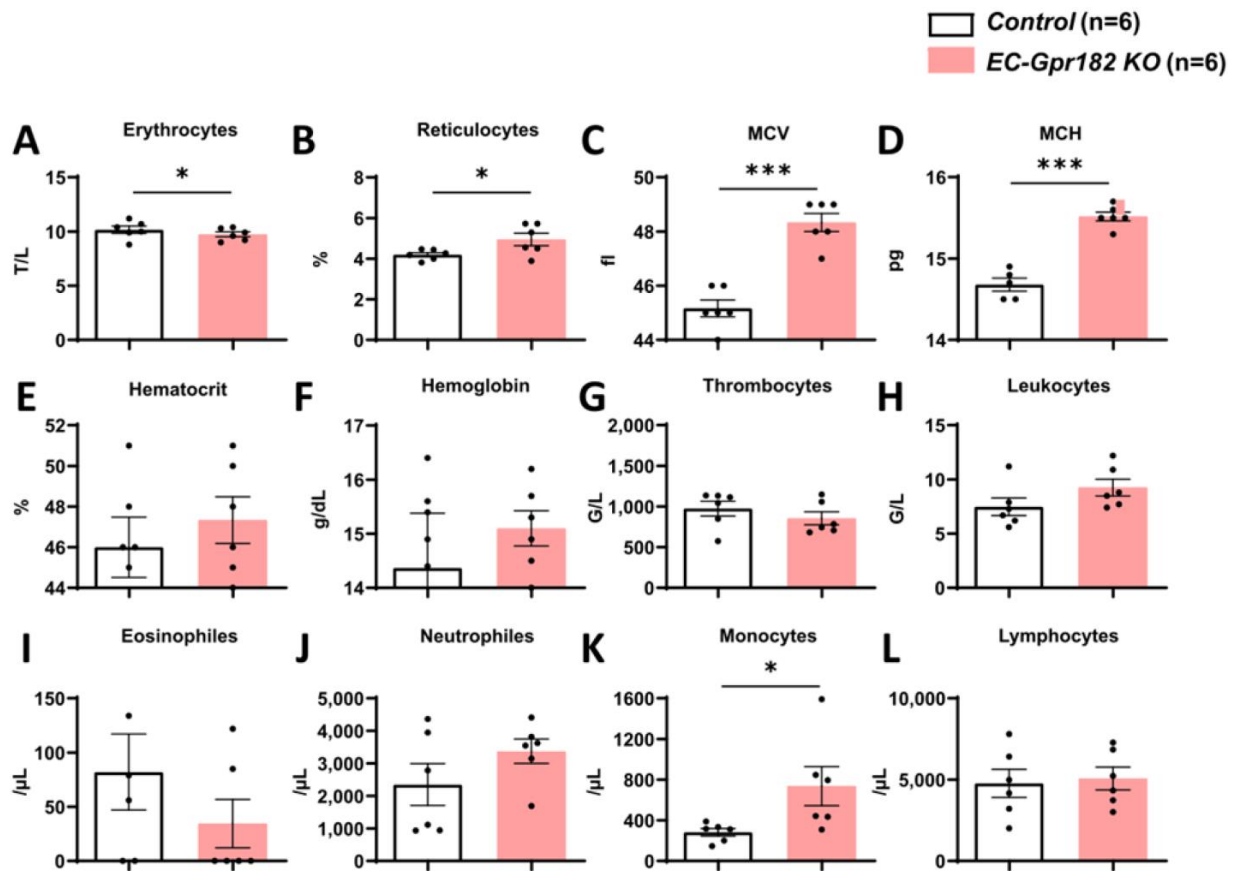


Figure 28: GPR182 deficiency leads mainly to an increased MCV/MCH, while erythrocytes and reticulocytes counts are slightly risen.

Blood cell count and parameters of circulating cells in EC-Gpr182-KO male and their control littermates (A-L). Data are means \pm SEM; differences between genotypes were analyzed using paired Student's t-test. * P < 0.05; ** P < 0.01

b) Hematopoiesis

Regarding the promising results shown in Figure 16, Prof. Dr. Michael Rieger (Department of Medicine, Hematology/Oncology, Goethe University Hospital, Frankfurt), also a member of my Thesis Advisory Committee, kindly offered his theoretical and experimental knowledge in hematopoiesis to validate these findings and analyze more accurately the phenotype we observed.

Antibodies' clones and gating strategy used in M. Rieger's lab were different (Figure 29A). Also, it allowed us to differentiate the different multipotent progenitors and their proliferating status.

First, we confirmed the decreased HSC population in *Gpr182* KO mice (Figure 29C); however, we determined that quiescent LT-HSC were declined while proliferating ST-HSC population were unchanged (Figure 29D-E). Additionally, hematopoietic progenitors (Figure 29B) and their proliferating rate were not affected (data not shown). Similarly, we obtained very similar results with the inducible endothelial-specific mouse line (figure F-I).

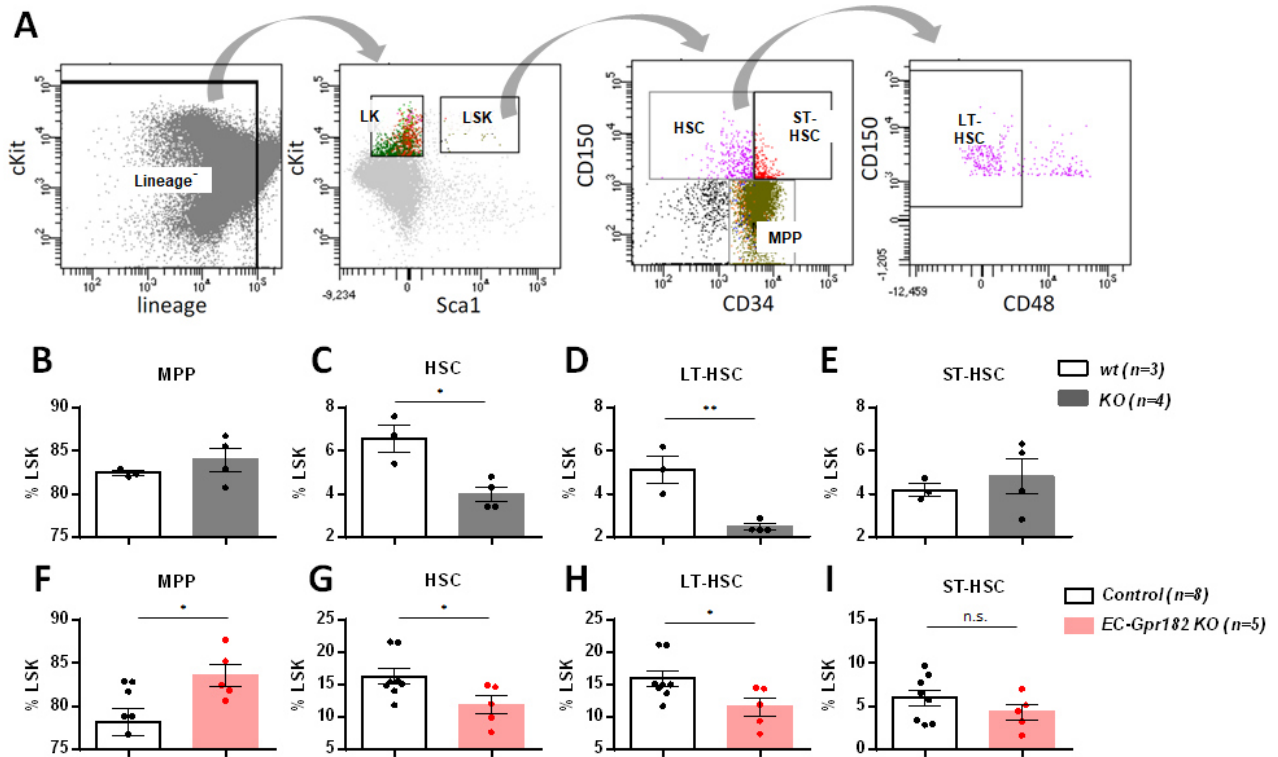


Figure 29: *Gpr182*-deficiency results in decreased bone marrow HSC

Gating strategy used to distinguish the different HSPC subpopulations (A). MPP, HSC, LT-HSC and ST-HSC subpopulations were quantified by flow cytometry in *GPR182*-deficient mice (B-E) and EC-*Gpr182*-KO animals (F-I). Data are means \pm SEM; differences between genotypes were analyzed using paired Student's t-test. n.s., nonsignificant * $P < 0.05$; ** $P < 0.01$

c) Increased extramedullary HSC population

Using flow cytometry, we observed an increased c-kit⁺ population in the spleen of *Gpr182* deficient mice (Figure 30A). Secondly, using the colony-forming unit assay (CFU), we quantified the HSCs *ex vivo* and confirmed the increased splenic HSC population in KO mice (Figure 30B). Furthermore, we obtained comparable results using the inducible endothelial-specific mice (Figure 30C-D).

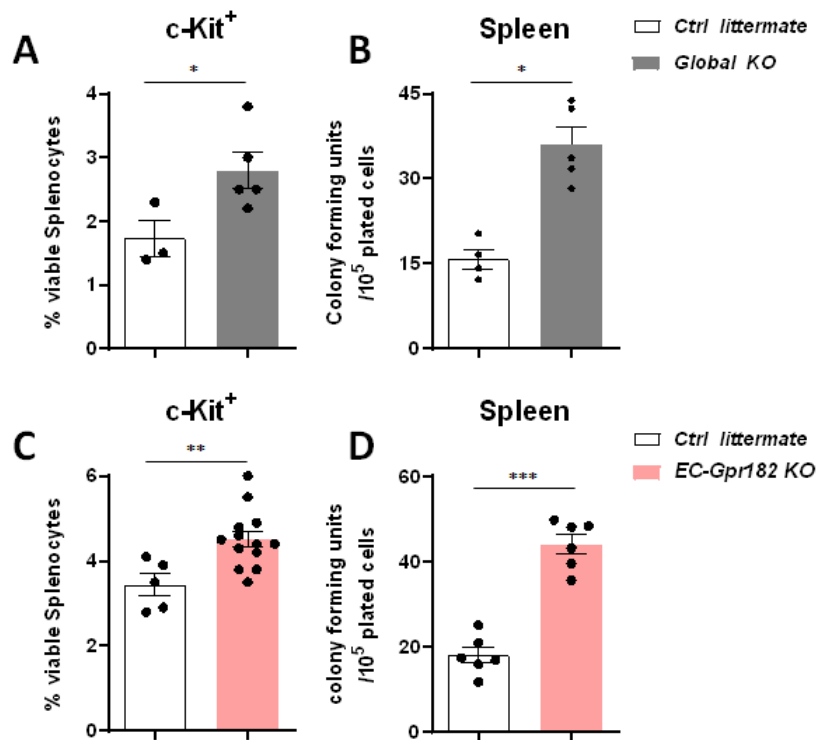


Figure 30: Increased HSC population within the spleen of KO mice

Measurement of the HSC population within the spleen of Gpr182-deficient mice by flow cytometry (A) and by colony-forming unit assay (CFU) (B). Similar experiments were performed using the EC-Gpr182-KO (C-D). Shown are mean values \pm SEM. * $P < 0.05$; ** $P < 0.01$; *** $P < 0.001$. Statistical analysis using an unpaired two-tailed Student's t test.

Subsequently, we questioned whether the splenic HSCs expansion resulted from an *in situ* proliferation of splenic HSC or merely resulted from the settlement toward the spleen of the egressed medullary HSCs.

d) Increased HSC population within the circulation

To test this hypothesis, we quantified the HSC fraction within the bloodstream and noticed a rise in colony-forming units in the blood of *Gpr182* deficient mice (Figure 31A). Furthermore, we made identical observation using the inducible endothelial-specific mouse line (Figure 31B).

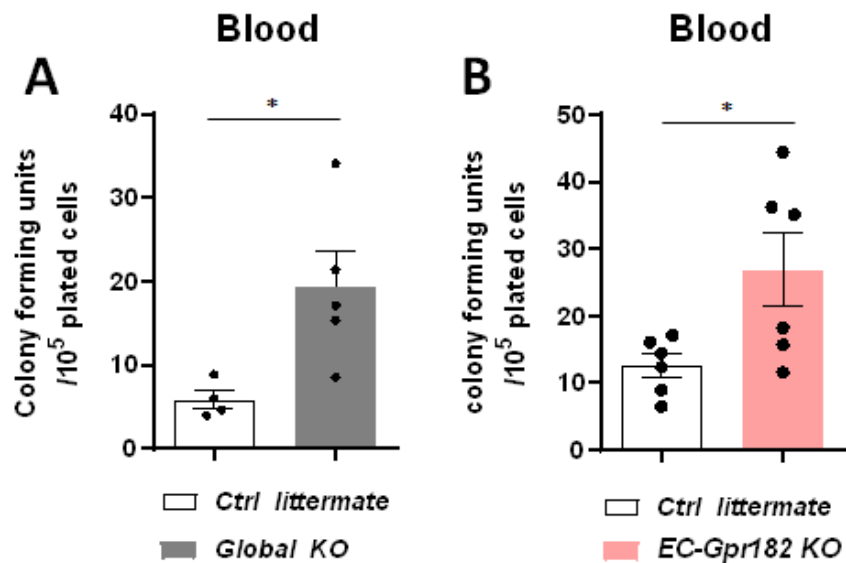


Figure 31: Increased HSC number within the bloodstream

Quantifying the HSC number within the bloodstream of *Gpr182*-deficient mice (A) and EC-*Gpr182*-KO (B) using the colony-forming unit assay (CFU). Shown are mean values \pm SEM. * $P < 0.05$. Statistical analysis using an unpaired two-tailed Student's t test.

7) Model

Altogether these results suggest that GPR182 behaves as a chemokine decoy receptor, shaping the chemokine's extracellular gradient and indirectly supporting an effective migration and maintenance of chemokine-responsive cells. Conversely, the lack of GPR182 results in improper shaping of chemokine gradient and misguided cell migration or cell retention.

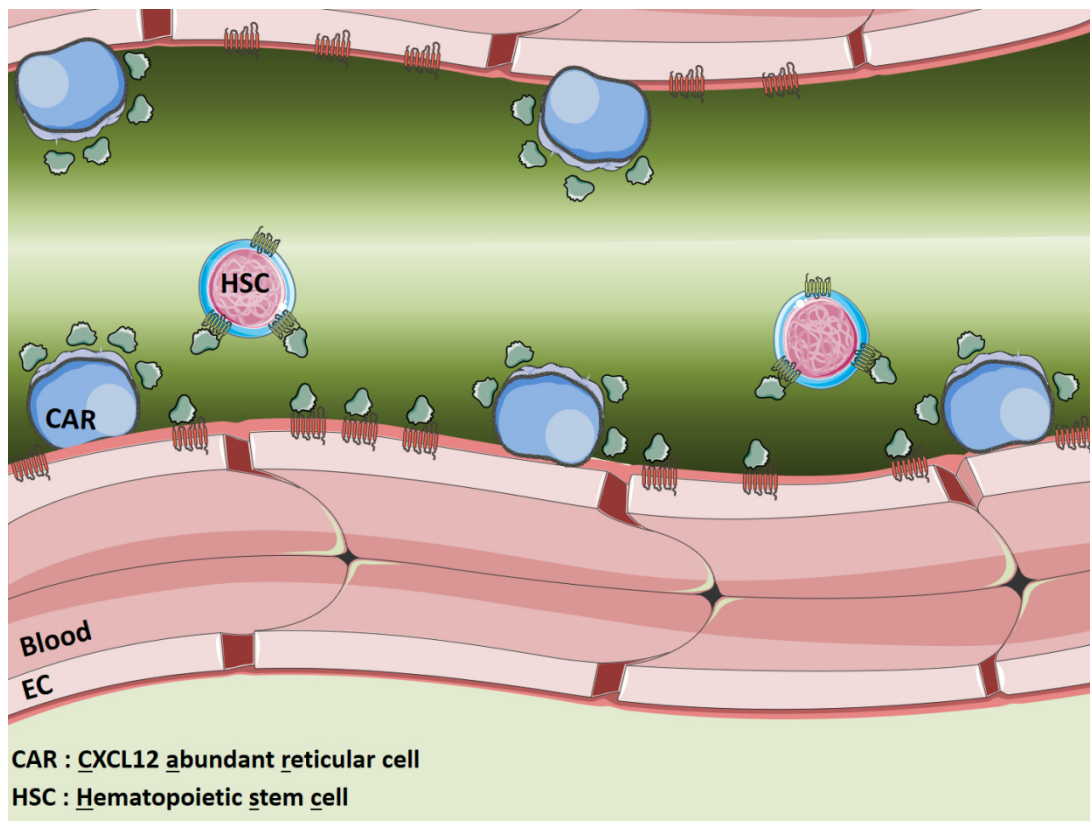


Figure 32: Model of GPR182 behaving as a chemokine decoy receptor

Created with [231]

Considering the bone marrow niche and its GPR182 positive vasculature, the loss of GPR182 implies the loss of an accurate CXCL12 distribution. We believe that in the absence of appropriate CXCL12 dissemination, LT-HSCs would be disoriented, dispersing within the niche and ultimately reaching the bloodstream. Hereafter, the

circulation would carry HSCs away into the splenic sinusoids where they “extravasate” and establish themselves. To sum up, the HSCs egress from the bone marrow and settle in the spleen.

To validate this model, we performed two additional experiments:

First, we studied the engraftment and the maintenance of HSCs of KO donor mice back into a physiological bone marrow niche to confirm that the lack of endothelial GPR182 did not intrinsically alter the HSCs.

Secondly, we studied the location and abundance of CXCL12 within the bone marrow niche to link the egress of HSCs observed in KO mice with the loss of the appropriate distribution of CXCL12.

a) Transplantation

To answer whether the loss of GPR182 affects intrinsically and irreversibly HSCs' behavior, we analyzed the engraftment efficiency and persistence of HSCs from donor knock-out mice and their control littermates back to a healthy HSC niche that expresses GPR182. We observed that HSC engraftment (Figure 32A) and persistence (Figure 32B) within the recipient niche were similar in both groups. Additionally, the RNA sequencing analysis of sorted HSCs from both KO mice and their control littermates did not reveal alterations in the HSCs transcriptome (data not shown).

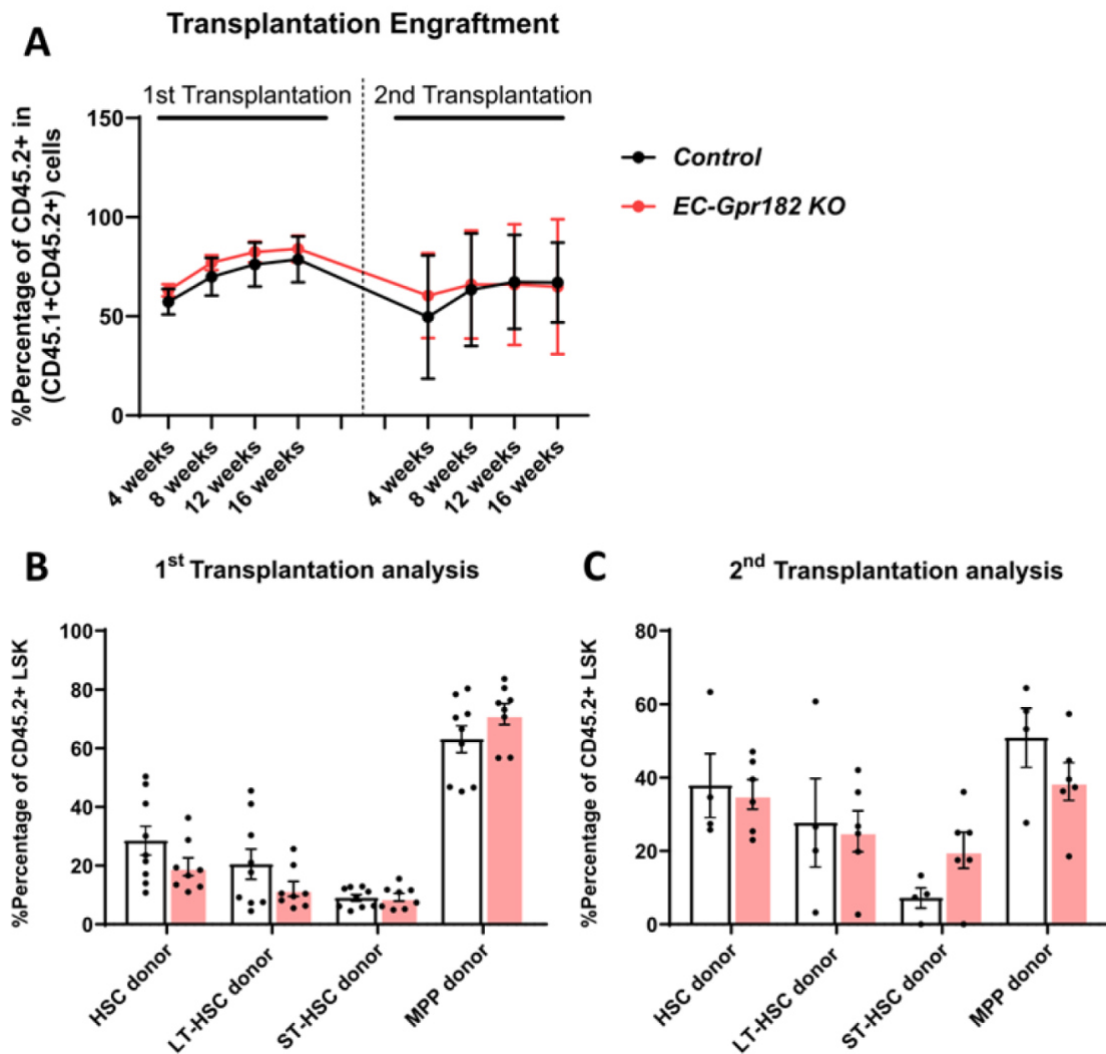


Figure 33: The engraftment and the persistence of *Gpr182-KO* donor- HSCs appears normal

The engraftment of HSC collected from *Gpr182KO* donor and their control littermates was monitored during two successive transplantation experiment (A). The quantitative analysis of the several HSPC subpopulations was performed by flow cytometry at the end of the first, and second transplantation experiment (B-C)

b) CXCL12 concentration and localization are not altered in the bone marrow niche

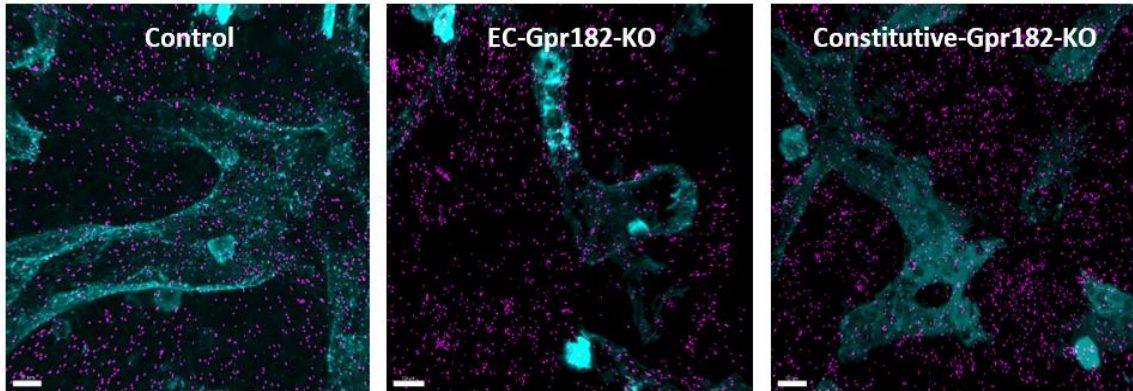
To investigate whether the egress of HSC in knock-out mice is linked to a misshaped distribution of CXCL12, we aimed to locate and quantified CXCL12 within the bone marrow. For this purpose, we requested and welcomed the support from Pr. Dr. Timm Schröder (Department of Biosystems Science and Engineering, ETH Zürich) who, recently analyzed the CXCL12 distribution and abundance within the bone marrow using the proximity ligation assay [176]. Unfortunately, their experiments conducted on global KO mice and inducible endothelial cell-specific mouse line did not reveal any significant alteration in the location nor abundance of CXCL12 in the HSC niche (Figure 33).

Figure 34: The localization and quantification of CXCL12 within the bone marrow niche is not altered by the lack of GPR182

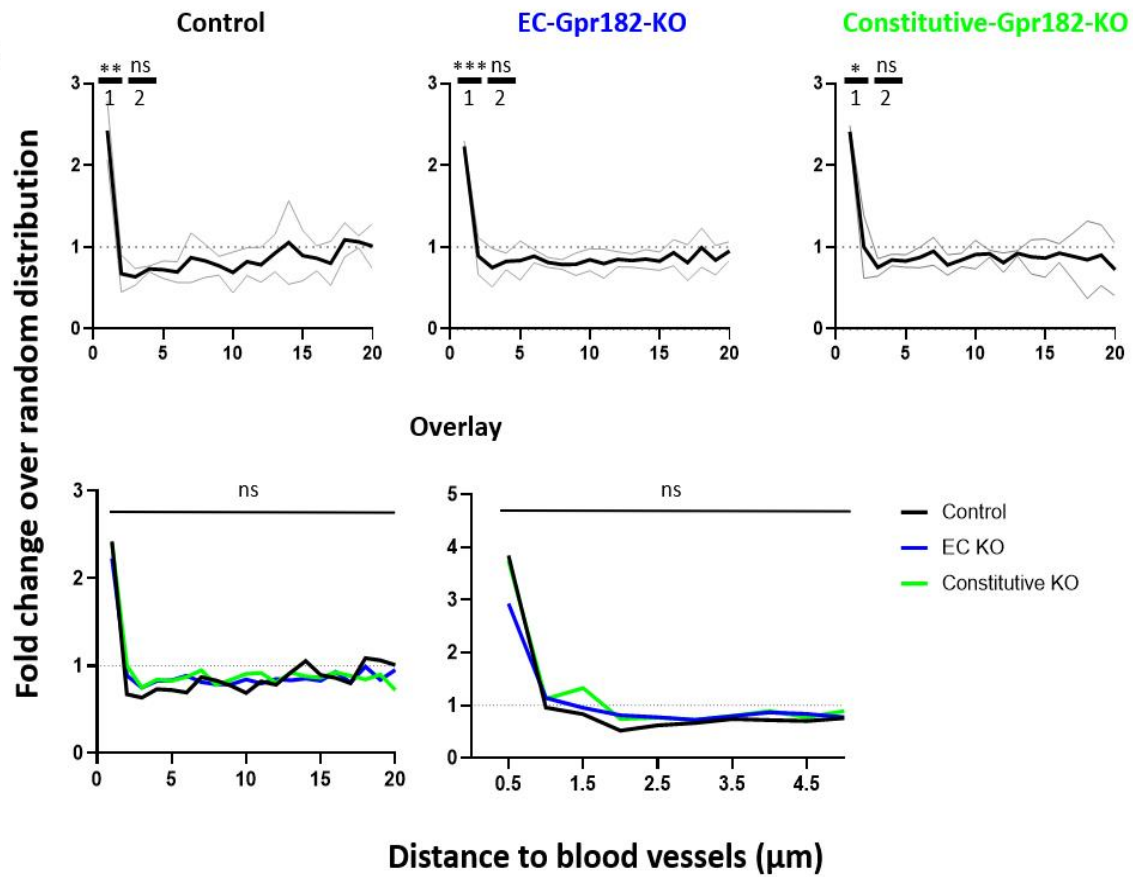
The localization of CXCL12 within the bone marrow niche was performed using the proximity ligation assay (PLA). Representative confocal images showing the CXCL12 distribution in wild-type, global KO, and EC-*Gpr182-KO* animals were taken (A). Quantification analysis were performed to calculate the CXCL12 concentration around the bone marrow vasculature in each of this mouse line (B).

Endomucin CXCL12 (PLA)

A



B



VIII. Discussion

Altogether, the work of this thesis shows that GPR182, an orphan GPCR specifically expressed in the endothelium, is a novel atypical chemokine receptor for the chemokines CXCL10, CXCL12 and CXCL13.

Indeed, an accumulation of evidence allowed us to consider GPR182 as a novel atypical chemokine receptor. First, the closest paralogue of GPR182, ACKR3, is an atypical chemokine receptor for CXCL11 and CXCL12 [2, 51, 177]. Secondly, similarly to all ACKRs, GPR182 lacks the *DRYLAIV* motif within the second intracellular loop [178], which is necessary for coupling to G-protein [101, 179]. Consequently, it was legitimate to observe chemokines' binding to GPR182 without triggering subsequent downstream signaling. Furthermore, the accumulation of chemokines in the plasma of mice lacking the receptor demonstrates that GPR182 functions as a scavenger receptor. Last but not least, we revealed the role of GPR182 in the maintenance and trafficking of chemokine-sensitive cells.

By definition, all ACKRs share some characteristics, mainly: the absence of G-protein signaling and chemokine internalization through β -arrestin recruitment [73, 101]. However, each ACKR exhibits a distinct relationship with β -arrestin. For instance, ACKR1 only interacts with β -arrestin upon ligand stimulation [75] while ACKR2 and ACKR3 have strong basal recruitment of β -arrestin that is strengthened after ligand binding [116, 180, 181]. Conversely, GPR182 display the strongest basal recruitment of β -arrestin, yet this cannot be reinforced upon ligand stimulation. Alongside the different interaction behavior with β -arrestin, the constitutive or ligand-dependent internalization behavior of ACKR diverges [182]. Such discrepancies go against the simplistic dogma that associates β -arrestin with receptor internalization [182]. Intriguingly, β -arrestin seem to carry very diversified roles. As mentioned, β -arrestin has long been connected with GPCR internalization since β -arrestin is a key player in recruiting the machinery for clathrin-coated pits formation and ultimately GPCR desensitization [183]. However, new

pieces of evidence exhibit β -arrestin as a proteic adaptor between GPCRs and E3 ligase [184]. Subsequently, the E3 ligase ubiquitinates the receptor, ending in the fusion of the receptor with the endosome system [185]. Additionally, further studies display that ACKR3 is constitutively ubiquitinated (and interacting with β -arrestin), and the deubiquitylation triggers the receptor internalization [186]. Conclusively, whether there is no doubt that ACKRs lack canonical G-protein signaling, outstanding questions remain to be solved to fully understand the role of β -arrestin for each ACKR likewise their ubiquitination and phosphorylation status function.

Overall, our data indicate that GPR182 plays a role in HSCs maintenance within the bone marrow niche. Given that the CXCL12/CXCR4 axis is recognized to play a crucial role in HSC maintenance [85, 187, 188], the most likely mechanism by which GPR182 retains HSCs is by shaping the extracellular abundance and location of CXCL12. However, our analysis using proximity ligation assay (PLA) did not expose such alteration of CXCL12 distribution in KO mice. Several reasons could explain such observations.

- First, our model suggested that GPR182 shapes CXCL12 gradients by binding and internalizing the chemokines, implying that GPR182 depletes CXCL12 from the matrix. Intriguingly, results obtained by PLA exposed the highest concentration of CXCL12 alongside the vasculature; thereby, validating the perivascular localization of HSCs but contradicting our model. Perhaps, our model should better imagine the vascular wall as a physical barrier, blocking the free-diffusion of CXCL12 to the bloodstream. Indeed, it is highly acknowledged that chemokines eagerly reach the circulation [189], especially when released in highly permeable vascular bed such as the bone marrow sinusoids [190, 191]. Therefore, in a revised model, GPR182 would delimit the presence of the chemokine to the bone marrow niche, thereby avoiding the egress of HSC out of the bone marrow niche.

- Secondly, it is technically unclear whether the PLA result represents the monomeric, dimeric or total CXCL12 which could substantially change the way to interpret the results. While no doubt persists regarding the role supported by CXCL12 in

the HSC niche; however, there is hitherto no investigation that explored the post-translational regulation of CXCL12 in the bone marrow niche.

- Moreover, we interpreted our phenotype based on the interaction between GPR182 and CXCL12. However, our analyses demonstrate that CXCL 10 and CXCL13 have a higher affinity for GPR182 (respectively, K_i : 10 and 9) than CXCL12 (K_d : 41nM). Our understanding of the bone marrow niche homeostasis is still scattered; besides exposing the crucial role of the CXCL12/CXCR4 axis in HSC maintenance, additional factors might certainly be involved. Interestingly, some evidence highlight that compared to other subpopulations, quiescent HSCs specifically express a pool of cytokines including CXCL10, CXCL13 and IFN- γ (IFN- γ : known as an inflammatory marker, but also the precursor of CXCL10) [192, 193], although the role of these chemokines and their receptors remain unexplored. Strikingly, baseline expression of IFN- γ plays a role in HSC mobilization [193], but IFN- γ does not have chemoattractant property underlining the hypothesis that the HSC depletion observed in IFN- γ KO was instead a hidden role of the chemoattractant CXCL10 than a direct role of IFN- γ .

Interestingly, our cytokines' level measurement in the blood suggests that the loss of GPR182 drastically impaired IL-7 and IL-15 homeostasis. The biological functions of these two cytokines remain poorly understood, although they appear to function together [194-197]. For instance, IL-7 and -15 are both expressed by CAR cells and play a role in HSC differentiation [198, 199]. Therefore, it would be appealing to investigate whether the loss of GPR182 alters the CAR cells expression of IL-7 and IL-15 and their role within the HSC niche.

Regardless of the precise mechanism, our data indicate that GPR182 plays a role in the HSC maintenance within the bone marrow niche. Unfortunately, we have no explanation regarding how the medullary hematopoiesis remains unchanged while experiencing the egress of LT-HSC. Moreover, why these egressed HSCs establish themselves in the spleen without triggering extramedullary hematopoiesis persists mysterious.

Besides playing a role in cell retention within a particular specialized environment, our data show that GPR182 may also play a role in pathogens-induced and sterile immunity. First, GPR182 loss of function results in accumulation in the plasma of chemokines

binding GPR182, implying that the lack of the receptor results in less effective chemokines gradients and putatively a reduced leukocytes migration. We considered it too difficult to specifically assess *in vivo* the sharpness of the CXCL12 gradient because of the versatile function of CXCL12 [200]. However, a plethora of studies restrict the function of CXCL10 to the migration of T cells, macrophages, dendritic cells and NK cells [201-203] and CXCL13 to the migration of B lymphocytes [204-207]. Therefore, the reduced extravasation of macrophages, T and B lymphocytes during our adoptive transfer experiment is consistent with the reduced efficiency of CXCL10 and -13 gradients in deficient mice. Similarly, reduced leukocytes recruitment within the tumor and thus reduced tumor immunity would be consistent with the bolder development of lung tumors in deficient mice [208-210]. However, further analysis would be required to demonstrate that a reduced leukocytes infiltration within the tumor is the root of enhanced tumor growth.

Finally, we could observe a moderate “splenomegaly” in deficient mice. Regarding the possible patho-physiological mechanisms causing splenomegaly [211], it appears most likely that the increased splenic size observed in GPR182 KO mice is a consequence of increased immunologic activity. Additionally, we observed alterations in the leukocyte composition of the spleen. As previously described, the reduced trafficking of CFSE positive leukocytes into the spleen in a brief period is consistent with the loss of gradient efficiency. However, following a prolonged duration of GPR182 deficiency, we could observe an accumulation of splenic macrophages that we cannot explain. Markedly, the macrophages accumulation seems correlated with the plasma level of CXCL10 though we cannot explain it. However, splenic macrophages are known for the homing and maintenance of splenic T cells through the expression of CXCL10 [212-214], which is consistent with the fact that we repeatedly noticed a reduction of T cells in the spleen of KO mice. Finally, we detected a drop in B cells composition three days after the deletion of GPR182. Such observation is consistent with the fact that CXCL13 is required for the homing and retention within the spleen [215, 216], although we noticed a compensation of the loss of CXCL13 function on prolonged duration and global KO.

Alongside the internalization of CXCL10, CXCL12 and CXCL13 GPR182 is indirectly involved in the CXCL10/CXCR3, CXCL12/CXCR4/ACKR3 and CXCL13/CXCR5 axes.

Such impairments might certainly be involved in a myriad of disease including inflammation such as non-exhaustively: cancer, non-alcoholic steatohepatitis (NASH), atherosclerosis, post-infarct induced heart failure, autoimmune encephalomyelitis (EAE model). Therefore, numerous and diversified investigations are required to shed light on the involvement of GPR182 in these pathologies.

GPR182 and ACKR3 differ from others ACKRs because of the relatively low number of ligands they bind: three chemokines for GPR182 and only two for ACKR3, while ACKR1 and ACKR2 roughly bind twenty chemokines each. Furthermore, GPR182 and ACKR3 are not entirely related to the chemokine receptor family since their position within the GPCR phylogenetic tree is on a separated branch between chemokine receptors and vaso-modulator receptors [2]. Indeed, ACKR3 is also known for scavenging adrenomedullin, a vasodilator peptide [Ref]. Although GPR182 has previously been proposed to bind adrenomedullin, the idea was then rejected due to its inability to signal through canonical pathways in response to adrenomedullin [48]. The demonstration that ACKR3 not only binds chemokines but also adrenomedullin permit another study to propose ACKR3 as a broad-scavenger receptor that also internalizes several opioid peptides [120]. Conclusively, we may question GPR182's capacity to scavenge other class of ligands such as opioid peptides and reconsider whether GPR182 scavenging ability of adrenomedullin. In addition, a genome-wide RNAi screening identified GPR182 as a potential scavenger receptor for LDL [217]. Coherently, our screening exposed increased β -arrestin recruitment to GPR182 in response to KOdiA-PC which, is a phospholipid found in LDL and oxLDL particles [218, 219]. Interestingly, KOdiA-PC is an extremely powerful epitope recognized by CD36 positive macrophages, responsible for the uptake of oxLDL and the establishment of atherosclerotic plates [218, 219]. Therefore, it would be appealing to test whether GPR182 binds and scavenges KOdiA-PC.

Our research starting from scratch barely uncovers few aspects of the *in vivo* functions of GPR182, consequently ignoring several areas which could be of interest. For example, it is widely accepted that an essential mechanism of GPCRs regulation is

receptor dimerization [220-222]. Here, we abstained from searching whether GPR182 is preferably found as a monomer or homodimers. More importantly, GPCR heterodimerization permits a quasi-infinite possibility in receptor signaling regulations. Several reports expose “conventional” heterodimerization between ACKR3 and CXCR4 [223]. However, with the recent evidence that ACKR3 is an opioid peptides receptor, no investigation attempted yet to expose ACKR3/opioid receptor dimers. However, previous work showed dimerization between CXCR4 and the delta-opioid receptor [224]. However, some studies highlighted ACKR3 heterodimerization and oligomerization with α -adrenergic receptors and CXCR4/ α -adrenergic receptors respectively [225]. Besides GPCR dimerization, ACKR3 interacts with receptor-activity-modifying protein-2 (RAMP2) and RAMP3 [120, 121, 174]. While the interaction of RAMPs does not directly modify the receptor signaling, it enhanced the plasma localization of ACKR3 [121]. If we did not seek whether GPR182 oligo/heterodimerizes, it would be reasonable to investigate a potential interaction between GPR182 and CXCR3, CXCR4 and CXCR5. In addition, regarding the wide range of ACKR3 functions, we cannot exclude the oligo/heterodimerization of GPR182 with non-chemokine GPCRs. Finally, if RAMPs did not enhance the signaling of GPR182, we could have investigated whether RAMPs would affect the recruitment of β -arrestin to GPR182 and consequently the plasma membrane location of the receptor.

Besides GPR182 potential regulation by receptor dimerization or RAMP interaction, we could have study the GPR182 functions within the organ which expresses the most GPR182: the liver and the lung. The role mediated by chemokines in the liver has been studied broadly. For instance, the CXCL12/CXCR4/ACKR3 axis is involved in regenerative processes following acute liver disease [226]. Therefore, it would be appealing to question whether GPR182 is a novel member of this trio. Nevertheless, this report shows that ACKR3 is not expressed by liver sinusoidal endothelial cells at baseline, and its expression is triggered only after liver damages. Since GPR182 is constitutively and highly expressed by liver endothelial cells and CXCL12 constitutively expressed in the healthy liver [227], it would be interesting to investigate their physiological function(s). Strikingly, the liver is the organ expressing the most GPR182 and CXCL13. CXCL13 was shown to recruit CXCR5 positive T cell in response to

hepatitis B virus [228]; however, constitutively high expression of a homeostatic chemokine like CXCL13 might certainly support additional hepatic functions than immune vigilance against hepatic viruses. As previously mentioned, it would also be a matter of interest to demonstrate whether GPR182 scavenges LDL. Given the substantial metabolic role of the liver in LDL uptake [229, 230]. Finally, we sparsely uncovered the deleterious effect of pulmonary GPR182 in tumor growth. Therefore, innumerable facets of GPR182 remained to be questioned and investigated.

Regarding the potential of GPR182 to be a broad scavenger receptor such as ACKR3, it would be attractive to design an educated approach to potentially identify novel ligands. One method would consist in studying the binding pocket of GPR182. For instance, understanding the chemicals properties required for binding a receptor has previously allowed the identification of novel ligands for ACKR3 [120]. Additionally, having a better understanding of the binding pocket of GPR182 would allow designing a potent and specific antagonist. Such antagonist would embody a new tool for further *in vitro* and *in vivo* study. Finally, GPCRs are recognized as the most successful target for drug design for clinical use [29]. For instance, our data indicate the role of GPR182 in leukocytes recruitment to potential inflammation sites. Therefore, we could target pharmacologically various pathological conditions involving excessive or sustained inflammation to lessen undesired inflammation and inflammation-induced fibrosis.

IX. Bibliography

1. Pflieger, J., K. Gresham, and W.J. Koch, *G protein-coupled receptor kinases as therapeutic targets in the heart*. Nat Rev Cardiol, 2019. **16**(10): p. 612-622.
2. Kufareva, I., et al., *Status of GPCR modeling and docking as reflected by community-wide GPCR Dock 2010 assessment*. Structure, 2011. **19**(8): p. 1108-26.
3. Kroeze, W.K., et al., *PRESTO-Tango as an open-source resource for interrogation of the druggable human GPCRome*. Nat Struct Mol Biol, 2015. **22**(5): p. 362-9.
4. Regard, J.B., I.T. Sato, and S.R. Coughlin, *Anatomical profiling of G protein-coupled receptor expression*. Cell, 2008. **135**(3): p. 561-71.
5. Rieger, M.A. and T. Schroeder, *Hematopoiesis*. Cold Spring Harb Perspect Biol, 2012. **4**(12).
6. Szekanecz, Z. and A.E. Koch, *Successes and failures of chemokine-pathway targeting in rheumatoid arthritis*. Nat Rev Rheumatol, 2016. **12**(1): p. 5-13.
7. Sahingur, S.E. and W.A. Yeudall, *Chemokine function in periodontal disease and oral cavity cancer*. Front Immunol, 2015. **6**: p. 214.
8. Crane, G.M., E. Jeffery, and S.J. Morrison, *Adult haematopoietic stem cell niches*. Nat Rev Immunol, 2017. **17**(9): p. 573-590.
9. Fredriksson, R., et al., *The G-protein-coupled receptors in the human genome form five main families. Phylogenetic analysis, paralogon groups, and fingerprints*. Mol Pharmacol, 2003. **63**(6): p. 1256-72.
10. Wettschureck, N. and S. Offermanns, *Mammalian G proteins and their cell type specific functions*. Physiol Rev, 2005. **85**(4): p. 1159-204.
11. Pierce, K.L., R.T. Premont, and R.J. Lefkowitz, *Seven-transmembrane receptors*. Nat Rev Mol Cell Biol, 2002. **3**(9): p. 639-50.
12. Schioth, H.B. and R. Fredriksson, *The GRAFS classification system of G-protein coupled receptors in comparative perspective*. Gen Comp Endocrinol, 2005. **142**(1-2): p. 94-101.
13. Kakarala, K.K. and K. Jamil, *Sequence-structure based phylogeny of GPCR Class A Rhodopsin receptors*. Mol Phylogenet Evol, 2014. **74**: p. 66-96.
14. Hollenstein, K., et al., *Insights into the structure of class B GPCRs*. Trends Pharmacol Sci, 2014. **35**(1): p. 12-22.
15. Chun, L., W.H. Zhang, and J.F. Liu, *Structure and ligand recognition of class C GPCRs*. Acta Pharmacol Sin, 2012. **33**(3): p. 312-23.
16. Seifert, J.R. and M. Mlodzik, *Frizzled/PCP signalling: a conserved mechanism regulating cell polarity and directed motility*. Nat Rev Genet, 2007. **8**(2): p. 126-38.
17. Strutt, H. and D. Strutt, *Differential stability of flamingo protein complexes underlies the establishment of planar polarity*. Curr Biol, 2008. **18**(20): p. 1555-64.
18. Bjarnadottir, T.K., R. Fredriksson, and H.B. Schioth, *The adhesion GPCRs: a unique family of G protein-coupled receptors with important roles in both central and peripheral tissues*. Cell Mol Life Sci, 2007. **64**(16): p. 2104-19.
19. Bjarnadottir, T.K., et al., *The human and mouse repertoire of the adhesion family of G-protein-coupled receptors*. Genomics, 2004. **84**(1): p. 23-33.

20. Lin, H.H., et al., *Autocatalytic cleavage of the EMR2 receptor occurs at a conserved G protein-coupled receptor proteolytic site motif*. J Biol Chem, 2004. **279**(30): p. 31823-32.
21. Sun, J.P., et al., *The very large G protein coupled receptor (Vlgr1) in hair cells*. J Mol Neurosci, 2013. **50**(1): p. 204-14.
22. Alexander, S.P.H., et al., *THE CONCISE GUIDE TO PHARMACOLOGY 2019/20: G protein-coupled receptors*. Br J Pharmacol, 2019. **176** Suppl 1: p. S21-S141.
23. Brinks, H.L. and A.D. Eckhart, *Regulation of GPCR signaling in hypertension*. Biochim Biophys Acta, 2010. **1802**(12): p. 1268-75.
24. Jones, B., et al., *Targeting GLP-1 receptor trafficking to improve agonist efficacy*. Nat Commun, 2018. **9**(1): p. 1602.
25. Danial, C., et al., *An Investigator-Initiated Open-Label Trial of Sonidegib in Advanced Basal Cell Carcinoma Patients Resistant to Vismodegib*. Clin Cancer Res, 2016. **22**(6): p. 1325-9.
26. Cummings, J., et al., *Pimavanserin for patients with Parkinson's disease psychosis: a randomised, placebo-controlled phase 3 trial*. Lancet, 2014. **383**(9916): p. 533-40.
27. Meltzer, H.Y., et al., *A randomized, double-blind, placebo-controlled trial of aripiprazole lauroxil in acute exacerbation of schizophrenia*. J Clin Psychiatry, 2015. **76**(8): p. 1085-90.
28. Earley, W., et al., *Cariprazine Treatment of Bipolar Depression: A Randomized Double-Blind Placebo-Controlled Phase 3 Study*. Am J Psychiatry, 2019. **176**(6): p. 439-448.
29. Hauser, A.S., et al., *Trends in GPCR drug discovery: new agents, targets and indications*. Nat Rev Drug Discov, 2017. **16**(12): p. 829-842.
30. Laschet, C., N. Dupuis, and J. Hanson, *The G protein-coupled receptors deorphanization landscape*. Biochem Pharmacol, 2018. **153**: p. 62-74.
31. Rodbell, M., et al., *The glucagon-sensitive adenyl cyclase system in plasma membranes of rat liver. V. An obligatory role of guanylnucleotides in glucagon action*. J Biol Chem, 1971. **246**(6): p. 1877-82.
32. Boyer, J.L., G.L. Waldo, and T.K. Harden, *Beta gamma-subunit activation of G-protein-regulated phospholipase C*. J Biol Chem, 1992. **267**(35): p. 25451-6.
33. Birnbaumer, L., *Expansion of signal transduction by G proteins. The second 15 years or so: from 3 to 16 alpha subunits plus betagamma dimers*. Biochim Biophys Acta, 2007. **1768**(4): p. 772-93.
34. Sunahara, R.K., C.W. Dessauer, and A.G. Gilman, *Complexity and diversity of mammalian adenylyl cyclases*. Annu Rev Pharmacol Toxicol, 1996. **36**: p. 461-80.
35. Plagge, A., G. Kelsey, and E.L. Germain-Lee, *Physiological functions of the imprinted Gnas locus and its protein variants Galpha(s) and XLalpha(s) in human and mouse*. J Endocrinol, 2008. **196**(2): p. 193-214.
36. Katada, T., et al., *The inhibitory guanine nucleotide-binding regulatory component of adenylate cyclase. Properties and function of the purified protein*. J Biol Chem, 1984. **259**(6): p. 3568-77.
37. Chikumi, H., et al., *Potent activation of RhoA by Galpha q and Gq-coupled receptors*. J Biol Chem, 2002. **277**(30): p. 27130-4.
38. Smrcka, A.V., et al., *Regulation of polyphosphoinositide-specific phospholipase C activity by purified Gq*. Science, 1991. **251**(4995): p. 804-7.

39. Dixon, R.A., et al., *Cloning of the gene and cDNA for mammalian beta-adrenergic receptor and homology with rhodopsin*. Nature, 1986. **321**(6065): p. 75-9.
40. Booden, M.A., D.P. Siderovski, and C.J. Der, *Leukemia-associated Rho guanine nucleotide exchange factor promotes G alpha q-coupled activation of RhoA*. Mol Cell Biol, 2002. **22**(12): p. 4053-61.
41. Logothetis, D.E., et al., *The beta gamma subunits of GTP-binding proteins activate the muscarinic K⁺ channel in heart*. Nature, 1987. **325**(6102): p. 321-6.
42. Garcia, D.E., et al., *G-protein beta-subunit specificity in the fast membrane-delimited inhibition of Ca²⁺ channels*. J Neurosci, 1998. **18**(22): p. 9163-70.
43. Rhee, S.G., *Regulation of phosphoinositide-specific phospholipase C*. Annu Rev Biochem, 2001. **70**: p. 281-312.
44. Gao, B.N. and A.G. Gilman, *Cloning and expression of a widely distributed (type IV) adenylyl cyclase*. Proc Natl Acad Sci U S A, 1991. **88**(22): p. 10178-82.
45. Wing, M.R., et al., *Activation of phospholipase C-epsilon by heterotrimeric G protein betagamma-subunits*. J Biol Chem, 2001. **276**(51): p. 48257-61.
46. Kurose, H., *Galpha12 and Galpha13 as key regulatory mediator in signal transduction*. Life Sci, 2003. **74**(2-3): p. 155-61.
47. Kapas, S., K.J. Catt, and A.J. Clark, *Cloning and expression of cDNA encoding a rat adrenomedullin receptor*. J Biol Chem, 1995. **270**(43): p. 25344-7.
48. Kennedy, S.P., et al., *Expression of the rat adrenomedullin receptor or a putative human adrenomedullin receptor does not correlate with adrenomedullin binding or functional response*. Biochem Biophys Res Commun, 1998. **244**(3): p. 832-7.
49. Sumanas, S., T. Joraniak, and S. Lin, *Identification of novel vascular endothelial-specific genes by the microarray analysis of the zebrafish cloche mutants*. Blood, 2005. **106**(2): p. 534-41.
50. Xiao, L., et al., *Identification of a stable molecular signature in mammary tumor endothelial cells that persists in vitro*. Angiogenesis, 2014. **17**(3): p. 511-8.
51. Kechele, D.O., et al., *Orphan Gpr182 suppresses ERK-mediated intestinal proliferation during regeneration and adenoma formation*. J Clin Invest, 2017. **127**(2): p. 593-607.
52. Schmid, W., et al., *Patient's and health care provider's perspectives on music therapy in palliative care - an integrative review*. BMC Palliat Care, 2018. **17**(1): p. 32.
53. Griffith, J.W., C.L. Sokol, and A.D. Luster, *Chemokines and chemokine receptors: positioning cells for host defense and immunity*. Annu Rev Immunol, 2014. **32**: p. 659-702.
54. Barker, C.E., et al., *CCL2 nitration is a negative regulator of chemokine-mediated inflammation*. Sci Rep, 2017. **7**: p. 44384.
55. Loos, T., et al., *Citrullination of CXCL10 and CXCL11 by peptidylarginine deiminase: a naturally occurring posttranslational modification of chemokines and new dimension of immunoregulation*. Blood, 2008. **112**(7): p. 2648-56.
56. Proost, P., et al., *Citrullination of CXCL8 by peptidylarginine deiminase alters receptor usage, prevents proteolysis, and dampens tissue inflammation*. J Exp Med, 2008. **205**(9): p. 2085-97.
57. Garton, K.J., et al., *Tumor necrosis factor-alpha-converting enzyme (ADAM17) mediates the cleavage and shedding of fractalkine (CX3CL1)*. J Biol Chem, 2001. **276**(41): p. 37993-8001.

58. Tsou, C.L., C.A. Haskell, and I.F. Charo, *Tumor necrosis factor-alpha-converting enzyme mediates the inducible cleavage of fractalkine*. J Biol Chem, 2001. **276**(48): p. 44622-6.
59. Hundhausen, C., et al., *The disintegrin-like metalloproteinase ADAM10 is involved in constitutive cleavage of CX3CL1 (fractalkine) and regulates CX3CL1-mediated cell-cell adhesion*. Blood, 2003. **102**(4): p. 1186-95.
60. Gough, P.J., et al., *A disintegrin and metalloproteinase 10-mediated cleavage and shedding regulates the cell surface expression of CXC chemokine ligand 16*. J Immunol, 2004. **172**(6): p. 3678-85.
61. Abel, S., et al., *The transmembrane CXC-chemokine ligand 16 is induced by IFN-gamma and TNF-alpha and shed by the activity of the disintegrin-like metalloproteinase ADAM10*. J Immunol, 2004. **172**(10): p. 6362-72.
62. Van Lint, P. and C. Libert, *Chemokine and cytokine processing by matrix metalloproteinases and its effect on leukocyte migration and inflammation*. J Leukoc Biol, 2007. **82**(6): p. 1375-81.
63. Janssens, R., S. Struyf, and P. Proost, *The unique structural and functional features of CXCL12*. Cell Mol Immunol, 2018. **15**(4): p. 299-311.
64. Connell, B.J., et al., *Heparan sulfate differentially controls CXCL12alpha- and CXCL12gamma-mediated cell migration through differential presentation to their receptor CXCR4*. Sci Signal, 2016. **9**(452): p. ra107.
65. Sarris, M., et al., *Inflammatory chemokines direct and restrict leukocyte migration within live tissues as glycan-bound gradients*. Curr Biol, 2012. **22**(24): p. 2375-82.
66. Weber, M., et al., *Interstitial dendritic cell guidance by haptotactic chemokine gradients*. Science, 2013. **339**(6117): p. 328-32.
67. Monneau, Y., F. Arenzana-Seisdedos, and H. Lortat-Jacob, *The sweet spot: how GAGs help chemokines guide migrating cells*. J Leukoc Biol, 2016. **99**(6): p. 935-53.
68. Salanga, C.L. and T.M. Handel, *Chemokine oligomerization and interactions with receptors and glycosaminoglycans: the role of structural dynamics in function*. Exp Cell Res, 2011. **317**(5): p. 590-601.
69. Dyer, D.P., et al., *The dependence of chemokine-glycosaminoglycan interactions on chemokine oligomerization*. Glycobiology, 2016. **26**(3): p. 312-26.
70. Liang, W.G., et al., *Structural basis for oligomerization and glycosaminoglycan binding of CCL5 and CCL3*. Proc Natl Acad Sci U S A, 2016. **113**(18): p. 5000-5.
71. von Hundelshausen, P., et al., *Heterophilic interactions of platelet factor 4 and RANTES promote monocyte arrest on endothelium*. Blood, 2005. **105**(3): p. 924-30.
72. Koenen, R.R., et al., *Disrupting functional interactions between platelet chemokines inhibits atherosclerosis in hyperlipidemic mice*. Nat Med, 2009. **15**(1): p. 97-103.
73. Hughes, C.E. and R.J.B. Nibbs, *A guide to chemokines and their receptors*. FEBS J, 2018. **285**(16): p. 2944-2971.
74. Hauser, M.A., et al., *Inflammation-Induced CCR7 Oligomers Form Scaffolds to Integrate Distinct Signaling Pathways for Efficient Cell Migration*. Immunity, 2016. **44**(1): p. 59-72.

75. Chakera, A., et al., *The duffy antigen/receptor for chemokines exists in an oligomeric form in living cells and functionally antagonizes CCR5 signaling through hetero-oligomerization*. Mol Pharmacol, 2008. **73**(5): p. 1362-70.
76. Mellado, M., et al., *Chemokine receptor homo- or heterodimerization activates distinct signaling pathways*. EMBO J, 2001. **20**(10): p. 2497-507.
77. Percherancier, Y., et al., *Bioluminescence resonance energy transfer reveals ligand-induced conformational changes in CXCR4 homo- and heterodimers*. J Biol Chem, 2005. **280**(11): p. 9895-903.
78. Sohy, D., et al., *Hetero-oligomerization of CCR2, CCR5, and CXCR4 and the protean effects of "selective" antagonists*. J Biol Chem, 2009. **284**(45): p. 31270-9.
79. Chen, C., et al., *Heterodimerization and cross-desensitization between the mu-opioid receptor and the chemokine CCR5 receptor*. Eur J Pharmacol, 2004. **483**(2-3): p. 175-86.
80. Tripathi, A., et al., *Heteromerization of chemokine (C-X-C motif) receptor 4 with alpha1A/B-adrenergic receptors controls alpha1-adrenergic receptor function*. Proc Natl Acad Sci U S A, 2015. **112**(13): p. E1659-68.
81. Kleist, A.B., et al., *New paradigms in chemokine receptor signal transduction: Moving beyond the two-site model*. Biochem Pharmacol, 2016. **114**: p. 53-68.
82. Kufareva, I., C.L. Salanga, and T.M. Handel, *Chemokine and chemokine receptor structure and interactions: implications for therapeutic strategies*. Immunol Cell Biol, 2015. **93**(4): p. 372-83.
83. Bachelerie, F., et al., *International Union of Basic and Clinical Pharmacology. [corrected]. LXXXIX. Update on the extended family of chemokine receptors and introducing a new nomenclature for atypical chemokine receptors*. Pharmacol Rev, 2014. **66**(1): p. 1-79.
84. Kehrl, J.H., *Chemoattractant receptor signaling and the control of lymphocyte migration*. Immunol Res, 2006. **34**(3): p. 211-27.
85. Sugiyama, T., et al., *Maintenance of the hematopoietic stem cell pool by CXCL12-CXCR4 chemokine signaling in bone marrow stromal cell niches*. Immunity, 2006. **25**(6): p. 977-88.
86. Gerszten, R.E., et al., *MCP-1 and IL-8 trigger firm adhesion of monocytes to vascular endothelium under flow conditions*. Nature, 1999. **398**(6729): p. 718-23.
87. Shimaoka, T., et al., *Cell surface-anchored SR-PSOX/CXC chemokine ligand 16 mediates firm adhesion of CXC chemokine receptor 6-expressing cells*. J Leukoc Biol, 2004. **75**(2): p. 267-74.
88. Kim, C.S., et al., *Potential involvement of CCL23 in atherosclerotic lesion formation/progression by the enhancement of chemotaxis, adhesion molecule expression, and MMP-2 release from monocytes*. Inflamm Res, 2011. **60**(9): p. 889-95.
89. Escribano, C., C. Delgado-Martin, and J.L. Rodriguez-Fernandez, *CCR7-dependent stimulation of survival in dendritic cells involves inhibition of GSK3beta*. J Immunol, 2009. **183**(10): p. 6282-95.
90. Lopez-Cotarelo, P., et al., *A novel MEK-ERK-AMPK signaling axis controls chemokine receptor CCR7-dependent survival in human mature dendritic cells*. J Biol Chem, 2015. **290**(2): p. 827-40.

91. Delgado-Martin, C., et al., *Chemokine CXCL12 uses CXCR4 and a signaling core formed by bifunctional Akt, extracellular signal-regulated kinase (ERK)1/2, and mammalian target of rapamycin complex 1 (mTORC1) proteins to control chemotaxis and survival simultaneously in mature dendritic cells.* J Biol Chem, 2011. **286**(43): p. 37222-36.
92. Ploix, C., D. Lo, and M.J. Carson, *A ligand for the chemokine receptor CCR7 can influence the homeostatic proliferation of CD4 T cells and progression of autoimmunity.* J Immunol, 2001. **167**(12): p. 6724-30.
93. Whiting, D., et al., *Chemokine monokine induced by IFN-gamma/CXC chemokine ligand 9 stimulates T lymphocyte proliferation and effector cytokine production.* J Immunol, 2004. **172**(12): p. 7417-24.
94. Karlmark, K.R., et al., *The fractalkine receptor CX(3)CR1 protects against liver fibrosis by controlling differentiation and survival of infiltrating hepatic monocytes.* Hepatology, 2010. **52**(5): p. 1769-82.
95. Schaerli, P., et al., *Cutaneous CXCL14 targets blood precursors to epidermal niches for Langerhans cell differentiation.* Immunity, 2005. **23**(3): p. 331-42.
96. Sanchez-Martin, L., et al., *The chemokine CXCL12 regulates monocyte-macrophage differentiation and RUNX3 expression.* Blood, 2011. **117**(1): p. 88-97.
97. Gibbons, D., et al., *Interleukin-8 (CXCL8) production is a signatory T cell effector function of human newborn infants.* Nat Med, 2014. **20**(10): p. 1206-10.
98. Aliberti, J., et al., *CCR5 provides a signal for microbial induced production of IL-12 by CD8 alpha+ dendritic cells.* Nat Immunol, 2000. **1**(1): p. 83-7.
99. Elsner, J., et al., *Human eotaxin represents a potent activator of the respiratory burst of human eosinophils.* Eur J Immunol, 1996. **26**(8): p. 1919-25.
100. Walz, A., et al., *[Ca²⁺]_i changes and respiratory burst in human neutrophils and monocytes induced by NAP-1/interleukin-8, NAP-2, and gro/MGSA.* J Leukoc Biol, 1991. **50**(3): p. 279-86.
101. Nibbs, R.J. and G.J. Graham, *Immune regulation by atypical chemokine receptors.* Nat Rev Immunol, 2013. **13**(11): p. 815-29.
102. Novitzky-Basso, I. and A. Rot, *Duffy antigen receptor for chemokines and its involvement in patterning and control of inflammatory chemokines.* Front Immunol, 2012. **3**: p. 266.
103. Rot, A., *Contribution of Duffy antigen to chemokine function.* Cytokine Growth Factor Rev, 2005. **16**(6): p. 687-94.
104. Lee, J.S., et al., *Duffy antigen facilitates movement of chemokine across the endothelium in vitro and promotes neutrophil transmigration in vitro and in vivo.* J Immunol, 2003. **170**(10): p. 5244-51.
105. Pruenster, M., et al., *The Duffy antigen receptor for chemokines transports chemokines and supports their promigratory activity.* Nat Immunol, 2009. **10**(1): p. 101-8.
106. Reutershan, J., et al., *DARC on RBC limits lung injury by balancing compartmental distribution of CXC chemokines.* Eur J Immunol, 2009. **39**(6): p. 1597-607.
107. Mei, J., et al., *CXCL5 regulates chemokine scavenging and pulmonary host defense to bacterial infection.* Immunity, 2010. **33**(1): p. 106-17.

108. Schnabel, R.B., et al., *Duffy antigen receptor for chemokines (Darc) polymorphism regulates circulating concentrations of monocyte chemoattractant protein-1 and other inflammatory mediators*. *Blood*, 2010. **115**(26): p. 5289-99.
109. Miller, L.H., et al., *Erythrocyte receptors for (Plasmodium knowlesi) malaria: Duffy blood group determinants*. *Science*, 1975. **189**(4202): p. 561-3.
110. Horuk, R., et al., *A receptor for the malarial parasite Plasmodium vivax: the erythrocyte chemokine receptor*. *Science*, 1993. **261**(5125): p. 1182-4.
111. Nedelec, Y., et al., *Genetic Ancestry and Natural Selection Drive Population Differences in Immune Responses to Pathogens*. *Cell*, 2016. **167**(3): p. 657-669 e21.
112. Quach, H., et al., *Genetic Adaptation and Neandertal Admixture Shaped the Immune System of Human Populations*. *Cell*, 2016. **167**(3): p. 643-656 e17.
113. Bonecchi, R., et al., *Differential recognition and scavenging of native and truncated macrophage-derived chemokine (macrophage-derived chemokine/CC chemokine ligand 22) by the D6 decoy receptor*. *J Immunol*, 2004. **172**(8): p. 4972-6.
114. Savino, B., et al., *Recognition versus adaptive up-regulation and degradation of CC chemokines by the chemokine decoy receptor D6 are determined by their N-terminal sequence*. *J Biol Chem*, 2009. **284**(38): p. 26207-15.
115. McCulloch, C.V., et al., *Multiple roles for the C-terminal tail of the chemokine scavenger D6*. *J Biol Chem*, 2008. **283**(12): p. 7972-82.
116. Galliera, E., et al., *beta-Arrestin-dependent constitutive internalization of the human chemokine decoy receptor D6*. *J Biol Chem*, 2004. **279**(24): p. 25590-7.
117. Weber, M., et al., *The chemokine receptor D6 constitutively traffics to and from the cell surface to internalize and degrade chemokines*. *Mol Biol Cell*, 2004. **15**(5): p. 2492-508.
118. Burns, J.M., et al., *A novel chemokine receptor for SDF-1 and I-TAC involved in cell survival, cell adhesion, and tumor development*. *J Exp Med*, 2006. **203**(9): p. 2201-13.
119. Balabanian, K., et al., *The chemokine SDF-1/CXCL12 binds to and signals through the orphan receptor RDC1 in T lymphocytes*. *J Biol Chem*, 2005. **280**(42): p. 35760-6.
120. Meyrath, M., et al., *The atypical chemokine receptor ACKR3/CXCR7 is a broad-spectrum scavenger for opioid peptides*. *Nat Commun*, 2020. **11**(1): p. 3033.
121. Mackie, D.I., et al., *RAMP3 determines rapid recycling of atypical chemokine receptor-3 for guided angiogenesis*. *Proc Natl Acad Sci U S A*, 2019. **116**(48): p. 24093-24099.
122. Klein, K.R., et al., *Decoy receptor CXCR7 modulates adrenomedullin-mediated cardiac and lymphatic vascular development*. *Dev Cell*, 2014. **30**(5): p. 528-40.
123. Gosling, J., et al., *Cutting edge: identification of a novel chemokine receptor that binds dendritic cell- and T cell-active chemokines including ELC, SLC, and TECK*. *J Immunol*, 2000. **164**(6): p. 2851-6.
124. Watts, A.O., et al., *beta-Arrestin recruitment and G protein signaling by the atypical human chemokine decoy receptor CCX-CKR*. *J Biol Chem*, 2013. **288**(10): p. 7169-81.

125. Bondue, B., V. Wittamer, and M. Parmentier, *Chemerin and its receptors in leukocyte trafficking, inflammation and metabolism*. Cytokine Growth Factor Rev, 2011. **22**(5-6): p. 331-8.
126. Leick, M., et al., *CCL19 is a specific ligand of the constitutively recycling atypical human chemokine receptor CRAM-B*. Immunology, 2010. **129**(4): p. 536-46.
127. Hartmann, T.N., et al., *Human B cells express the orphan chemokine receptor CRAM-A/B in a maturation-stage-dependent and CCL5-modulated manner*. Immunology, 2008. **125**(2): p. 252-62.
128. Lim, K., et al., *Neutrophil trails guide influenza-specific CD8(+) T cells in the airways*. Science, 2015. **349**(6252): p. aaa4352.
129. Thanabalasuriar, A., et al., *iNKT Cell Emigration out of the Lung Vasculature Requires Neutrophils and Monocyte-Derived Dendritic Cells in Inflammation*. Cell Rep, 2016. **16**(12): p. 3260-3272.
130. Nagarsheth, N., M.S. Wicha, and W. Zou, *Chemokines in the cancer microenvironment and their relevance in cancer immunotherapy*. Nat Rev Immunol, 2017. **17**(9): p. 559-572.
131. Norlander, A.E., M.A. Saleh, and M.S. Madhur, *CXCL16: a chemokine-causing chronic kidney disease*. Hypertension, 2013. **62**(6): p. 1008-10.
132. van der Vorst, E.P., Y. Doring, and C. Weber, *Chemokines*. Arterioscler Thromb Vasc Biol, 2015. **35**(11): p. e52-6.
133. Medzhitov, R., *Origin and physiological roles of inflammation*. Nature, 2008. **454**(7203): p. 428-35.
134. Fullerton, J.N. and D.W. Gilroy, *Resolution of inflammation: a new therapeutic frontier*. Nat Rev Drug Discov, 2016. **15**(8): p. 551-67.
135. Sender, R., S. Fuchs, and R. Milo, *Are We Really Vastly Outnumbered? Revisiting the Ratio of Bacterial to Host Cells in Humans*. Cell, 2016. **164**(3): p. 337-40.
136. Bennett, G.D. and M.M. Kay, *Homeostatic removal of senescent murine erythrocytes by splenic macrophages*. Exp Hematol, 1981. **9**(3): p. 297-307.
137. de Back, D.Z., et al., *Of macrophages and red blood cells; a complex love story*. Front Physiol, 2014. **5**: p. 9.
138. Klei, T.R., et al., *From the Cradle to the Grave: The Role of Macrophages in Erythropoiesis and Erythrophagocytosis*. Front Immunol, 2017. **8**: p. 73.
139. Tavian, M., M.F. Hallais, and B. Peault, *Emergence of intraembryonic hematopoietic precursors in the pre-liver human embryo*. Development, 1999. **126**(4): p. 793-803.
140. Huyhn, A., et al., *Characterization of hematopoietic progenitors from human yolk sacs and embryos*. Blood, 1995. **86**(12): p. 4474-85.
141. Civin, C.I., et al., *Antigenic analysis of hematopoiesis. III. A hematopoietic progenitor cell surface antigen defined by a monoclonal antibody raised against KG-1a cells*. J Immunol, 1984. **133**(1): p. 157-65.
142. Gekas, C., et al., *The placenta is a niche for hematopoietic stem cells*. Dev Cell, 2005. **8**(3): p. 365-75.
143. Hirsch, E., et al., *Impaired migration but not differentiation of haematopoietic stem cells in the absence of beta1 integrins*. Nature, 1996. **380**(6570): p. 171-5.

144. Potocnik, A.J., C. Brakebusch, and R. Fassler, *Fetal and adult hematopoietic stem cells require beta1 integrin function for colonizing fetal liver, spleen, and bone marrow*. *Immunity*, 2000. **12**(6): p. 653-63.
145. Fan, N., et al., *Extramedullary hematopoiesis in the absence of myeloproliferative neoplasm: Mayo Clinic case series of 309 patients*. *Blood Cancer J*, 2018. **8**(12): p. 119.
146. Badr, N.M., C. Roberts, and A.M. Shaaban, *Extramedullary Haematopoiesis in Axillary Lymph Nodes of Breast Carcinoma Patients Receiving Neoadjuvant Chemotherapy: A Potential Diagnostic Pitfall*. *Pathobiology*, 2019. **86**(2-3): p. 167-172.
147. Bowen, J.M., et al., *Extramedullary hematopoiesis in a sentinel lymph node as an early sign of chronic myelomonocytic leukemia*. *Case Rep Pathol*, 2015. **2015**: p. 594970.
148. Kiel, M.J., et al., *SLAM family receptors distinguish hematopoietic stem and progenitor cells and reveal endothelial niches for stem cells*. *Cell*, 2005. **121**(7): p. 1109-21.
149. Morrison, S.J. and D.T. Scadden, *The bone marrow niche for haematopoietic stem cells*. *Nature*, 2014. **505**(7483): p. 327-34.
150. Calvi, L.M., et al., *Osteoblastic cells regulate the haematopoietic stem cell niche*. *Nature*, 2003. **425**(6960): p. 841-6.
151. Zhang, J., et al., *Identification of the haematopoietic stem cell niche and control of the niche size*. *Nature*, 2003. **425**(6960): p. 836-41.
152. Lo Celso, C., et al., *Live-animal tracking of individual haematopoietic stem/progenitor cells in their niche*. *Nature*, 2009. **457**(7225): p. 92-6.
153. Nombela-Arrieta, C., et al., *Quantitative imaging of haematopoietic stem and progenitor cell localization and hypoxic status in the bone marrow microenvironment*. *Nat Cell Biol*, 2013. **15**(5): p. 533-43.
154. Kiel, M.J., et al., *Hematopoietic stem cells do not depend on N-cadherin to regulate their maintenance*. *Cell Stem Cell*, 2009. **4**(2): p. 170-9.
155. Kunisaki, Y., et al., *Arteriolar niches maintain haematopoietic stem cell quiescence*. *Nature*, 2013. **502**(7473): p. 637-43.
156. Kusumbe, A.P., S.K. Ramasamy, and R.H. Adams, *Coupling of angiogenesis and osteogenesis by a specific vessel subtype in bone*. *Nature*, 2014. **507**(7492): p. 323-328.
157. Barker, J.E., *Sl/Slid hematopoietic progenitors are deficient in situ*. *Exp Hematol*, 1994. **22**(2): p. 174-7.
158. Barker, J.E., *Early transplantation to a normal microenvironment prevents the development of Steel hematopoietic stem cell defects*. *Exp Hematol*, 1997. **25**(6): p. 542-7.
159. Fleischman, R.A. and B. Mintz, *Prevention of genetic anemias in mice by microinjection of normal hematopoietic stem cells into the fetal placenta*. *Proc Natl Acad Sci U S A*, 1979. **76**(11): p. 5736-40.
160. Zhou, B.O., et al., *Leptin-receptor-expressing mesenchymal stromal cells represent the main source of bone formed by adult bone marrow*. *Cell Stem Cell*, 2014. **15**(2): p. 154-68.

161. Ding, L. and S.J. Morrison, *Haematopoietic stem cells and early lymphoid progenitors occupy distinct bone marrow niches*. Nature, 2013. **495**(7440): p. 231-5.
162. Mendez-Ferrer, S., et al., *Haematopoietic stem cell release is regulated by circadian oscillations*. Nature, 2008. **452**(7186): p. 442-7.
163. Qian, H., et al., *Critical role of thrombopoietin in maintaining adult quiescent hematopoietic stem cells*. Cell Stem Cell, 2007. **1**(6): p. 671-84.
164. Kimura, S., et al., *Hematopoietic stem cell deficiencies in mice lacking c-Mpl, the receptor for thrombopoietin*. Proc Natl Acad Sci U S A, 1998. **95**(3): p. 1195-200.
165. Takubo, K., et al., *Regulation of the HIF-1alpha level is essential for hematopoietic stem cells*. Cell Stem Cell, 2010. **7**(3): p. 391-402.
166. Spencer, J.A., et al., *Direct measurement of local oxygen concentration in the bone marrow of live animals*. Nature, 2014. **508**(7495): p. 269-73.
167. Wilkinson, A.C., et al., *Branched-chain amino acid depletion conditions bone marrow for hematopoietic stem cell transplantation avoiding amino acid imbalance-associated toxicity*. Exp Hematol, 2018. **63**: p. 12-16 e1.
168. Taya, Y., et al., *Depleting dietary valine permits nonmyeloablative mouse hematopoietic stem cell transplantation*. Science, 2016. **354**(6316): p. 1152-1155.
169. Benedikter, B.J., et al., *Ultrafiltration combined with size exclusion chromatography efficiently isolates extracellular vesicles from cell culture media for compositional and functional studies*. Sci Rep, 2017. **7**(1): p. 15297.
170. Li, W.C., K.L. Ralphs, and D. Tosh, *Isolation and culture of adult mouse hepatocytes*. Methods Mol Biol, 2010. **633**: p. 185-96.
171. Bale, S.S., et al., *Long-term coculture strategies for primary hepatocytes and liver sinusoidal endothelial cells*. Tissue Eng Part C Methods, 2015. **21**(4): p. 413-22.
172. Duchene, J., et al., *Atypical chemokine receptor 1 on nucleated erythroid cells regulates hematopoiesis*. Nat Immunol, 2017. **18**(7): p. 753-761.
173. Tunaru, S., et al., *20-HETE promotes glucose-stimulated insulin secretion in an autocrine manner through FFAR1*. Nat Commun, 2018. **9**(1): p. 177.
174. Lorenzen, E., et al., *Multiplexed analysis of the secretin-like GPCR-RAMP interactome*. Sci Adv, 2019. **5**(9): p. eaaw2778.
175. Inoue, A., et al., *Illuminating G-Protein-Coupling Selectivity of GPCRs*. Cell, 2019. **177**(7): p. 1933-1947 e25.
176. Kunz, L. and T. Schroeder, *A 3D Tissue-wide Digital Imaging Pipeline for Quantitation of Secreted Molecules Shows Absence of CXCL12 Gradients in Bone Marrow*. Cell Stem Cell, 2019. **25**(6): p. 846-854 e4.
177. Naumann, U., et al., *CXCR7 functions as a scavenger for CXCL12 and CXCL11*. PLoS One, 2010. **5**(2): p. e9175.
178. Le Mercier, A., et al., *GPR182 is an endothelium-specific atypical chemokine receptor that maintains hematopoietic stem cell homeostasis*. Proc Natl Acad Sci U S A, 2021. **118**(17).
179. Bachelierie, F., et al., *An atypical addition to the chemokine receptor nomenclature: IUPHAR Review 15*. Br J Pharmacol, 2015. **172**(16): p. 3945-9.
180. Coggins, N.L., et al., *CXCR7 controls competition for recruitment of beta-arrestin 2 in cells expressing both CXCR4 and CXCR7*. PLoS One, 2014. **9**(6): p. e98328.

181. Luker, K.E., et al., *Constitutive and chemokine-dependent internalization and recycling of CXCR7 in breast cancer cells to degrade chemokine ligands*. *Oncogene*, 2010. **29**(32): p. 4599-610.
182. Vacchini, A., M. Locati, and E.M. Borroni, *Overview and potential unifying themes of the atypical chemokine receptor family*. *J Leukoc Biol*, 2016. **99**(6): p. 883-92.
183. Tian, X., D.S. Kang, and J.L. Benovic, *beta-arrestins and G protein-coupled receptor trafficking*. *Handb Exp Pharmacol*, 2014. **219**: p. 173-86.
184. Skieterska, K., P. Rondou, and K. Van Craenenbroeck, *Regulation of G Protein-Coupled Receptors by Ubiquitination*. *Int J Mol Sci*, 2017. **18**(5).
185. Marchese, A., et al., *G protein-coupled receptor sorting to endosomes and lysosomes*. *Annu Rev Pharmacol Toxicol*, 2008. **48**: p. 601-29.
186. Canals, M., et al., *Ubiquitination of CXCR7 controls receptor trafficking*. *PLoS One*, 2012. **7**(3): p. e34192.
187. Greenbaum, A., et al., *CXCL12 in early mesenchymal progenitors is required for haematopoietic stem-cell maintenance*. *Nature*, 2013. **495**(7440): p. 227-30.
188. Aiuti, A., et al., *The chemokine SDF-1 is a chemoattractant for human CD34+ hematopoietic progenitor cells and provides a new mechanism to explain the mobilization of CD34+ progenitors to peripheral blood*. *J Exp Med*, 1997. **185**(1): p. 111-20.
189. Middleton, J., et al., *Leukocyte extravasation: chemokine transport and presentation by the endothelium*. *Blood*, 2002. **100**(12): p. 3853-60.
190. Perlin, J.R., A. Sporrij, and L.I. Zon, *Blood on the tracks: hematopoietic stem cell-endothelial cell interactions in homing and engraftment*. *J Mol Med (Berl)*, 2017. **95**(8): p. 809-819.
191. Itkin, T., et al., *Distinct bone marrow blood vessels differentially regulate haematopoiesis*. *Nature*, 2016. **532**(7599): p. 323-8.
192. Sinclair, A., et al., *CXCR2 and CXCL4 regulate survival and self-renewal of hematopoietic stem/progenitor cells*. *Blood*, 2016. **128**(3): p. 371-83.
193. Matatall, K.A., et al., *Type II interferon promotes differentiation of myeloid-biased hematopoietic stem cells*. *Stem Cells*, 2014. **32**(11): p. 3023-30.
194. Thiant, S., et al., *Plasma levels of IL-7 and IL-15 in the first month after myeloablative BMT are predictive biomarkers of both acute GVHD and relapse*. *Bone Marrow Transplant*, 2010. **45**(10): p. 1546-52.
195. Pratt, L.M., et al., *IL15 levels on day 7 after hematopoietic cell transplantation predict chronic GVHD*. *Bone Marrow Transplant*, 2013. **48**(5): p. 722-8.
196. Adachi, T., et al., *Hair follicle-derived IL-7 and IL-15 mediate skin-resident memory T cell homeostasis and lymphoma*. *Nat Med*, 2015. **21**(11): p. 1272-9.
197. Deshpande, P., et al., *IL-7- and IL-15-mediated TCR sensitization enables T cell responses to self-antigens*. *J Immunol*, 2013. **190**(4): p. 1416-23.
198. Cordeiro Gomes, A., et al., *Hematopoietic Stem Cell Niches Produce Lineage-Instructive Signals to Control Multipotent Progenitor Differentiation*. *Immunity*, 2016. **45**(6): p. 1219-1231.
199. Cui, G., et al., *Characterization of the IL-15 niche in primary and secondary lymphoid organs in vivo*. *Proc Natl Acad Sci U S A*, 2014. **111**(5): p. 1915-20.
200. Britton, C., M.C. Poznansky, and P. Reeves, *Polyfunctionality of the CXCR4/CXCL12 axis in health and disease: Implications for therapeutic*

- interventions in cancer and immune-mediated diseases*. FASEB J, 2021. **35**(4): p. e21260.
201. Bujak, M., et al., *Induction of the CXC chemokine interferon-gamma-inducible protein 10 regulates the reparative response following myocardial infarction*. Circ Res, 2009. **105**(10): p. 973-83.
 202. Barreira da Silva, R., et al., *Dipeptidylpeptidase 4 inhibition enhances lymphocyte trafficking, improving both naturally occurring tumor immunity and immunotherapy*. Nat Immunol, 2015. **16**(8): p. 850-8.
 203. Ryu, J.K., et al., *Blood coagulation protein fibrinogen promotes autoimmunity and demyelination via chemokine release and antigen presentation*. Nat Commun, 2015. **6**: p. 8164.
 204. Cosgrove, J., et al., *B cell zone reticular cell microenvironments shape CXCL13 gradient formation*. Nat Commun, 2020. **11**(1): p. 3677.
 205. Kanemitsu, N., et al., *CXCL13 is an arrest chemokine for B cells in high endothelial venules*. Blood, 2005. **106**(8): p. 2613-8.
 206. Legler, D.F., et al., *B cell-attracting chemokine 1, a human CXC chemokine expressed in lymphoid tissues, selectively attracts B lymphocytes via BLR1/CXCR5*. J Exp Med, 1998. **187**(4): p. 655-60.
 207. Leon, B., et al., *Regulation of T(H)2 development by CXCR5+ dendritic cells and lymphotoxin-expressing B cells*. Nat Immunol, 2012. **13**(7): p. 681-90.
 208. House, I.G., et al., *Macrophage-Derived CXCL9 and CXCL10 Are Required for Antitumor Immune Responses Following Immune Checkpoint Blockade*. Clin Cancer Res, 2020. **26**(2): p. 487-504.
 209. Karin, N., *CXCR3 Ligands in Cancer and Autoimmunity, Chemoattraction of Effector T Cells, and Beyond*. Front Immunol, 2020. **11**: p. 976.
 210. Wald, O., O.M. Shapira, and U. Izhar, *CXCR4/CXCL12 axis in non small cell lung cancer (NSCLC) pathologic roles and therapeutic potential*. Theranostics, 2013. **3**(1): p. 26-33.
 211. Chapman, J., et al., *Splenomegaly*, in *StatPearls*. 2021: Treasure Island (FL).
 212. Majumder, S., et al., *CXCL10 is critical for the generation of protective CD8 T cell response induced by antigen pulsed CpG-ODN activated dendritic cells*. PLoS One, 2012. **7**(11): p. e48727.
 213. Khan, I.A., et al., *IP-10 is critical for effector T cell trafficking and host survival in Toxoplasma gondii infection*. Immunity, 2000. **12**(5): p. 483-94.
 214. Singh, N. and S. Sundar, *Inflammatory chemokines and their receptors in human visceral leishmaniasis: Gene expression profile in peripheral blood, splenic cellular sources and their impact on trafficking of inflammatory cells*. Mol Immunol, 2017. **85**: p. 111-119.
 215. Forster, R., et al., *A putative chemokine receptor, BLR1, directs B cell migration to defined lymphoid organs and specific anatomic compartments of the spleen*. Cell, 1996. **87**(6): p. 1037-47.
 216. Ansel, K.M., et al., *A chemokine-driven positive feedback loop organizes lymphoid follicles*. Nature, 2000. **406**(6793): p. 309-14.
 217. Kraehling, J.R., et al., *Genome-wide RNAi screen reveals ALK1 mediates LDL uptake and transcytosis in endothelial cells*. Nat Commun, 2016. **7**: p. 13516.

218. Podrez, E.A., et al., *Identification of a novel family of oxidized phospholipids that serve as ligands for the macrophage scavenger receptor CD36*. J Biol Chem, 2002. **277**(41): p. 38503-16.
219. Nie, S., et al., *Detection of atherosclerotic lesions and intimal macrophages using CD36-targeted nanovesicles*. J Control Release, 2015. **220**(Pt A): p. 61-70.
220. Angers, S., A. Salahpour, and M. Bouvier, *Dimerization: an emerging concept for G protein-coupled receptor ontogeny and function*. Annu Rev Pharmacol Toxicol, 2002. **42**: p. 409-35.
221. George, S.R., B.F. O'Dowd, and S.P. Lee, *G-protein-coupled receptor oligomerization and its potential for drug discovery*. Nat Rev Drug Discov, 2002. **1**(10): p. 808-20.
222. Lohse, M.J., *Dimerization in GPCR mobility and signaling*. Curr Opin Pharmacol, 2010. **10**(1): p. 53-8.
223. Levoye, A., et al., *CXCR7 heterodimerizes with CXCR4 and regulates CXCL12-mediated G protein signaling*. Blood, 2009. **113**(24): p. 6085-93.
224. Pello, O.M., et al., *Ligand stabilization of CXCR4/delta-opioid receptor heterodimers reveals a mechanism for immune response regulation*. Eur J Immunol, 2008. **38**(2): p. 537-49.
225. Albee, L.J., et al., *alpha1-Adrenergic Receptors Function Within Hetero-Oligomeric Complexes With Atypical Chemokine Receptor 3 and Chemokine (C-X-C motif) Receptor 4 in Vascular Smooth Muscle Cells*. J Am Heart Assoc, 2017. **6**(8).
226. Ding, B.S., et al., *Divergent angiocrine signals from vascular niche balance liver regeneration and fibrosis*. Nature, 2014. **505**(7481): p. 97-102.
227. Liepelt, A. and F. Tacke, *Stromal cell-derived factor-1 (SDF-1) as a target in liver diseases*. Am J Physiol Gastrointest Liver Physiol, 2016. **311**(2): p. G203-9.
228. Li, Y., et al., *CXCL13-mediated recruitment of intrahepatic CXCR5(+)CD8(+) T cells favors viral control in chronic HBV infection*. J Hepatol, 2020. **72**(3): p. 420-430.
229. Macchi, C., et al., *PCSK9: a view beyond the canonical cholesterol lowering impact*. Am J Pathol, 2021.
230. Arvind, A., et al., *Lipid and Lipoprotein Metabolism in Liver Disease*, in *Endotext*, K.R. Feingold, et al., Editors. 2000: South Dartmouth (MA).
231. <https://smart.servier.com/>

X. Publications

The Orphan G-Protein Coupled Receptor 182 Is a Negative Regulator of Definitive Hematopoiesis through Leukotriene B4 Signaling

Hyoun-Bum Kwon, Duncan I. Mackie, Remy Bonnavion, Alan Le Mercier, Christian S. M. Helker, Taekwon Son, Stefan Guenter, D. Stephen Serafin, Kyu-Won Kim, Stefan Offermanns, Kathleen M. Caron,* and Didier Y. R. Stainier*

Cite This: *ACS Pharmacol. Transl. Sci.* 2020, 3, 676–689

Read Online

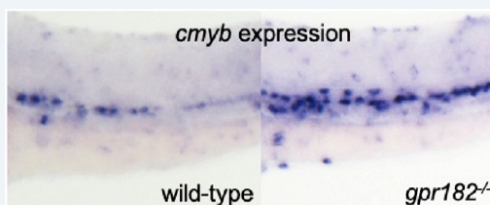
ACCESS |

Metrics & More

Article Recommendations

Supporting Information

ABSTRACT: The G protein-coupled receptor 182 (GPR182) is an orphan GPCR, the expression of which is enriched in embryonic endothelial cells (ECs). However, the physiological role and molecular mechanism of action of GPR182 are unknown. Here, we show that GPR182 negatively regulates definitive hematopoiesis in zebrafish and mice. In zebrafish, *gpr182* expression is enriched in the hemogenic endothelium (HE), and *gpr182*^{-/-} display an increased expression of HE and hematopoietic stem cell (HSC) marker genes. Notably, we find an increased number of myeloid cells in *gpr182*^{-/-} compared to wild-type. Further, by time-lapse imaging of zebrafish embryos during the endothelial-to-hematopoietic transition, we find that HE/HSC cell numbers are increased in *gpr182*^{-/-} compared to wild-type. *GPR182*^{-/-} mice also exhibit an increased number of myeloid cells compared to wild-type, indicating a conserved role for GPR182 in myelopoiesis. Using cell-based small molecule screening and transcriptomic analyses, we further find that GPR182 regulates the leukotriene B4 (LTB4) biosynthesis pathway. Taken together, these data indicate that GPR182 is a negative regulator of definitive hematopoiesis in zebrafish and mice, and provide further evidence for LTB4 signaling in HSC biology.



KEYWORDS: G protein-coupled receptor, GPR182, hematopoietic stem cell, definitive hematopoiesis, myelopoiesis, Leukotriene B4

G-protein coupled receptors (GPCRs) are the most tractable class of proteins, with ~30–40% of all drugs currently on the market targeting their activity.^{1–3} To date, many GPCRs remain categorized as “orphan” GPCRs, sparking much interest and investment to discover selective modulators of their activity for the development of novel therapeutics. As such, it is critical to define the function and molecular mechanism of these orphan receptors to understand the physiological impact of their inhibition. GPCRs constitute the largest receptor family and are involved in a variety of physiological processes that range from sensing external signals including light, odor, taste, and touch to mediating signal transduction pathways, such as in the autonomic nervous system and during inflammation.⁴ However, the role of GPCRs in hematopoiesis remains poorly characterized.

Historically, zebrafish have been recognized as an excellent genetic model system to study hematopoiesis because of a high level of similarity with mammals.⁵ Namely, zebrafish and mammals share all major types of blood cells, and these cells are produced via similar processes called primitive and definitive hematopoiesis.⁶ In zebrafish, primitive hematopoiesis occurs in the anterior lateral plate mesoderm, which gives rise to myeloid

cells, and in the posterior lateral plate mesoderm, which gives rise to primitive erythrocytes.⁵ Definitive hematopoiesis produces hematopoietic stem cells (HSCs) capable of self-renewing and contributing to all blood lineages.⁷ HSCs first appear at approximately 30–32 h post fertilization (hpf) from hemogenic endothelial cells located at the ventral wall of the dorsal aorta (VDA), which is functionally equivalent to the aorta-gonad-mesonephros (AGM) region in amniotes.^{8,9} HSCs (marked by *runx1* and *c-myb* expression) migrate to the caudal hematopoietic tissue (CHT) where they expand and further develop before moving to the kidney, which is the zebrafish equivalent to the mammalian bone marrow.¹⁰

GPR182 is a class A orphan GPCR. Initially, it was thought that GPR182 was a putative adrenomedullin receptor; however, it was later shown that adrenomedullin signals through a

Received: February 19, 2020

Published: June 24, 2020





GPR182 is an endothelium-specific atypical chemokine receptor that maintains hematopoietic stem cell homeostasis

Alan Le Mercier^{a,1}, Remy Bonnavaion^{a,1,2}, Weijia Yu^b, Mohamad Wessam Alnouri^a, Sophie Ramas^a, Yang Zhang^c, Yannick Jäger^a, Kenneth Anthony Roquid^a, Hyun-Woo Jeong^d, Kishor Kumar Sivaraj^d, Haaglim Cho^a, Xinyi Chen^a, Boris Strilic^a, Tjeerd Sijmonsma^{b,e}, Ralf Adams^d, Timm Schroeder^e, Michael A. Rieger^{b,e,f,g}, and Stefan Offermanns^{a,f,g,h,i,2}

^aDepartment of Pharmacology, Max Planck Institute for Heart and Lung Research, Bad Nauheim, 61231, Germany; ^bDepartment of Medicine, Hematology/Oncology, Goethe University Hospital, 60590 Frankfurt, Germany; ^cDepartment of Biosystems Science and Engineering, Eidgenössische Technische Hochschule (ETH) Zurich, 4058 Basel, Switzerland; ^dDepartment of Tissue Morphogenesis, Max Planck Institute for Molecular Biomedicine, 48149 Münster, Germany; ^eGerman Cancer Consortium and German Cancer Research Center, Heidelberg, 69120, Germany; ^fFrankfurt Cancer Institute, 60590 Frankfurt, Germany; ^gCardio-Pulmonary Institute, 60590 Frankfurt, Germany; ^hGerman Centre for Cardiovascular Research, Rhine-Main site, Frankfurt and Bad Nauheim, 60590, Germany; and ⁱCentre for Molecular Medicine, Medical Faculty, Goethe University Frankfurt, 60590 Frankfurt, Germany

Edited by Robert J. Lefkowitz, Howard Hughes Medical Institute, Durham, NC, and approved March 8, 2021 (received for review October 15, 2020)

G protein-coupled receptor 182 (GPR182) has been shown to be expressed in endothelial cells; however, its ligand and physiological role has remained elusive. We found GPR182 to be expressed in microvascular and lymphatic endothelial cells of most organs and to bind with nanomolar affinity the chemokines CXCL10, CXCL12, and CXCL13. In contrast to conventional chemokine receptors, binding of chemokines to GPR182 did not induce typical downstream signaling processes, including G_q- and G_i-mediated signaling or β-arrestin recruitment. GPR182 showed relatively high constitutive activity in regard to β-arrestin recruitment and rapidly internalized in a ligand-independent manner. In constitutive GPR182-deficient mice, as well as after induced endothelium-specific loss of GPR182, we found significant increases in the plasma levels of CXCL10, CXCL12, and CXCL13. Global and induced endothelium-specific GPR182-deficient mice showed a significant decrease in hematopoietic stem cells in the bone marrow as well as increased colony-forming units of hematopoietic progenitors in the blood and the spleen. Our data show that GPR182 is a new atypical chemokine receptor for CXCL10, CXCL12, and CXCL13, which is involved in the regulation of hematopoietic stem cell homeostasis.

GPCR | orphan | chemokine

G protein-coupled receptors (GPCRs) represent the largest group of transmembrane receptors encoded in the genome, and they are the largest group of proteins targeted by approved drugs (1, 2). GPCRs are very versatile and can bind ligands of different physicochemical properties, including ions, lipids, biogenic amines, peptides, or proteins, such as chemokines (3). Primarily by activation of heterotrimeric G proteins, GPCRs regulate multiple functions in basically all cells of mammalian organisms (4). Despite their large physiological and pharmacological relevance, the endogenous ligands, activating mechanisms and physiological functions of more than 100 GPCRs, are still not known and these receptors are therefore referred to as “orphan” receptors (3, 5). G protein-coupled receptor 182 (GPR182) is an orphan receptor, although it has been suggested to bind adrenomedullin (6), but this observation could not be confirmed (7). GPR182 was initially described to be widely expressed in various organs (8). More-detailed analyses in developing zebrafish and in mice revealed that Gpr182 is preferentially expressed in the vascular endothelium (9, 10). Widespread expression in endothelial cells of adult mice was shown using a mouse line expressing β-galactosidase under the control of the Gpr182-promoter (11), and expression of GPR182 in sinusoidal endothelial cells was reported based on immunohistochemical analysis (12). Whereas the role of GPR182 in endothelial cells is unknown, GPR182 expression was also reported in intestinal stem

cells, where the receptor was shown to negatively regulate proliferation during regeneration and adenoma formation (11).

Chemokine receptors are a family of 22 GPCRs that respond to 52 chemokines (13). Upon activation, they induce G protein-mediated intracellular signaling processes which, in many cases, regulate the migration of leukocytes (14). However, more recent work has shown that the function of chemokines goes beyond the regulation of leukocyte migration and can also affect other cell functions and cell types (13, 15, 16). In addition, and in contrast to other groups of GPCRs, the chemokine receptor family contains several members, which bind chemokines but are unable to signal through G proteins. These so-called “atypical chemokine receptors” (ACKRs) can indirectly regulate the interactions between chemokines and conventional chemokine receptors by controlling chemokine localization, distribution, and abundance (13, 16, 17). As most conventional chemokine receptors, ACKRs typically bind subgroups of chemokines. For instance, ACKR1 binds various

Significance

G protein-coupled receptors (GPCRs) are important regulators of cellular and biological functions and are primary targets of therapeutic drugs. About 100 mammalian GPCRs are still considered orphan receptors because they lack a known endogenous ligand. We report the deorphanization of GPR182, which is expressed in endothelial cells of the microvasculature. We show that GPR182 is an atypical chemokine receptor, which binds CXCL10, 12, and 13. However, binding does not induce downstream signaling. Consistent with a scavenging function of GPR182, mice lacking GPR182 have increased plasma levels of chemokines. In line with the crucial role of CXCL12 in hematopoietic stem cell homeostasis, we found that loss of GPR182 results in increased egress of hematopoietic stem cells from the bone marrow.

Author contributions: R.B., M.A.R., and S.O. designed research; A.L.M., R.B., W.Y., M.W.A., S.R., Y.Z., Y.J., K.A.R., H.-W.J., K.K.S., H.C., X.C., B.S., and T.S. performed research; R.A. and T.S. contributed new reagents/analytic tools; A.L.M., R.B., W.Y., M.W.A., S.R., Y.Z., and S.O. analyzed data; A.L.M., R.B., and S.O. wrote the paper; and R.A. discussed data.

The authors declare no competing interest.

This article is a PNAS Direct Submission.

This open access article is distributed under Creative Commons Attribution-NonCommercial-NoDerivatives License 4.0 (CC BY-NC-ND).

¹A.L.M. and R.B. contributed equally to this work.

²To whom correspondence may be addressed. Email: remy.bonnavaion@mpi-bn.mpg.de or Stefan.Offermanns@mpi-bn.mpg.de.

This article contains supporting information online at <https://www.pnas.org/lookup/suppl/doi:10.1073/pnas.2021596118/-DCSupplemental>.

Published April 19, 2021.

XI. Schriftliche Erklärung

Name/Vorname: Le Mercier Alan

Geburtsdatum: 18 März 1990

Schriftliche Erklärung

Nach bestandener Doktorprüfung lege ich hiermit die Bescheinigung der Universitätsbibliothek über die Abgabe der erforderlichen Pflichtexemplare meiner Dissertation sowie die Pflichtexemplare meiner Dissertation für das Dekanat vor.

Diese Pflichtexemplare lege ich in der Version vor, die auch den Gutachtern (Referent, Korreferent/en) im Promotionsverfahren vorgelegen hat. Ich versichere mit meiner Unterschrift, dass ich außer den Ergänzungen

- zum/ zu den Korreferenten,
- dem Tag der mündlichen Prüfung

auf der Seite 2 meiner Dissertation keine Änderungen vorgenommen habe.

(Datum, Unterschrift)